Ohio River Valley Soils Seminar XLVIII

Infrastructure Innovation in Geotechnical Design

November 17, 2017
Hilton Netherland Plaza
35 West 5th Street
Cincinnati, Ohio

Planned Agenda – Friday, November 17, 2017

6:30-7:30 am	Exhibitor Registration and Setup
7:30-8:15 am	**Registration**
8:15-8:30 am	**Welcome Remarks:** Mark Salveter, P.E., Geopier Foundation Company
8:30-9:10 am	"Case Studies in Geotechnical Instrumentation" – David Westendorf, P.E., Terracon Consultants, Inc.
9:10-10:10 am	"Case Study – USACE Low Mobility Grout, Full Depth Reclamation, and Roller Compacted Concrete at Fort Campbell, KY" – Steven W. Shifflett, P.E., US Army Corps of Engineers – Louisville District
10:10-10:50 am	"Innovative Design for the Merchants Bridge West Approach Reconstruction for TRRA in St. Louis, MO" – Lyndsie Janbakhsh, P.E. and Kevin Kriete, P.E., HDR, Inc.
10:50-11:05 am	**Break**
11:05-11:45 am	"Innovations in Rehabilitation of Aging Bridge Abutments" – Justin Anderson, M.E., P.E., GeoStabilization International
11:45-12:35 pm	**Lunch**
12:35-12:45 pm	Keynote Speaker Introduction – Akshat Saxena, E.I., Geotechnology, Inc.
12:45-1:40 pm	**Keynote Speaker:** "Three-dimensional Levee and Floodwall Underseepage" – Timothy D. Stark, Ph.D., P.E., University of Illinois, Urbana-Champaign
1:40-2:20 pm	"Asphalt Resurfacing after a Geohazard Repair" – Paul Travis, E.I., P.L.S., and Justin Anderson, MS, P.E., Geostabilization International
2:20-3:00 pm	"Earthquake Hazard Mitigation in Memphis" – Ashraf S. Elsayed, Ph.D., P.E., D.GE, Geotechnology, Inc.
3:00-3:20 pm	**Break**
3:20-4:00 pm	"Geotechnical Challenges – The I-40/I-240 Interchange Phase II" – Ashraf S. Elsayed, Ph.D., P.E., D.GE, Geotechnology, Inc.
4:00-4:35 pm	"Dam Structures Improvements for a Transportation Project" – Richard L. Williams, Ph.D., P.E., Stantec Consulting Services, Inc.
4:35-4:45 pm	**Closing Remarks:** Mark Salveter, P.E., Geopier Foundation Company

Proceedings of the 48th Annual Ohio River Valley Soils Seminar

Infrastructure Innovation in Geotechnical Design

November 17, 2017
Hilton Netherland Plaza
35 West 5th Street
Cincinnati, Ohio

Sponsored by:

ASCE Cincinnati Section Geotechnical Group

Kentucky Geotechnical Engineering Group, ASCE

University of Cincinnati
Department of Civil and Environmental Engineering

University of Kentucky
Department of Civil Engineering

University of Louisville
Department of Civil and Environmental Engineering

ORVSS XLVIII Planning Committee:

Akshat Saxena, E.I.
Geotechnology, Inc.
(Chair)

Mark Salveter, P.E.
Geopier Foundation Company

Aaron Klingshirn, P.E.
Richard Goettle, Inc.

Tumal Karunaratne, E.I.
Civil Solutions Associates

Donald B. Thelen, P.E.
Geotechnology, Inc.

Joseph D. Hauber, P.E.
Geotechnology, Inc.

Table of Contents

Case Studies in Geotechnical Instrumentation

David W. Westendorf, P.E.[1]

Abstract: The use of instrumentation and geo-structural monitoring to monitor geohazards, improve earthwork schedules, and, improve foundation efficiency continues to gain momentum and usage. This presentation will review several geotechnical instrumentation infrastructure projects and the unique equipment used and challenges encountered on each project. Projects encompassing landslides, reservoirs, and pipelines will be introduced with an emphasis on the technologies utilized. Projects include the Riverside Drive Landslide and Wall which included strain gages, inclinometers, load cells, and piezometers to monitor a large landslide in Cincinnati, Ohio. The next project shared will be a large scale instrumentation system, including bedrock joint/fracture monitoring at the McCook Reservoir project in Chicago. The application of geotechnical instrumentation continues to evolve at an increasing pace. Such applications will improve geo-structural design, accelerate construction schedules, and afford designers, owners, and contractor's the data needed so projects can be completed efficiently and safely.

[1] Senior Geotechnical Engineer, Terracon Consultants, Inc., Cincinnati, Ohio.
Email: david.westendorf@terracon.com

Case Studies in Geotechnical Instrumentation

Case Studies:

- Riverside Drive Landslide & Wall, Cincinnati, Ohio
- McCook Quarry/Reservoir, Chicago, Illinois

David Westendorf, P.E.

- Senior Geotechnical Engineer w/ Terracon Consultants
- Cincinnati, Ohio Office
- B.S. Civil Engineering- University of Toledo
- M.S. Civil Engineering- University of Illinois Urbana-Champaign

Terracon

Riverside Drive Landslide & Wall Monitoring

Cincinnati, Ohio

Highlights:

- Long-term creep in area
- Accelerated in 2016
- Terracon performed geotechnical study, design alternatives, and provided design loads for emergency design-build wall construction
- 1,200-foot wall constructed by Goettle
- Terracon installed instrumentation to monitor water main, slope, soldier piles, and tiebacks

Terracon

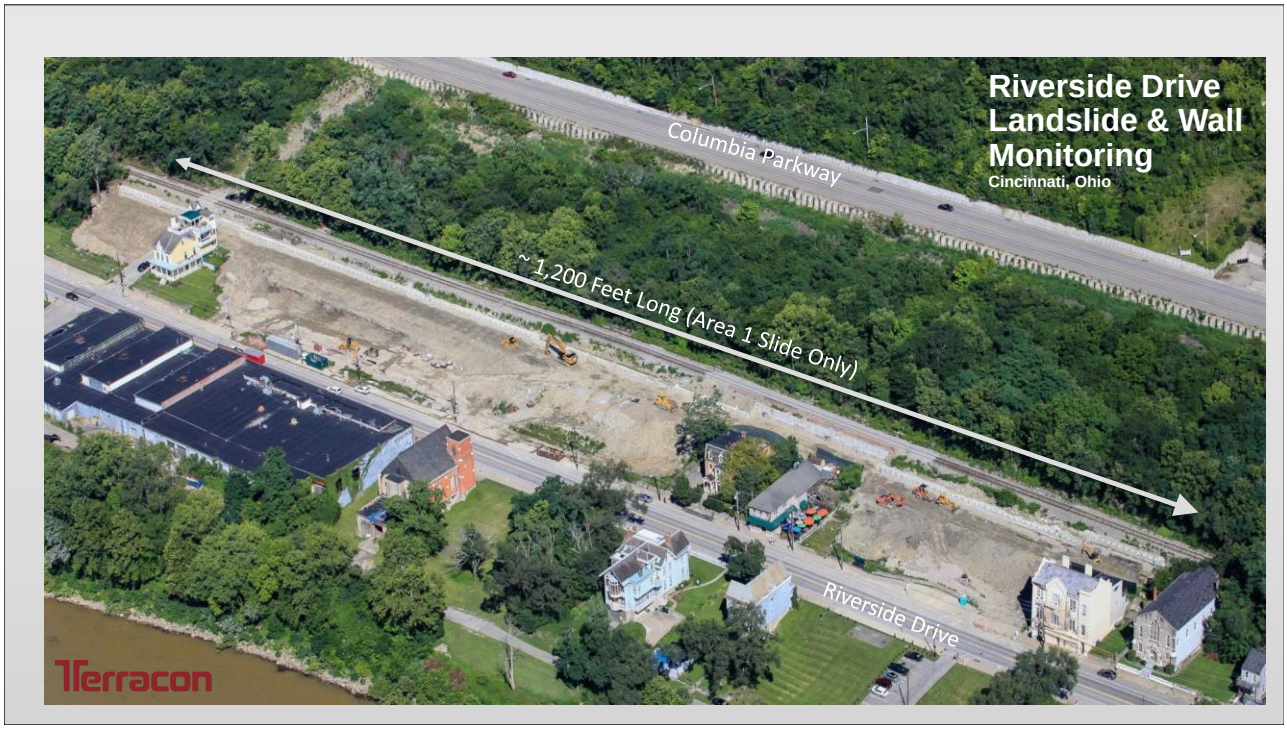
Riverside Drive
Landslide & Wall
Monitoring
Cincinnati, Ohio
Columbia Parkway
~1,200 Feet Long (Area 1 Slide Only)
Riverside Drive
Terracon

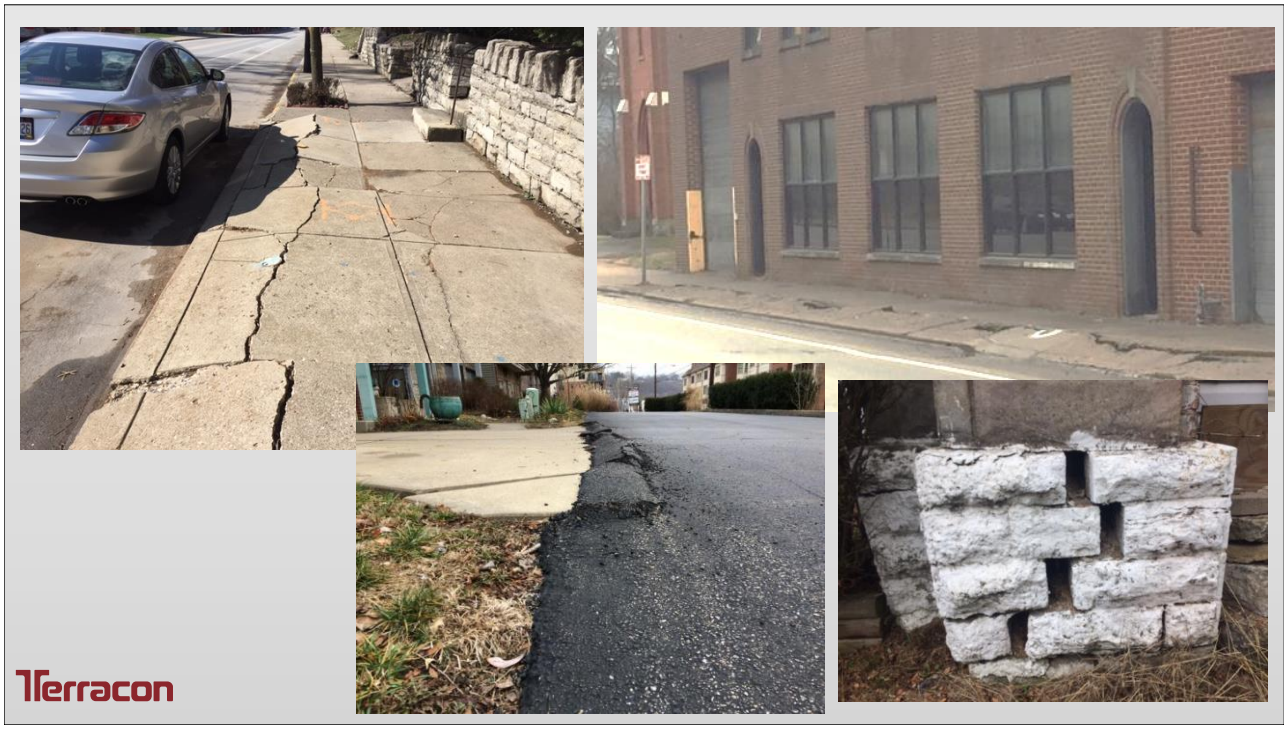
Terracon

Riverside Drive Landslide & Wall Monitoring

Cincinnati, Ohio

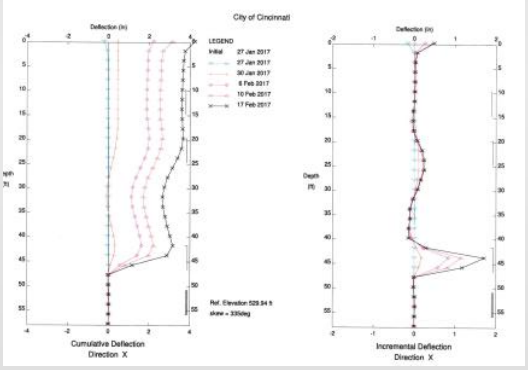

Riverside Drive Landslide & Wall Monitoring

Cincinnati, Ohio

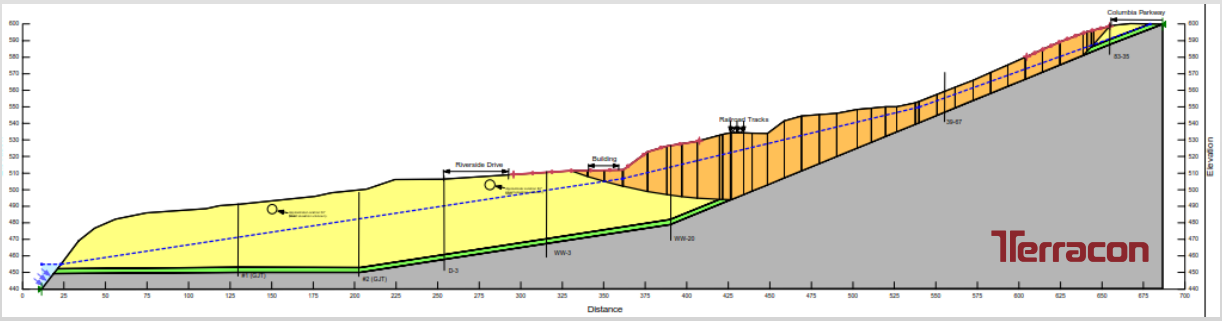

Riverside Drive Landslide & Wall Monitoring

Cincinnati, Ohio

- Repair was constructed by Goettle Construction and consisted of soldier pile & tieback wall, horizontal drains, and re-grading
- Soldier piles were W36x210 or W36x232 in 48 Inch Drilled Pier
- 7-strand tieback anchors
- Cap Beam (5'x4'2")
- Horizontal Drains- 3 degrees uphill, ~150 feet long
- Wall completed in Summer 2017
- Area 2 wall beginning late 2017

Riverside Drive Landslide & Wall Monitoring

Cincinnati, Ohio

Instrumentation System

- Inclinometers
  - In Slope
  - In Wall
- Piezometers
- Strain Gages
  - On Water Mains
  - On Retaining Wall
- Load Cells
  - Tiebacks
- Mix of Manual Readings & Dataloggers

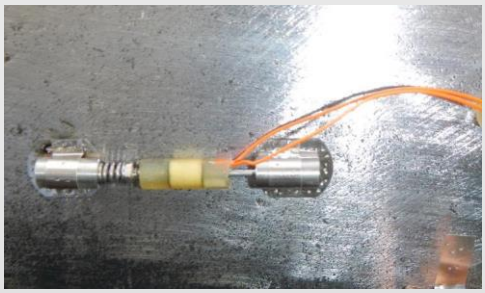

Water Main Strain Gages

- Geokon 4150 VW Strain Gages
- 3 per Water Main Section (90° Apart)
- 3 Sections Instrumented
- Gages were spot welded and epoxied to cast iron water main

- Saw trend of increasing load on mains but traffic and construction noise reduced effectiveness of some gages

Riverside Drive Landslide & Wall Monitoring

Cincinnati, Ohio

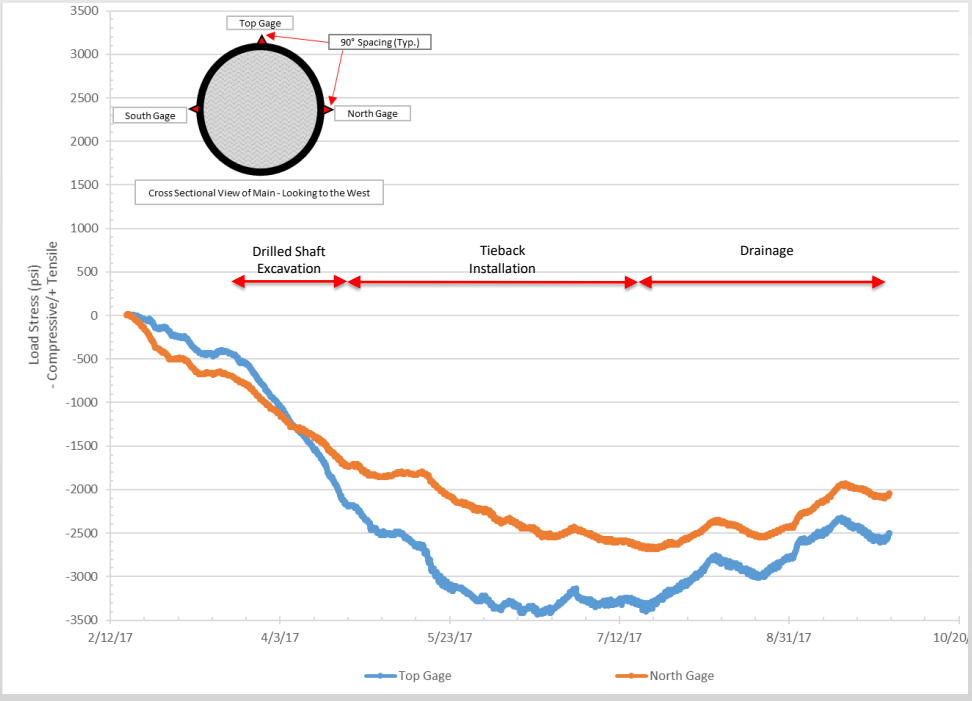

Riverside Drive Landslide & Wall Monitoring

Cincinnati, Ohio

Terracon

Riverside Drive Landslide & Wall Monitoring

Cincinnati, Ohio

Piezometers

- Installed 9 Vibrating Wire Piezometers
- Geokon 4500S VW Piezometers
- Installed alone or with inclinometers
- Piezometers were direct grouted
- Data collected with VW dataloggers or manual readings

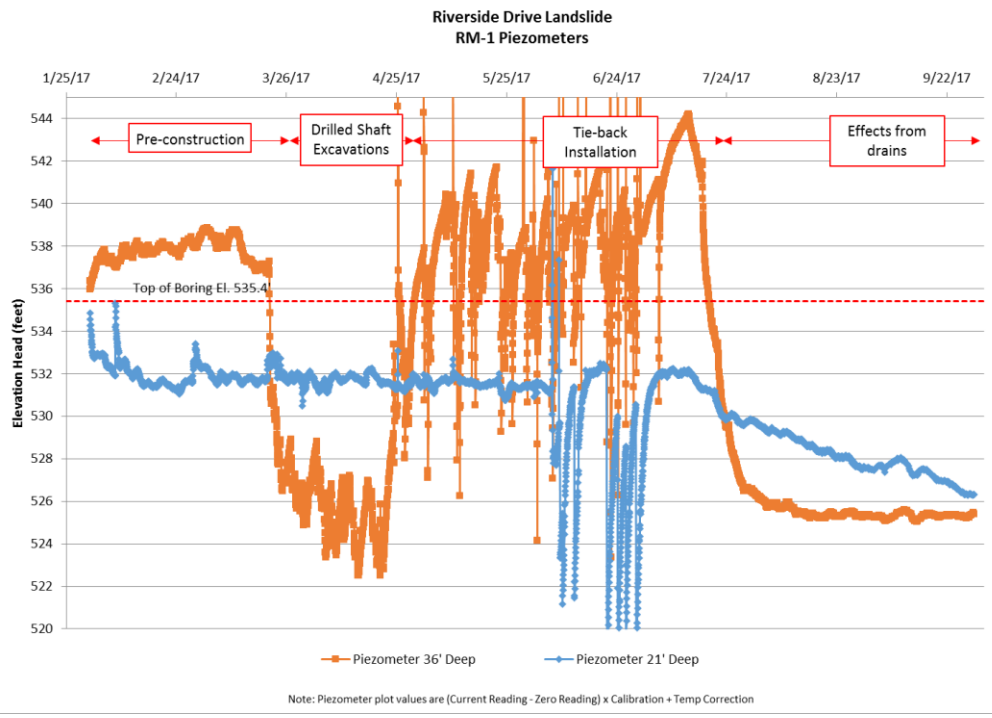

Riverside Drive Landslide & Wall Monitoring

Cincinnati, Ohio

Riverside Drive Landslide & Wall Monitoring

Cincinnati, Ohio

Retaining Wall Instrumentation

- 10 Geokon Model 4000 VW Strain Gages Per Beam @ 2 Locations
- Gages Installed on Flange in Pairs
- Inclinometer Casing Attached to Beam in 6 Locations
- Geokon Model 4900 VW Load Cell Installed on Tiebacks @ 2 Locations
- All gages connected to vibrating wire datalogger mounted to wall
- Monitoring began before installation to measure effects of construction activities and will continue well into future
- Terracon Instrumentation Engineer w/ assistance from Goettle personnel installed instrumentation

Riverside Drive Landslide & Wall Monitoring

Cincinnati, Ohio

Riverside Drive Landslide & Wall Monitoring

Cincinnati, Ohio

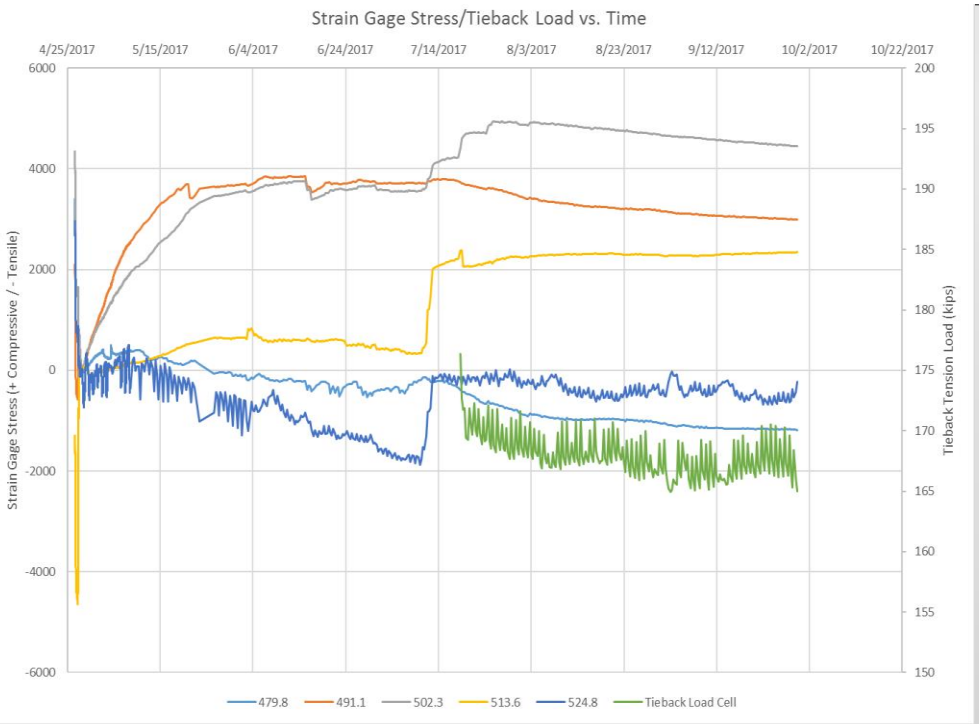

Riverside Drive Landslide & Wall Monitoring

Cincinnati, Ohio

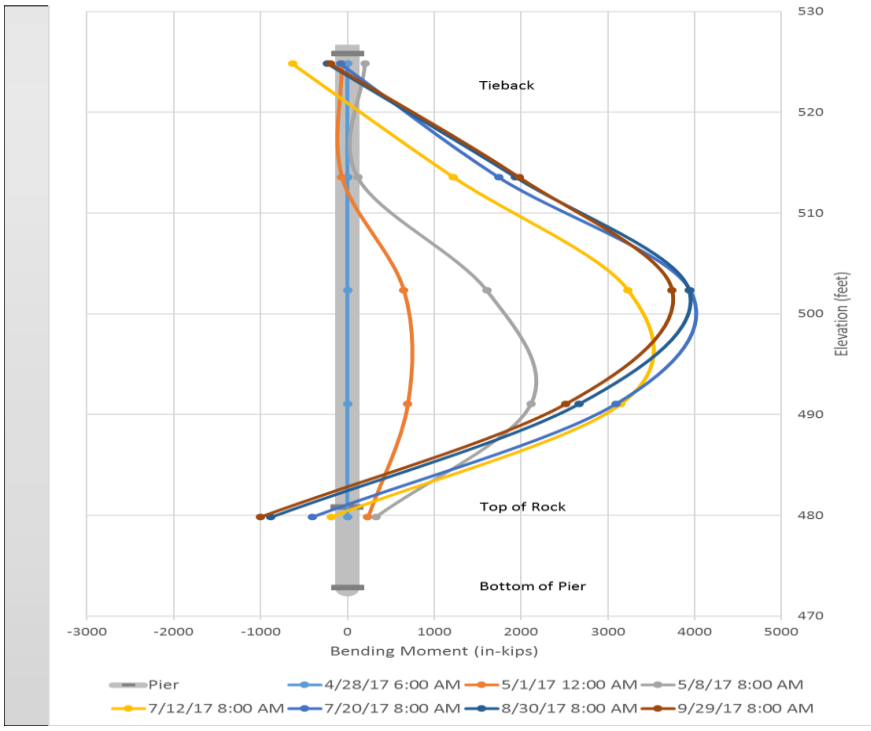

Riverside Drive Landslide & Wall Monitoring

Cincinnati, Ohio

Riverside Drive Landslide & Wall Monitoring

Cincinnati, Ohio

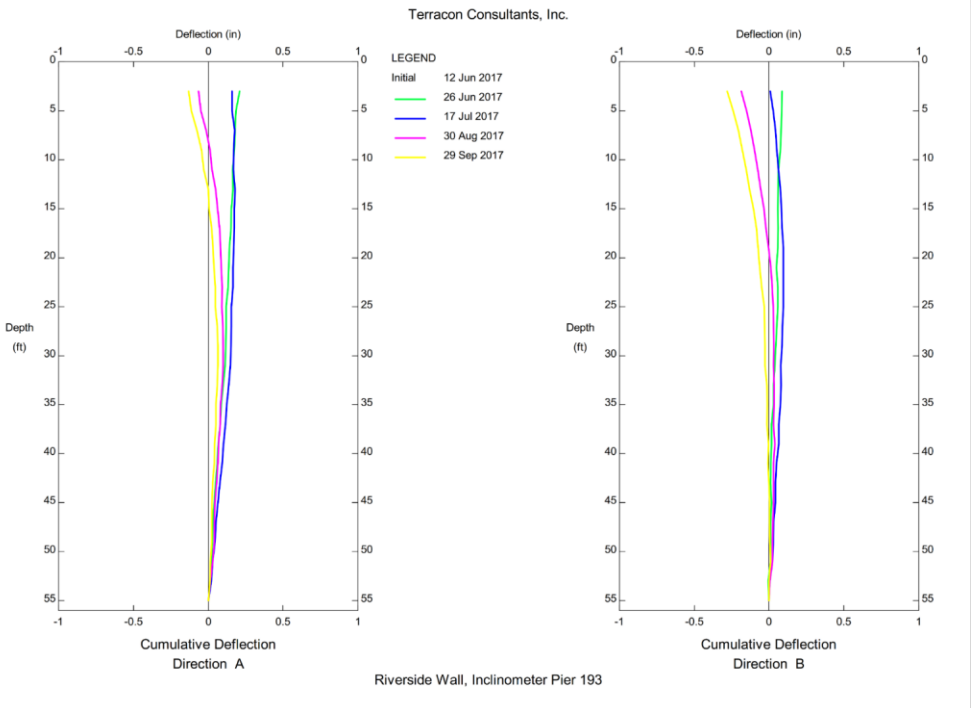

McCook Reservoir

Chicago, Illinois

Highlights:

- Located between I-55, Chicago Sanitary & Ship Canal, and Des Plaines River
- Approx. 1.1 mile long, 300 feet deep, 500-900 feet wide
- 10 billion gallon combined sewer overflow storage
- Construction to be completed in 2029
  - Stage 1 in 2017
- Limestone currently being quarried
- Metropolitan Water Reclamation District of Greater Chicago (MWRDGC) is the local sponsor and will own and operate the reservoir when construction is completed
- USACE overseeing the construction

Terracon

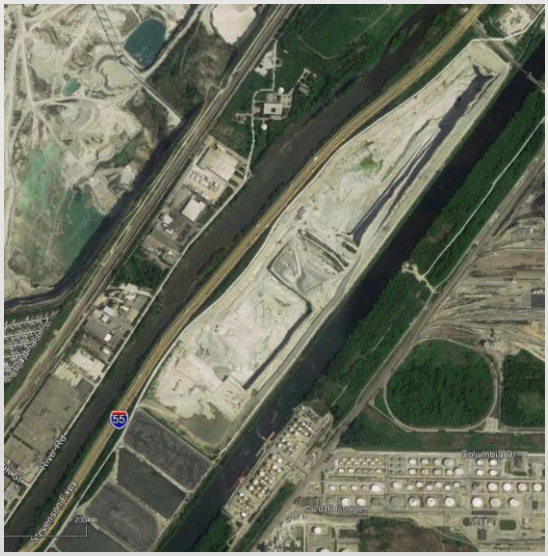

McCook Reservoir

- Construction of reservoir has included cutoff walls, grout curtains, overburden slopes, retaining walls, soil nails, rock wall stability, and an extensive instrumentation system
- Terracon partnered with TTL Associates in 2014 to consolidate, upgrade, adjust, and make additions to the existing instrumentation system for the USACE. Work is ongoing.
- System currently consists of 143 sensors located in 17 locations around this phase of the project.

Terracon

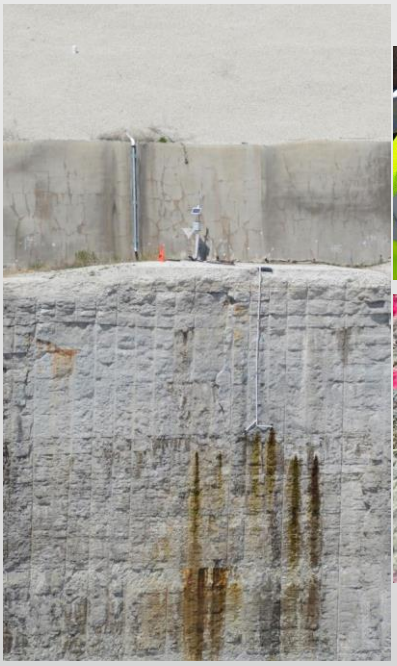

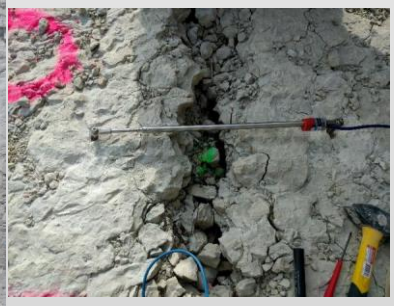

McCook Reservoir

- Sensors include:
  - VW Piezometers
  - VW In-Place Inclinometers
  - VW Extensometers
    - Single & Multi-Point
  - Time Domain Reflectometry (TDR)
  - VW Crackmeters
  - Webcams
  - Weather Station
- Wireless Data Acquisition System
  - Dataloggers communicate wirelessly with base station.
  - Base station has modem and transmits data to server setup by Canary Systems
  - Data shared on website.
- Downhole Video/Gamma Logging on New Boreholes

Terracon

McCook Reservoir

- Adjusting In-Place Inclinometer Spacing
  - Inclinometer strings are 200'+long
  - Manual readings of full 300'+ casing taken during removal
- Installation of one new inclinometer ~270 feet deep & one new piezometer string about ~270 feet deep
- Repairs & Improvements to the Extensometers
- Installation of Crackmeters
- Upgrades to dataloggers/server (by Canary Systems)
- Improvements to instrumentation protection & wiring

Terracon

McCook Reservoir

Terracon

McCook Reservoir

Terracon

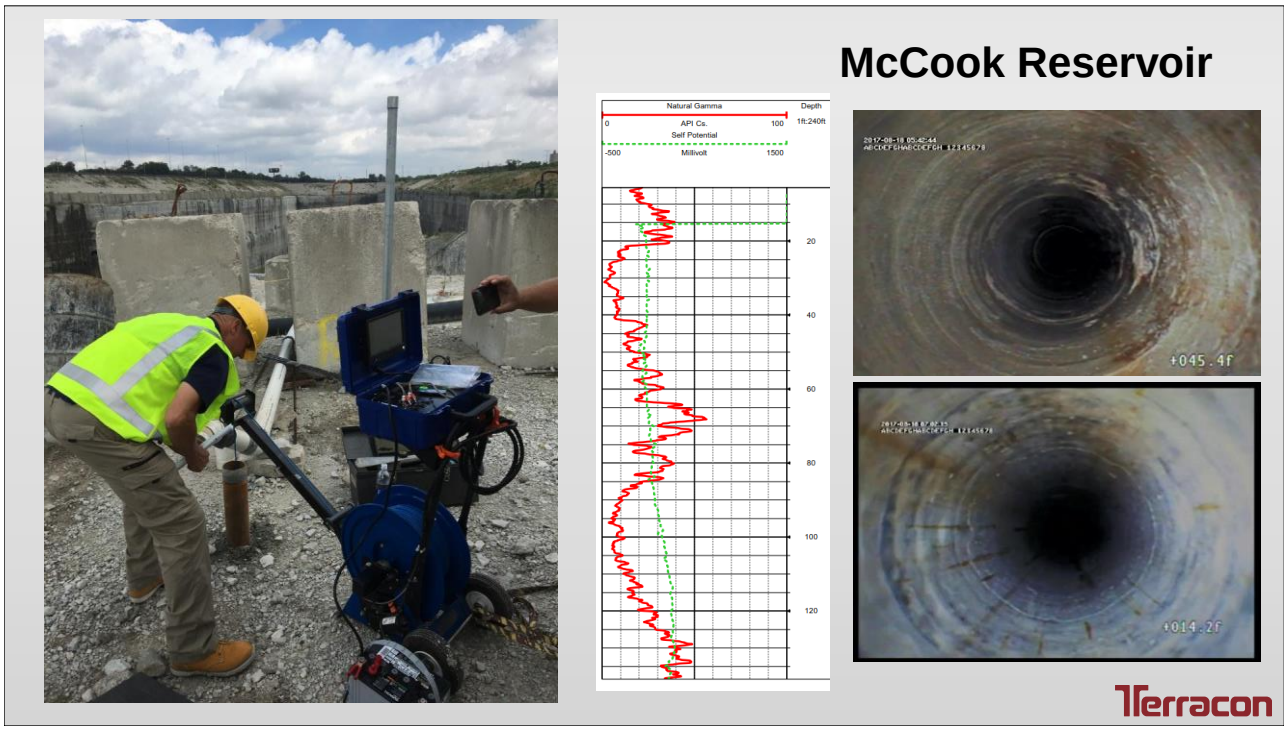
McCook Reservoir
Natural Gamma
Depth
0
API Cs.
100
1ft:240ft
Self Potential
-500
Millivolt
1500
20
40
60
80
100
120
+045.4f
+014.2f
Terracon


CANARY
McCook Automated Data Acquisition System (ADAS)
CANARY
Terracon

Thanks To:

- GCWW & City of Cincinnati
- Goettle Construction
- USACE
- TTL
- George Webb, Russ Gatermann & Everyone From Terracon That Helped On These Projects

Terracon

NOTES

NOTES

NOTES

Case Study – USACE Low Mobility Grout, Full Depth Reclamation, and Roller Compacted Concrete at Fort Campbell, KY

Steven W. Shifflett, P.E.[1]

Abstract: Development in the early part of the 21st century has unique challenges as the best sites have often already been developed. Fort Campbell, a military installation located outside of Hopkinsville, KY along the TN/KY state line is not immune from this issue. This Case Study will summarize the Geotechnical Investigation and summarize the design, coordination, construction and lesson's learned associated with large cuts and fills, Mechanically Stabilized Earth (MSE) and cantilever retaining wall construction, Full Depth Reclamation (FDR), asphalt stabilized base courses, Roller Compacted Concrete (RCC), and low mobility grouting to support shallow foundations in karst geology.

The chosen site consisted of 27 acres split into two nearly adjacent sites. The northern facility (106th TEMF) consisted of 12 acres occupying a previously developed area with heavy duty asphalt pavements and the southernmost facility (101st TEMF) was 15 acres scheduled for development on a wooded hillside in a highly karstic area. Due to this unique combination the site was passed over for other developments and was characterized as one of the "Three Worst Sites" at Fort Campbell. The project required the construction of two – 27,000 square foot maintenance facilities on shallow foundations along with storage and support facilities including heavy duty hardstand pavements, utility upgrades, and improved site access.

During the geotechnical investigation a 6 foot air/water filled void was encountered under the footprint of the 101st TEMF at a shallow depth within the potential zone of influence of the facility. Additional investigations followed including the use of geophysics to further evaluate the risks posed from karst on site. Relocating the facility was not feasible due to the turning radii required for the vehicles. Abandoning the site would have limited the effectiveness of the facility for the 101st Airborne and resulted in severe operational delays and cost overruns. A low mobility grouting program was designed and executed to support the project and to eliminate the need for deep foundations. The grouting program included over 231 grout injections at a cost of approximately $225,000 per facility. The grouting program was unique in that it was exploratory in nature specifically targeting areas below the shallow footings within the zone of influence of the structure for treatment. This allowed the weathered karst bedrock to be mapped and for treatment of potential low stress zones.

[1] Acting Chief, Geotechnical Design & Levee Safety U.S. Army Corps of Engineers - Louisville District, Louisville, Kentucky. Email: Steven.W.Shifflett@usace.army.mil

The 101st TEMF would require approximately 10 feet of cut and 21 feet of fill at the lowest point which required construction of 3 retaining walls utilizing a Mechanically Stabilized Earth (MSE) wall system in conjunction with earthen slopes and a gravity T-wall along the northern perimeter. The 106th TEMF was nearly at grade and utilized full depth reclamation to recycle the asphalt on site as part of a chemical stabilized subgrade. Due to the large surface area of the project and the severe traffic loadings anticipated the use of Roller Compacted Concrete (RCC) was recommended to save costs.The use of instrumentation and geo-structural monitoring to monitor geohazards, improve earthwork schedules, and, improve foundation efficiency continues to gain momentum and usage. This presentation will review several geotechnical instrumentation infrastructure projects and the unique equipment used and challenges encountered on each project. Projects encompassing landslides, reservoirs, and pipelines will be introduced with an emphasis on the technologies utilized. Projects include the Riverside Drive Landslide and Wall which included strain gages, inclinometers, load cells, and piezometers to monitor a large landslide in Cincinnati, Ohio. The next project shared will be a large scale instrumentation system, including bedrock joint/fracture monitoring at the McCook Reservoir project in Chicago. The application of geotechnical instrumentation continues to evolve at an increasing pace. Such applications will improve geo-structural design, accelerate construction schedules, and afford designers, owners, and contractor's the data needed so projects can be completed efficiently and safely.

CASE STUDY - USACE LOW MOBILITY GROUT, FDR, AND RCC AT FORT CAMPBELL

ORVSS XLVIII
Steven W. Shifflett, P.E.
Chief, Geotechnical Design and Levee Safety Section
USACE Louisville District
November 2017

US Army Corps of Engineers
Louisville District

Standard Disclaimer

THE VIEWS EXPRESSED IN THIS PRESENTATION ARE SPECIFIC TO THE PRESENTER AND THE STUDY AREAS EXAMINED. VIEWS EXPRESSED DO NOT CONSTITUTE FORMAL POLICY DIRECTIVES, RECOMMENDATIONS, OR ENDORSEMENTS BY THE USACE LOUISVILLE DISTRICT.

PRESENTATION OUTLINE

- Vehicle Sustainment Brigade Complex Site Characterization
- Low Mobility Grouting (LMG)
- Subgrade Stabilization – Full Depth Reclamation (FDR) and Lime Stabilization
- Roller Compacted Concrete (RCC)

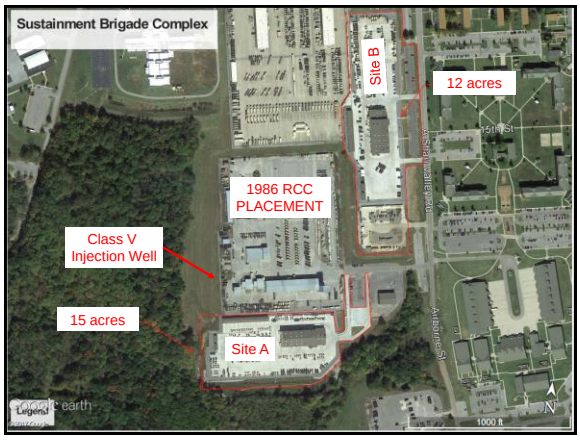

Vehicle Sustainment Brigade Complex TEMFs

- Two TEMF sites were designed and developed on one contract to support the 101st Airborne Transportation Brigade. Each TEMF would be 30,000 sf with unit support structures.
- The project included developing a 15 acre undeveloped hill side (Site A) and an existing 12 acre parking lot (Site B).
- Site A required 8 feet of cut and up to 20 feet of fill and multiple retaining walls.
- The TEMF's were identified to support heavy military equipment with gross weights ranging in excess of 130-200 kips.
- Both sites were designed for subgrade stabilization, stabilized drainage layers, and RCC pavement.

Geology

- The project site is located in the Mississippian Plateau
- Underlain by the Ste. Genevieve and St. Louis Limestones of the Slade Formation.
- Regional geomorphology – High Karst Potential. Mammoth Cave 100 miles to the northeast.
- Proximal sites to the north, west, and south have a documented history of sinkhole development.

Karst Maps (USGS)

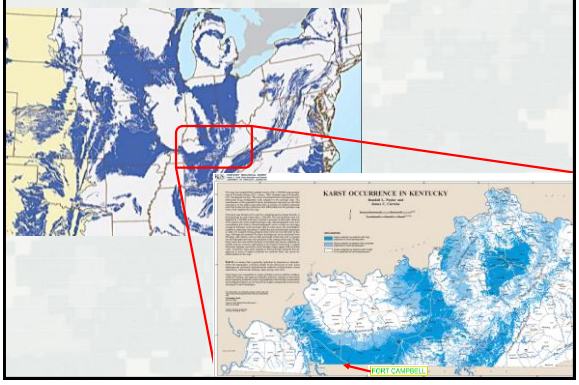

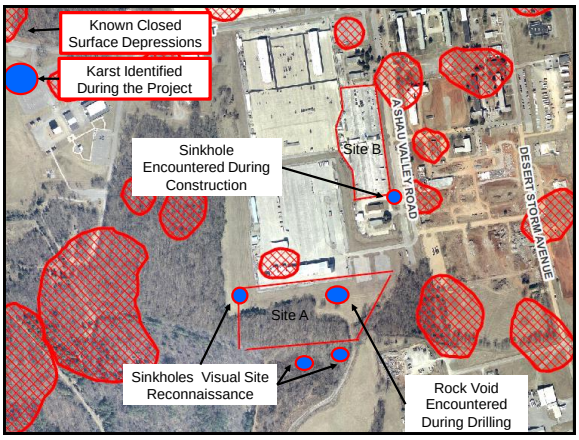

Site Layout, BLP, and Topo Site A

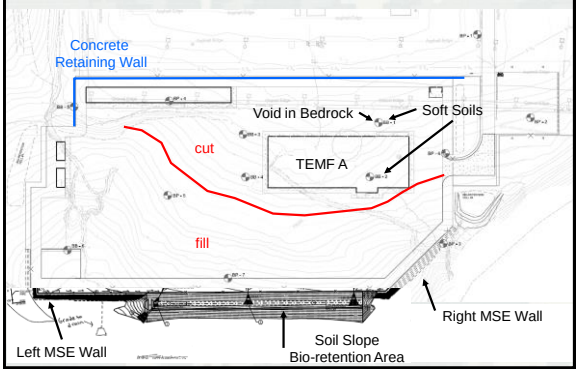

Geotechnical Field Investigation

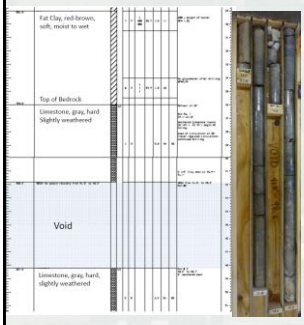

Building Boring Comparison SPT N-Values

Depth, ft	BB-1	BB-2	BB-3	BB-4
0-1.5	15	36	10	9
1.5-3	31	39	17	14
4-5.5		24	23	27
9-10.5	16	14	16	21
14-15.5	15	9	18	18
19-20.5	8	2		
24-25.5	4	1		
29-30.5	0	2		
34-35.5	2			

BB-1 and BB-3 were to have the upper 10 feet of soil stripped

Electrical Resistivity Imaging

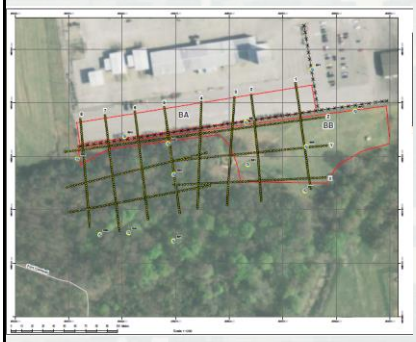

- AGI Super Sting R8 IP system.
- 11 traverses totaling 4,000 linear feet
- Void not detected, but additional zones of weathered bedrock were identified
- The test results were consistent with potential karst geology but did not provide conclusive evidence

Electrical Resistivity Imaging

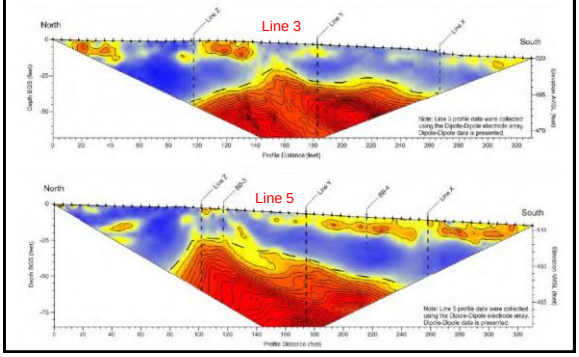

Rock Pinnacles Encountered West of the Building

Site Development

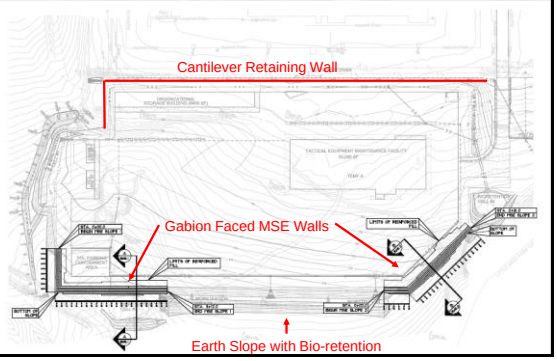

MSE Wall Design

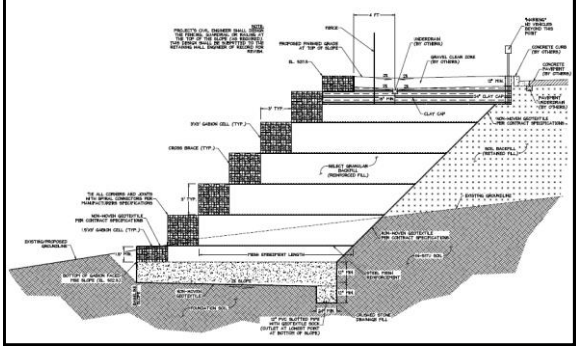

Site Development

Soil Excavation for MSE Walls

Final Gabion Faced MSE Retaining Walls

Why Low Mobility Grouting???

- Could not relocate site or building
- Karst features were confirmed on site in the structural zone of influence for the facility.
- Very soft soils present above the top of rock with up to 10 feet of soil to be cut based on grading plan.

Objectives of the Low Mobility Grouting Program

1. Allow pre-construction improvements rather then post construction remediation
2. Three low mobility grout injections were advanced below each footing to identify top of rock elevations and to evaluate the risk from the epikarst on site
3. Cap any potential karst defects at the bedrock contact beneath structural areas of the building
4. Use low mobility grouting to strengthen very soft soils in structural areas – Shallow foundations; reduce settlement

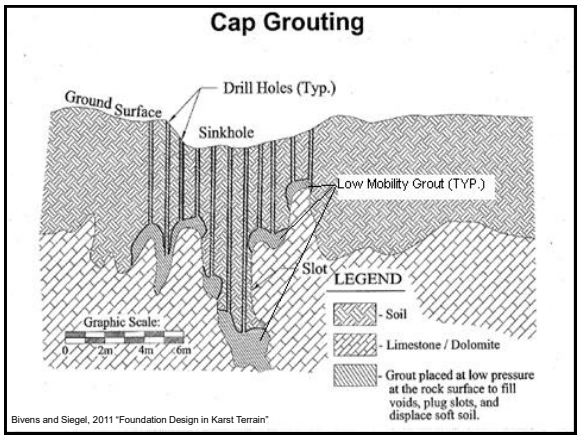

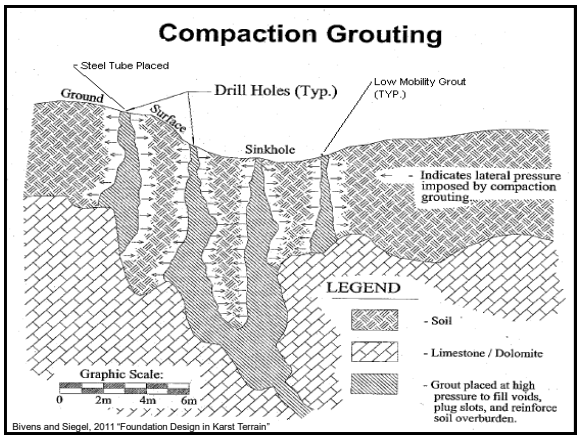

Grout Mix

- Proprietary Mix used by the Contractor Hayward Baker
- Sanded Cementitious grout
- W/C ratio 0.3-0.4 with up to 80% fly ash
- with a target slump of 4 inches
- 7 day strength of 1,000 psi/28 days 1800psi

Equipment

- The RTG-16 Rig advances casing into the ground
- 4" hose fed grout by a portable grout pump.

- Line pressure and volume continuously monitored.

Grouting Termination Criteria

- Grout Injection shall continue within each 2 feet zones beneath the injection pipe until one or more of the following occurs:

1. A maximum volume of **25 cubic feet** of grout is injected immediately above the bedrock surface **for cap grouting.**
2. A maximum volume of **10 cubic feet of grout/foot** is injected **from bedrock up to 15 feet below the ground surface, and 2.5 cubic feet of grout/foot is injected between 15 feet and 5 feet below the ground.**
3. Grout Injections terminate when the volume limits above are exceeded or the flow rate results in pressures in excess of 400 psi.
4. Movement of the ground surface is detected.
5. The final 10 feet of grout shall be placed by gravity without excess pressure.

Sample Grout Log

DEPTH (FT)		TIME		MAX GAUGE	MAX HEADER	GROUT QUANTITY		COMMENTS
TOP	BOTTOM	START	STOP	PRESSURE (PSI)	PRESSURE (PSI)	STROKES	CF	
33	34	4:13:02 PM	4:13:10 PM	200	50	40	25.2	Max Qty
31	33	4:13:10 PM	4:14:42 PM	200	50	48	30.24	Max Qty
29	31	4:14:42 PM	4:16:47 PM	200	50	32	20.16	Max Qty
27	29	4:16:47 PM	4:18:19 PM	200	50	32	20.16	Max Qty
25	27	4:18:19 PM	4:20:19 PM	200	50	32	20.16	Max Qty
23	25	4:20:19 PM	4:22:32 PM	200	50	32	20.16	Max Qty
21	23	4:22:32 PM	4:24:13 PM	200	50	32	20.16	Max Qty
19	21	4:24:14 PM	5:06:21 PM	200	50	32	20.16	Max Qty
17	19	5:06:21 PM	5:09:20 PM	250	50	32	20.16	Max Qty
15	17	5:09:20 PM	5:10:22 PM	400	50	7	4.41	Max Psi
13	15	5:10:22 PM	5:11:00 PM	310	50	1	0.63	Max Psi
11	13	5:11:00 PM	5:11:29 PM	350	50	1	0.63	Max Psi
9	11	5:11:29 PM	5:12:10 PM	350	50	1	0.63	Max Psi
0	9	5:12:10 PM	5:13:44 PM	350	50	3	1.89	Pump and Pull
					TOTALS	325	204.75	
							7.58 cy	

Low Mobility Grouting in clay soils provide consolidation as an injected grout bulb exerts forces in 3-D.

Big Picture Considerations: flow rate, pressure at the depth of injection, soil type and injected volume

Pressure/Elevation Plan View

Includes injection location, top of rock elevation, cap grouting pressure, grout column pressure just above cap grouting.

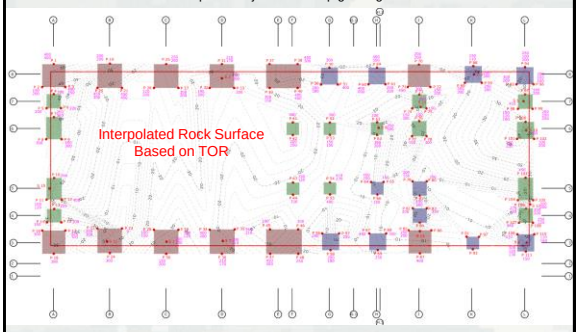

Top of Rock Profile Based on Grouting and Rock Probe Surveys

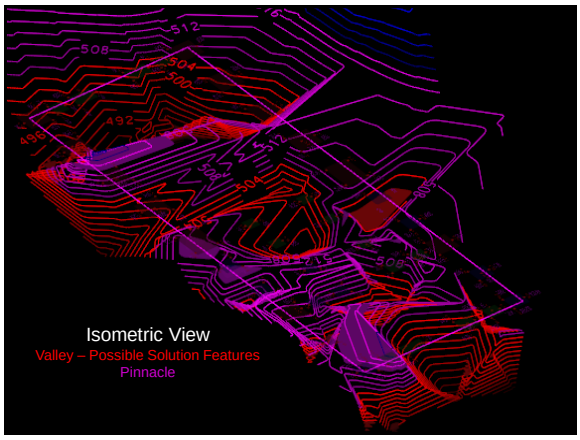

Results Summary

- 216 original grout injection points requiring 5,776 lf of casing
- Low Mobility Cap Grouting = 81 cubic yards TEMF A only
- Low Mobility Grouting = 1,025 cubic yards (377 TEMFA and 648 TEMF B)
- 15 tertiary holes were required as shown in the following figure.
- Total cost was approximately $450,000

SPT and Borehole Locations

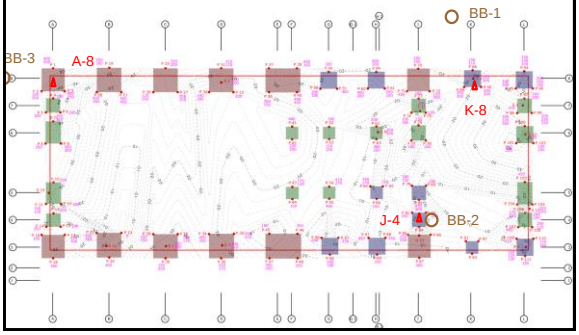

SPT Verification

Depth, ft	BB-1	K-8	BB-2	J-4	BB-3	A-8
0-1.5	15	stripped	36	stripped	10	stripped
1.5-3	31	stripped	39	36	17	stripped
4-5.5		stripped	24	40	23	stripped
9-10.5	16	11	14	38	16	34
14-15.5	15	12	9	30	18	46
19-20.5	8	23	2	32		47
24-25.5	4	29	1	28		53
29-30.5	0	23	2	35		48
34-35.5	2	27				45
39-40.5		39				43

A-8 and K-8 had 8 feet of material stripped off prior to drilling

Hydrofracture Risk

1. Uncontrolled grouting at excessive pressures results in hydrofracture, wasted grout, and can change the groundwater flow regime.
2. A calculated hydrofracture pressure is an ultra conservative number based on soil assumptions.
   - Neglects pump efficiency, head loss, viscosity, density, etc.

$Pf = \sigma_3 + qu$ *Mori and Tamura, 1987

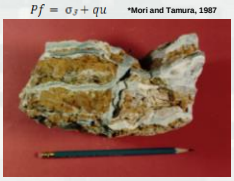

Photo courtesy of Patoka Lake Spillway Grouting, USACE

Chang & Huang 2016 method

$P_f = K_p \sigma_h' + 2c' K_p^{0.5} + u$

where $K_p = \tan^2(45° + \frac{\phi'}{2}) + 3$

c' = effective cohesion (assume = 0

Since $P_f > P_{op}$, soil does not fracture

Lesson's Learned for Pre-Treatment of Karst Bedrock

- Use CPT's or Air Track Rigs to delineate variations in rock topography.
- Utilize the ASCE Compaction Grouting Consensus Guide.
- Geologic conditions at the site should dictate theoretical volume cutoffs, flow rate, and grouting pressures.

FULL DEPTH RECLAMATION (FDR)

FDR is a technique that pulverizes and mixes the full flexible pavement section and a portion of the underlying subgrade to blend the material into a stabilized subbase suitable for compaction and chemical stabilization.

Why FDR???

Design efforts were mandated by Fort Campbell to recycle waste pavements on site (LEED)

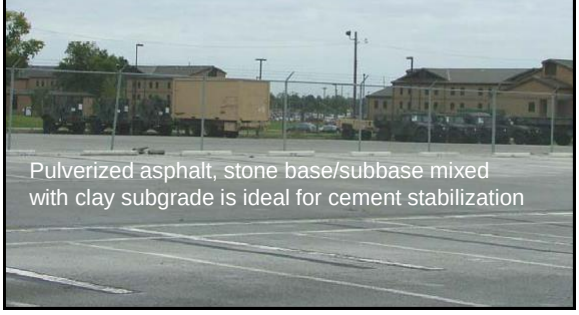

Pulverized asphalt, stone base/subbase mixed with clay subgrade is ideal for cement stabilization

FDR Construction Process

Pulverize, Shape, Add Cement, Mix in Place, Compact, and Surface

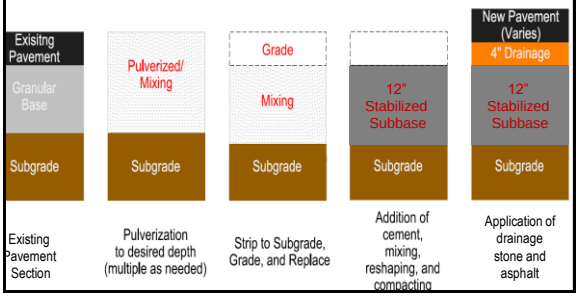

Inside a Reclaimer

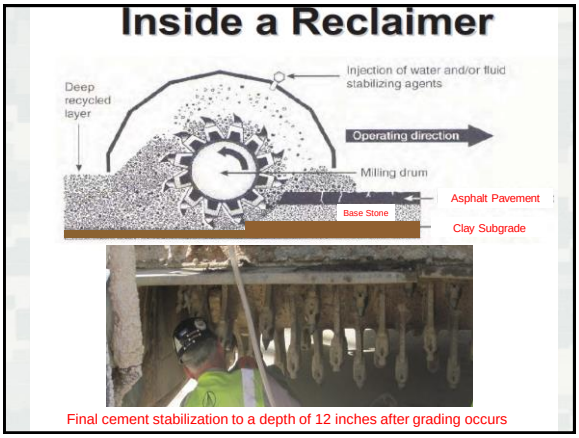

Final cement stabilization to a depth of 12 inches after grading occurs

FDR CONSTRUCTION PROCESS

1. Pulverize and Mixing
2. Shape and Grade
3. Application/mixing of Cement
4. Compaction
5. Finishing
6. Curing and Protection

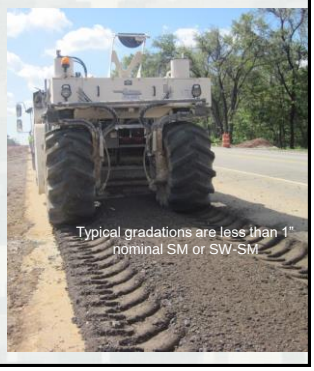

FDR Gradation

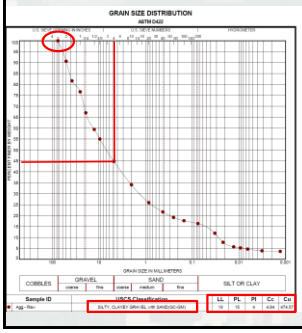

What is a Coarse Soil-Cement Gradation

- Coarse gradations consist of pulverized material that classify as gravels instead of sands per the USCS.
- ASTM D558, the mix design procedure, scalps out all aggregates greater than ¾" and the material is mostly sand and silt.
- An accepted mix design procedure does not exist for 3" minus gravel gradations.

BUILDING STRONG®

Coarse Soil-Cement Mix Designs

- Use the ASTM D558 procedure and design the cement dosage based on the scalped gradation.
- PCA recommends adding additional cement to compensate for the larger aggregate – But how much???
- More cement is not always better and can actually decrease strength and durability.
- Coarse soil-cement mixtures should be designed based on durability rather than strength (ASTM D559 and ASTM D560).
- **PCA has identified coarse soil cement as an area for future research as there is a general "lack of long term field performance information".**

BUILDING STRONG®

PCA Research

PCA Research (Provided by Wayne Adaska, PCA)

(45 to 60 % plus No.4 material)

AVERAGE CEMENT REQUIREMENT FOR DURABILITY – 6.3 % by wt.

AVERAGE CEMENT CONTENT FOR STRENGTH – of 650 psi at 7 days - 3.8 % by wt.

Average freeze-thaw results:

Durability of Soil Cement Mixtures Optimized for Strength

weight loss ——— 74 %

condition of specimens - poor

Mix Design Soil Compaction Method

Summary of Laboratory Results

Sheet 1 of 1

SAMPLE ID	Depth	USCS Classification and Soil Description	Compressive Strength (psi)	Liquid Limit	Plastic Limit	Plasticity Index	% <#200 Sieve	% Gravel	% Sand	% Silt	% Clay	Water Content (%)	Dry Density (pcf)
Agg - 5%	0												
Agg - 5%-1	0	Silty Clayey Gravel with Sand	458									8.3	129.6
Agg - 5%-2	0	Silty Clayey Gravel with Sand	502									8.3	129.6
Agg - 5%-3	0	Silty Clayey Gravel with Sand	420									8.3	129.6
Agg - 6%	0												
Agg - 6%-1	0	Silty Clayey Gravel with Sand	616									9.1	128.8
Agg - 6%-2	0	Silty Clayey Gravel with Sand	641									9.1	128.8
Agg - 6%-3	0	Silty Clayey Gravel with Sand	549									9.1	128.8
Agg - 7%	0												
Agg - 7%-1	0	Silty Clayey Gravel with Sand	513									10.6	127.5
Agg - 7%-2	0	Silty Clayey Gravel with Sand	572									10.6	127.5
Agg - 7%-3	0	Silty Clayey Gravel with Sand	477									10.6	127.5
Agg - Rav	0	SILTY, CLAYEY GRAVEL with SAND(GC-GM)		19	15	4	16.3	55.2	28.4	12.0	4.4	4.3	

JMF approved at 6.5% cement based on JMF and PCA Data.

FDR at TEMF B

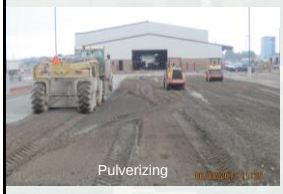
Pulverizing


Addition of Cement

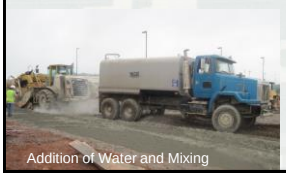
Addition of Water and Mixing

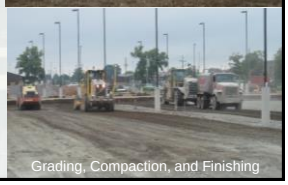
Grading, Compaction, and Finishing

Lesson's Learned from FDR

- Strength is not the primary design factor in coarse soil-cement mix designs.
- Design for durability (ASTM D560).
- Standard Density vs. Modified Density
- ASTM D558 is the approved mix design procedure. Correlations to ASTM D1557 are not accurate.

ROLLER COMPACTED CONCRETE (RCC) CONSTRUCTION

What is Roller Compacted Concrete (RCC) ???

RCC Pavement is a dense combination of multiple coarse/fine aggregates, cement, and water

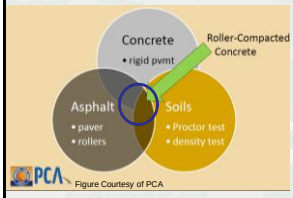

- No Slump concrete (consistency of DGA or FDR)
- Mix proportions per the Soil Compaction Method
- Placed by high density asphalt pavers
- Consolidated with vibratory rollers
- No forms or finishing – Similar to slip forming PCC
- No reinforcing steel – Aggregate Interlock
- Early load carrying capacity

RCC combines various production elements of PCC, Asphalt and soils

How Does RCC Work????

Conventional PCC Placement

- Continuous and Batch Type Mixers
- Proportioned as a Lean Concrete
- Similar Curing Requirements
- Similar Strength Testing Requirements

Conventional HMA Placement

- Similar Aggregate Gradations
- High Density Asphalt Paver
- Vibratory and Static Rolling
- Density checked per ASTM D6368

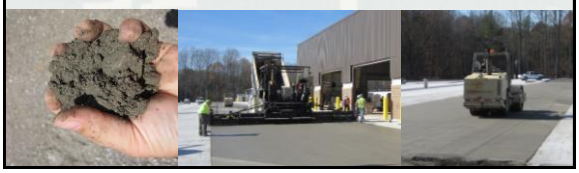

Why Use RCC at Fort Campbell???

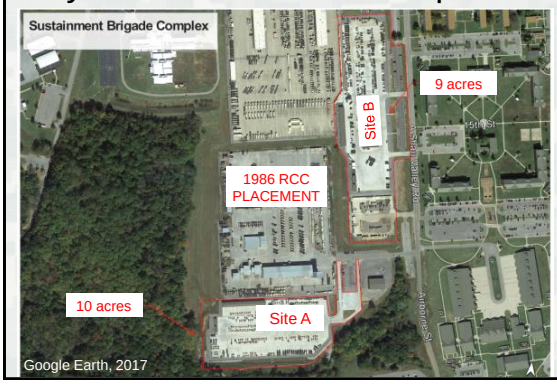

Design Traffic Loading

M1074 PLS with Trailer
- Gross weight is 86,300 lbs.
- 140,000 lbs. fully loaded
- Tire Pressure - 103 psi over 83 in^2

M1070 HET Tractor W/M1000 Trailer
- Gross Weight 103,000 lbs.
- 230,000 lbs. fully loaded
- Tire Pressure - 82 psi over 42 in^2

1986 RCC Placement at FTC

- **The pavement is over 30 years old.**
- Spread with bulldozers – Placed with rough surface
- Compacted with rollers
- This site is frequently referenced in publications

USACE RCC DESIGN - REFERENCES

- **Guide for Roller-Compacted Concrete Pavements from the National Concrete Pavement Technology Center 2010**
- Wayne Adaska, Director of Pavements, Portland Cement Association
- IS009 PCA Guide Specification for Construction of RCC Pavement (2004)
- ACI 325-10R-95 Report on RCC Pavements
- Tennessee Ready Mixed Concrete Association (TRMCA)
- Kentucky Ready Mix Concrete Association (KRMCA)
- TDOT Special Provisions Regarding RCC Pavement

Advantages of RCC

Dense, well graded, aggregate blend improves:

- Workability
- Compaction
- Surface finish
- Strength
- Durability
- AAR/ACR resistance
- Abrasion resistant
- Low water permeability
- Reduces segregation

Soil Compaction Method

- Determine the aggregate blend
- Determine the optimum density and moisture content for compaction
- Determine the percentage of cement

How to Determine the Aggregate Grading Limits

Suggested Blend Gradation

Size Number	Percent Passing
1-in (25 mm)	100
3/4-in (19mm)	90-100
1/2-in (12.5 mm)	70-90
3/8-in (9.5 mm)	60-85
No. 4 (4.75 mm)	40-65
No. 16 (1.18 mm)	20-40
No. 100 (150 µm)	6-18
No. 200 (75 µm)	2-8

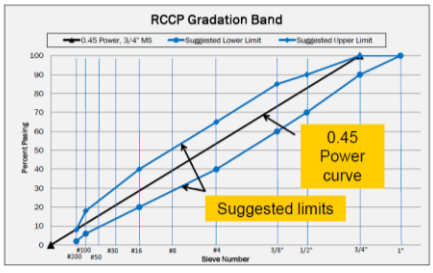

Guide For Roller Compacted Concrete Pavement, 2010

Optimum Moisture, Max Density and Cement Dosage

MIX DESIGN: Coarse Aggregate - 1,600 #, Fine Aggregate – 1,800#, Type I/II Cement – 380#, Fly Ash – 160#

Density – 98% ASTM D1557

Mix No. 1
γ dry max = 146.1 pcf
Opt. w = 6.6%
16% Cementitious
30% Fly Ash

Mix No. 2
γ dry max = 146.3 pcf
Opt. w = 6.8%
17% Cementitious
30% Fly Ash

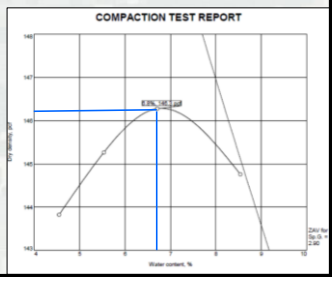

Compressive and Flexural Strengths

Days	7	14	28
Mix No. 1 – Avg. Comp, Strength (psi)	3,270	4,390	5,390
Mix No. 2 – Avg. Comp. Strength (psi)	4,270	4,960	6,010

* There is no ASTM Standard for fabricating RCC Beams. Fabricated beams should be avoided when working with RCC

ASTM C1435

TEMF Lighting and Grounding Rod Plan

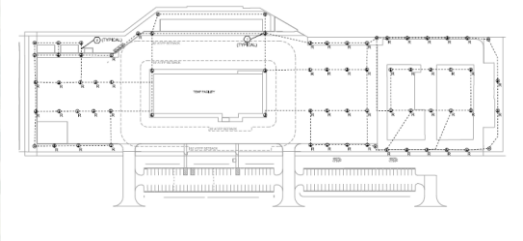

Relocate all lighting to gravel clear zones and utility strips.
Relocate all grounding points to utility strips

Pavement Design

Utility Trench

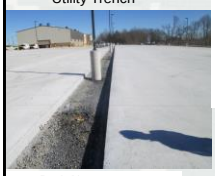

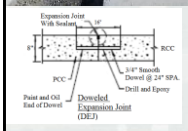

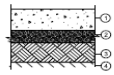

C1 ROLLER COMPACTED CONCRETE PAVEMENT

4" Stabilized Drainage Layer

8" RCC Pavement

Paving Plan For TEMF B

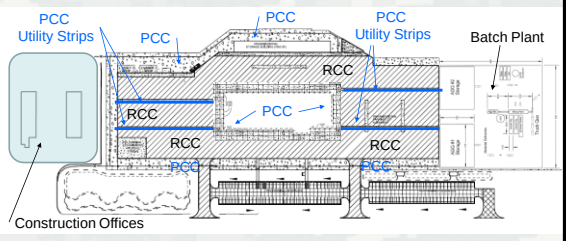

Paving Plan For TEMF A

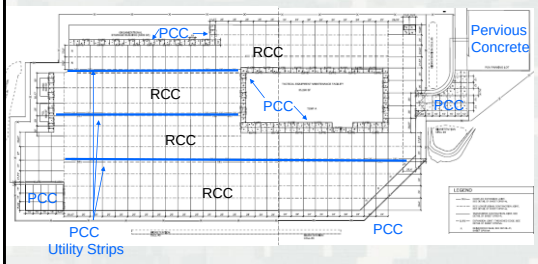

Production and Paving

Rigid and Dense at Placement

Field Density Testing

*Based on 264 Tests in November and December 2013

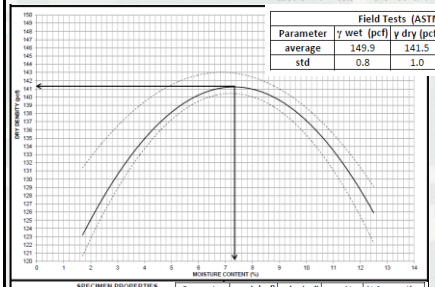

Field Tests (ASTM D6938)				
Parameter	γ wet (pcf)	γ dry (pcf)	w %	% Compaction
average	149.9	141.5	5.9	99.5
std	0.8	1.0	0.3	0.6

SPECIMEN PROPERTIES	
AVG. MAX DRY DENSITY:	141.3 pcf
AVG. OPTIMUM MOISTURE:	7.3%

Parameter	γ wet (pcf)	γ dry (pcf)	w %	% Compaction
average	150.5	140.3	7.3	98
std	1.1	1.1	0.3	0

Rolling Operations



RCC Finished Surface




RCC Joints



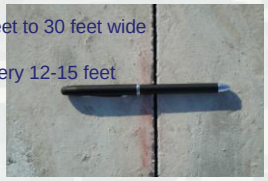

Paving Lanes varied from 12 feet to 30 feet wide

Control joints were sawn every 12-15 feet

RCC Joints

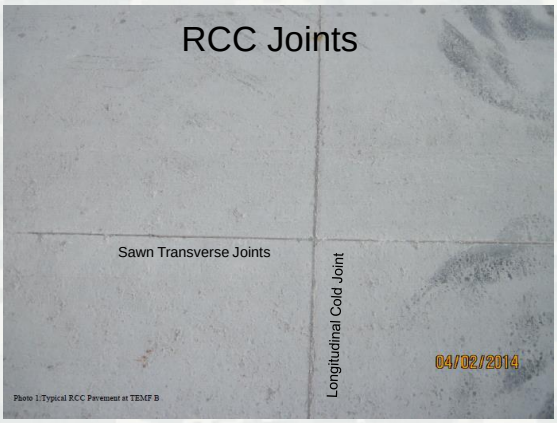

RCC Typical Joints

RCC Header and Over-pave

The beginning and end of production runs are sawn back to the joint line on the paving plan.

Over-pave areas targeted for sawn beams and pavement cores

Saves Production Time

Prevented Patching

Obtaining Cores and Beams

On-Site Laboratory Testing Facility

Results of Laboratory Testing

- Compressive Strength (ASTM C39) Cast Cylinders

  Project Requirement of 4,500 psi @28 days

- Flexural Strength (ASTM C78) of Sawn Beams (ASTM C42)

  Project Requirement of 500 psi @28 days

Compressive Strength Averages (Fabricated Cylinders ASTM C1435)

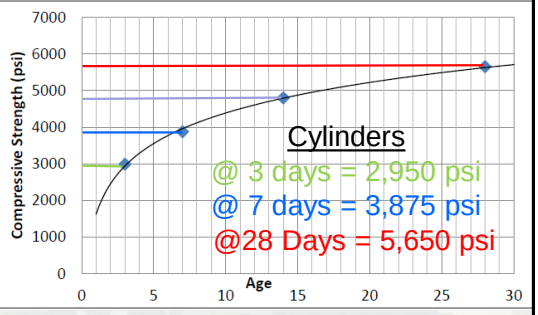

Compressive Strength Plot

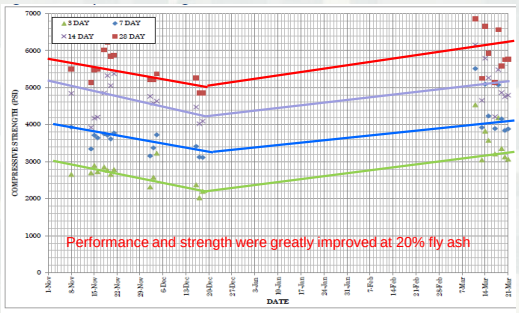

Changed mix from 30% fly ash to 20% fly ash in March 2014

Flexural Strength ASTM C78

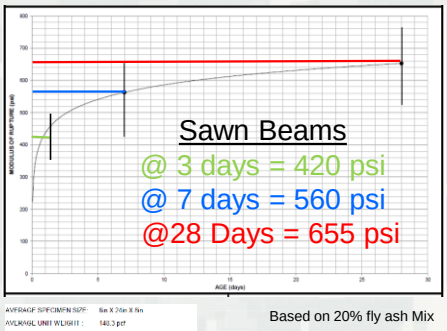

Based on 20% fly ash Mix

Early Load Carrying Capacity of RCC & PCC

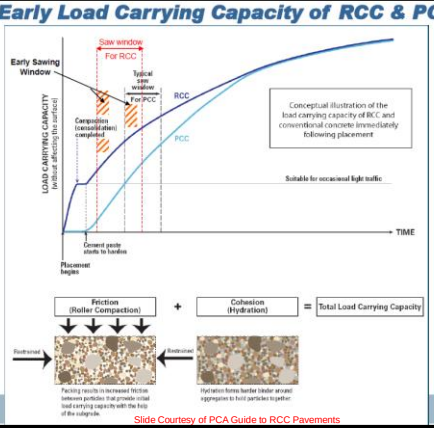

Slide Courtesy of PCA Guide to RCC Pavements

RCC vs PCC

- The results of the Fort Campbell RCC project are in agreement with PCA findings.
- RCC was able to be trafficked in a window of 2 or 3 days depending on ambient air conditions.
- RCC and PCC have similar compressive and flexural strengths at 7 and 28 days.
- Re-tempering RCC is not possible. After it is batched the properties of the mix are difficult to alter.
- RCC ASR resistance – inconclusive.

Fort Campbell ASR is Real!!!

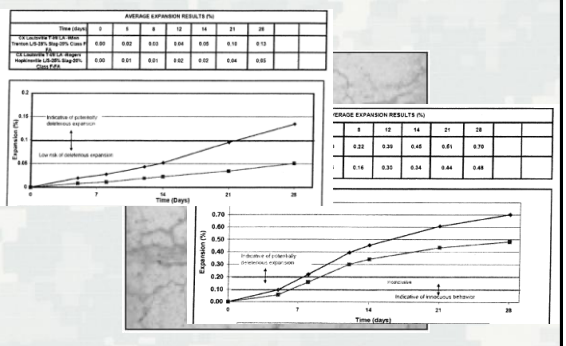

Lesson's Learned From RCC

- Costs for RCC are approximately equal to PCC based on the USACE Specification.
- Consolidate utilities and lighting areas to minimize pavement disruptions.
- Limit fly ash percentages to 20% or less.
- Remove cores and beams from over pave areas for testing.
- RCC has early strength gain which helped accelerate the overall project schedule.

Future Research

- LMG – Better correlate the relationship between grouting theory and hydrofracture.
- FDR - Study the long term performance of coarse graded soil-cement mixtures.
- RCC - Study the long term performance of RCC vs. PCC (aggregates, cement, climate, QC)

Wrap Up

Special Thanks:

- Mike Bivens, Rembco Geotechnical Contractors, inc.
- Wayne Adaska, Director of Pavements, PCA
- Hayward Baker
- Chris Carwie, A.G.Peltz Group, LLC - RCC Construction

References:

ASCE Compaction Grouting Consensus Guide, 2010.

Bivens and Siegel, "Foundation Design in Karst Terrain", 2011.

Chang and Huang, "Ground Response and Grout Distribution by Field Soil Grouting, *Proceedings of the Institution of Civil Engineers - Geotechnical Engineering,* P 35-48, 2016.

Full Depth Recycling with Cement, PCA, 2002

PCA Guide for Roller-Compacted Concrete Pavements, *National Concrete Pavement Technology Center*, 2010.

Mori, Akira & Tamura, Masahito. (1987). Hydrofracturing pressure of cohesive soils. *Soils and Foundations*. 27. 14-22. 10.3208/sandf1972.27.14.

Shifflett, Steven, "Pre-Construction Rock Treatment and Soil Modification Program Using Low Mobility Grout to Mitigate Future Sinkhole Development, *2015 International Sinkhole Conference Proceedings,* 2015.

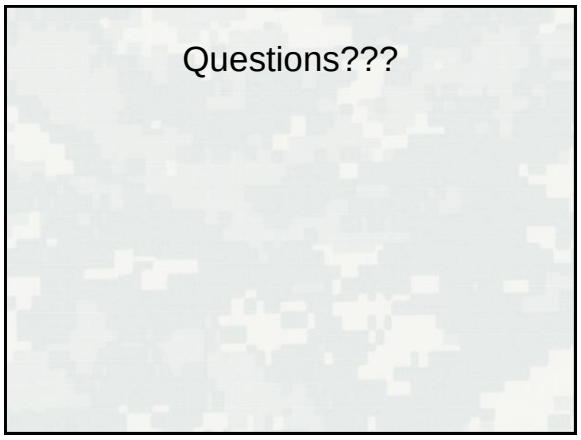
Questions???

INNOVATIVE DESIGN FOR THE MERCHANTS BRIDGE WEST APPROACH RECONSTRUCTION FOR TRRA IN ST. LOUIS, MO

Lyndsie Janbakhsh, P.E.[1], Kevin Kriete, P.E.[1]

[1]HDR, Lexington, KY and St. Louis, MO

ABSTRACT

When faced with unique project restraints, the Merchants Bridge Design Team adapted an innovative approach for the Merchants Bridge West Approach reconstruction of the Terminal Railroad Association (TRRA) track in St. Louis, Missouri. The reconstruction of the Merchants Bridge west approach began in January 2015 and concluded in April 2017.

The project begins at existing Bent W6 which was the western limit of a previous partial reconstruction of the Merchants Bridge over Mississippi River in 2005 and extends westerly to the existing concrete abutments. Due to TRRA's requirement that rail operations be maintained during construction, the existing bridge, consisting of an open deck steel trestle supported on steel frame bents, was designed to be fully encapsulated within the lightweight concrete (LCC) embankment. Conventional MSE wall panels were selected to contain the LCC and auger-cast piles placed underneath the MSE wall panel footings to increase the bearing capacity where it exceeded the allowable bearing capacity of the soil. A reinforced rock mat was used to distribute the load of the embankment to the auger-cast piles to help reduce differential settlement.

The Design Team performed advanced service and seismic load design utilizing finite element numerical analyses as well as other traditional methods. "Hard points" identified within the embankment were analyzed for increased stresses in the LCC fill. Liquefaction potential and seismic design was analyzed using the AREMA Level 1, 2, and 3 earthquake event criteria due to proximity of the New Madrid and Wabash Valley seismic zones.

Additionally, several existing utilities were present under the footprint of the proposed embankment. Utility bridges were proposed to minimize the impacts on the utilities but construction constraints challenged placement and methods of installation. To fully understand the utility "bridge" concept, many methods were considered and analyzed to estimate the settlement of each impacted utility, and the most suitable alternatives were selected.

The design for Merchants Bridge West Approach Reconstruction has the following advantages. (1) Track operations could be maintained throughout construction with minimal closure time. (2) Cellular concrete is lighter and stronger than compacted soil backfill, increasing stability and decreasing settlement impacts. (3) Increased seismic stability due to the embankment behaving like a large block that moves uniformly. (4) Utility bridge solutions work with limited overhead clearance under the existing tracks.

PROJECT OVERVIEW

The TRRA currently operates two bridges crossing the Mississippi River in St. Louis, Missouri. These crossings are critical to efficient railroad operations across the United States. The northern most crossing is officially named the Merchants Memorial Mississippi Rail Bridge and more commonly known as the Merchants Bridge. This project reconstructed the western approach of Merchants Bridge.

The West Approach is located adjacent to Ferry Street in north St. Louis. In 2005 a section of the west approach extending from the Mississippi River main spans to Bent W6 was reconstructed. The original substructure reconstructed as part of this project extends west from Bent W6 to the existing concrete abutments. The project included a double track structure at Bent W6 that continues westerly to a wye, where the structure splits into two legs. One leg continues to the west and currently carries a single operating track. The other leg turns to the south and carries two tracks toward downtown St. Louis. This leg crosses Ferry Street. The project location map is shown in Figure 1.

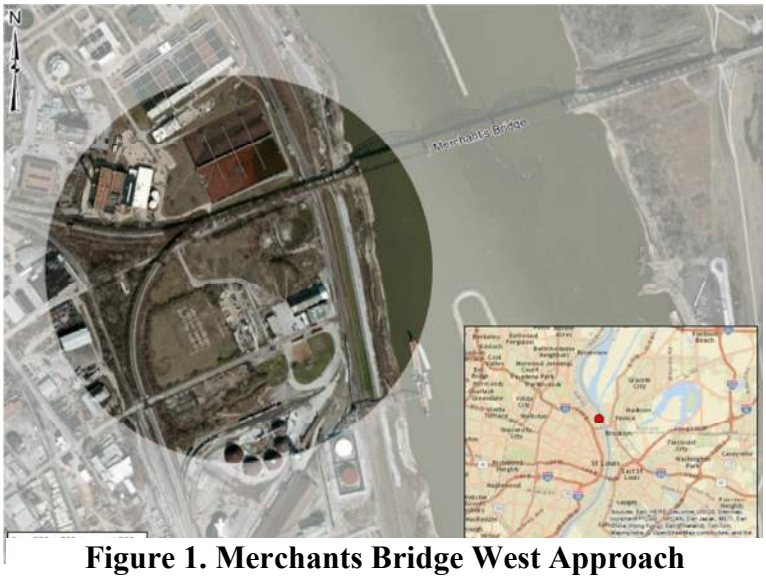

Figure 1. Merchants Bridge West Approach Reconstruction Project Location Map

The existing bridge approach consisted of an open deck trestle structure consisting of built-up steel stringer spans supported on steel towers. Based upon the as-built drawings, the tower legs were supported on 6-foot diameter by 8-foot deep concrete caissons supported on timber piling at the 4 straddle bents closest to the W6 pier. The remaining tower legs for the existing Merchants west approach were supported on cast-in place concrete foundations. The piles are assumed to be founded in the medium dense sands that underlie the 35 to 45 foot thick layer of soft clay fill and fine alluvium.

PROJECT CONSTRAINTS

A number of project constraints required unique solutions to be incorporated into the design. The constraints can be categorized as either operational or physical constraints and are described in further detail in the following sections.

Operational Constraints. Operational constraints are requirements imposed by TRRA in order to maintain operational goals during construction. For this project TRRA required rail traffic to remain fully operational throughout construction. The

only planned closure of the tracks allowed was during the final installation of trackwork.

To find a solution the design team developed a plan to leave the existing substructure in place. An embankment built primarily of lightweight cellular concrete formed between two precast concrete panel walls would be built to encapsulate the existing west approach. Leaving the existing structure intact allowed rail operations to continue without minimizing daily capacity or restricting train loads and eliminated costs and track time delays associated with temporary solutions.

With the permission of TRRA, the design team also limited rail traffic to only the northern most track, closing the southern track for the majority of construction. Closing the south track increased access under and near the track, decreased construction time, and allowed for construction phasing while still leaving rail traffic operational.

Physical Constraints. Physical constraints are imposed by existing physical features on or adjacent to the site that impose limitations or added consideration to the design. The physical constraints for this project include low overhead clearance below the existing structure (see Figure 2) and existing utilities that cross underneath the west approach.

Since the existing structure is to remain intact during construction the design team had to consider how construction equipment could access certain parts of the project site. Cross braces on the existing bents limited access to these areas by any typical construction equipment. Special provisions had to be made to address construction methods such as proof rolling alternatives to ensure the subgrade was adequate where proof rolling was not possible. The team also had to consider these areas in the design. Part of the structure foundation design required auger-cast piles. However, due to the size of the construction equipment, auger-cast piles are not possible in these cross-over areas or in some other low overhead clearance areas. Therefore the design had to include analyses on alternatives to auger-cast piles such as micropiles which allowed access to areas where low overhead clearance was a concern and areas where deep foundation elements would be placed in the center of the embankment, such as between the cross braced bents.

Figure 2. The Existing Merchants Bridge West Approach Substructure to be encapsulated in the new proposed embankment structure.

One of the most challenging constraints this project posed was the utilities on site. This project had numerous water, gas, and sewer pipe lines adjacent to or crossing the proposed embankment. The water company opted to move their lines so that it was not impacted by the new structure. However, the gas and sewer companies

required the design team to minimize impact to the existing lines that would stay in place. Due to height of the embankment and the subsurface soils on site, the anticipated settlement on site ranged from 2 to 7.5 inches with an average of approximately 4.5 inches. The utility companies needed to limit the settlement impact to 0.5 to 1.0 inches. The utilities were also located at differing depths which impacted the design differently. The gas utility lines were considered embedded at shallow depths (approximately 2 to 5 feet below existing ground surface elevation) while the sewer pipe elevations were deeply embedded (approximately 25 feet below existing ground surface elevation according to as-built plans). The problems presented by the utilities on site required the design team to propose a unique solution for each utility location.

SITE CHARACTERIZATION

Subsurface data for the project site consisted of multiple subsurface investigations and available research of the area. The primary subsurface investigation for this project was performed at the site by TSI Engineering, Inc. (TSI) in September of 2012, which included ten (10) standard penetration test borings located along the proposed structure. A supplemental investigation was performed in November of 2013 to obtain undisturbed samples for lab testing purposes. Other boring data that was located near the project site included a subsurface investigation consisting of six standard penetration test and rock core sample borings performed by Shannon & Wilson, Inc. in 2003, as part of the 2005 reconstruction project adjacent to the current proposed site. The subsurface conditions at the project site generally consist of (1) a relatively thin layer of soft, lean clay fill overlying (2) soft, lean clay fine alluvium over (3) medium dense coarse alluvium extending down to (4) limestone bedrock. The limestone bedrock generally dips from west to east towards the Mississippi River. Figure 3 presents a subsurface profile along the centerline of the proposed Merchants Bridge west approach reconstruction.

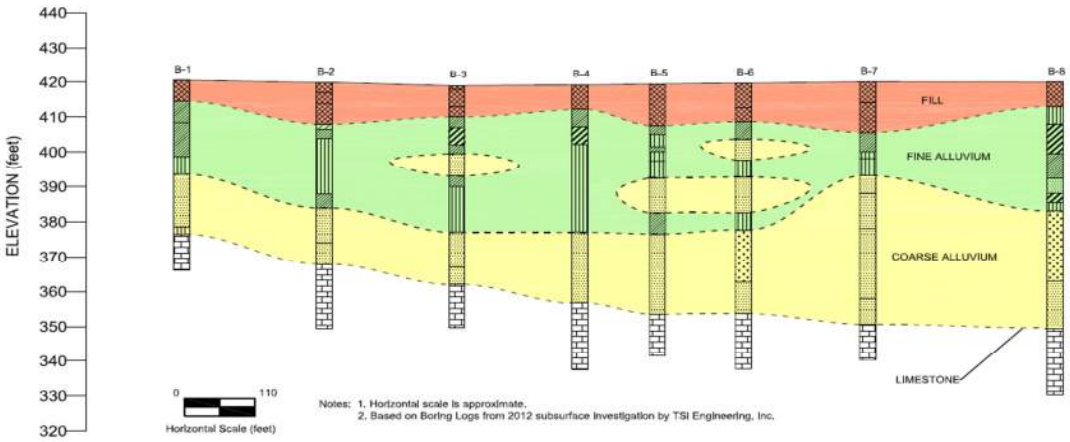

Figure 3. Subsurface Profile along project alignment.

The project limits are protected from Mississippi River flooding by an existing levee reducing the risk of uplift on the embankment due to flooding. However, the ground water table was still considered to be influenced by the adjacent Mississippi River. Water surface elevation measurements collected near the project site within the Mississippi River were reviewed and the average water surface elevation measured between October 1, 2007 and January 6, 2015 was selected as the design groundwater table elevation. Figure 4 presents the water surface elevation measurements along with seasonal averages and the overall average from October 1, 2007 to January 6, 2015. The source data was obtained from the USGS.

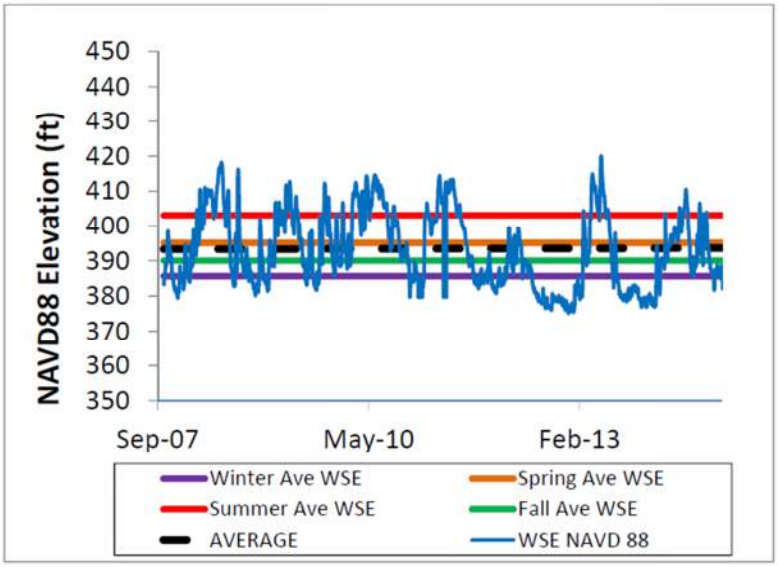

Figure 4. Water Surface Elevation measurements with seasonal averages of Mississippi River near project site.

The project site is located near known active seismic source areas such as the New Madrid seismic zone (NMSZ) situated about 150 miles to the southeast of the site, the Wabash Valley seismic zone (WVSZ), and the Commerce geophysical lineament (CGL). The probabilistic earthquake assessment for the project site was based on these seismic zones. The acceleration response spectra for three probabilistic design earthquakes were in accordance to the American Railway Engineering and Maintenance-of-Way Association (AREMA) 2014 Design Standards. The design response spectra at 5% damping for the three AREMA recommended earthquake levels at a site classification D, are defined as follows: (1) Level 1 correlating to a 100-year return period, (2) Level 2 or a 500-year return period, and (3) Level 3 ranging from a 1000-year to 2400-year return period (See Figure 5).

Based on Liquefaction Hazard Mapping by Pearce and Baldwin (2008) and liquefaction triggering analyses conducted during design, the project area soils would fall below the liquefaction threshold during a Level 1 event. At a Level 2 earthquake event the anticipated settlement due to liquefaction would be on the order of less than one-half inch. Furthermore, at the 1000-year return period (the lower end of the Level 3 earthquake event) significant liquefaction still only occurs at near 50 percent of the project site. At the upper end of the Level 3 earthquake event (2400-year return period) liquefaction may be pervasive across the entire project site. Figure 6 illustrates the range of liquefaction potential for the range of Level 3 earthquake events.

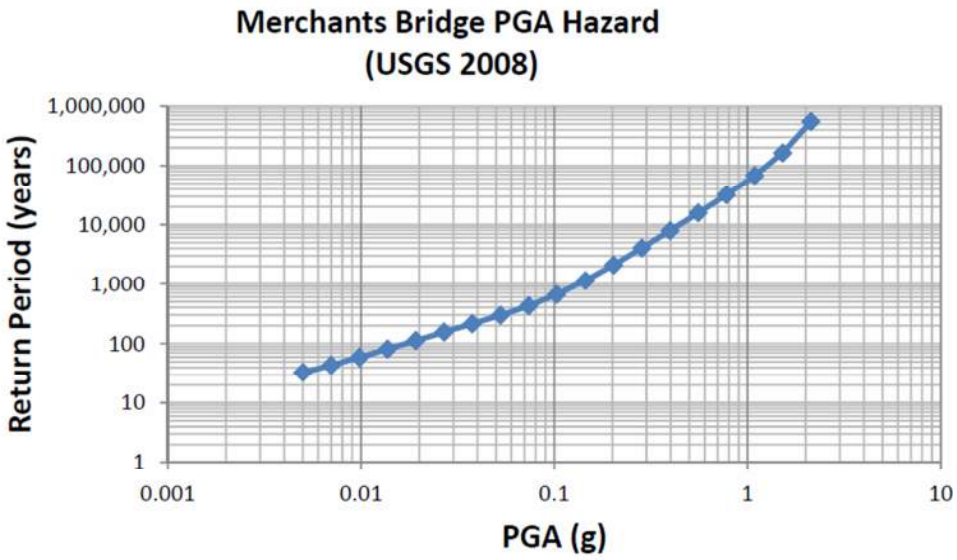

Figure 5. Merchants Bridge Peak Ground Accelerations as a function of Return Period.

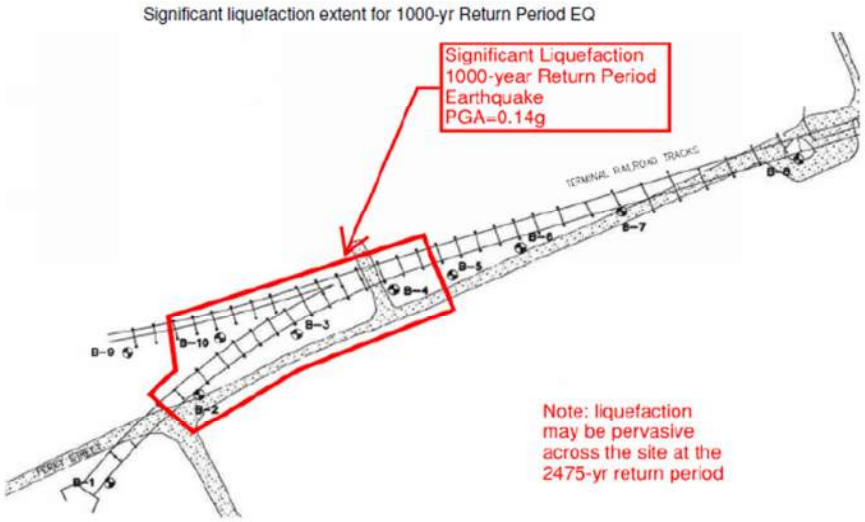

Figure 6. Liquefaction potential for the Merchants Bridge Project site.

DESIGN AND PERFORMANCE CRITERIA

Performance and design criteria for the Merchants Bridge west approach reconstruction can be categorized by seismic performance goals, service loading criteria, and light weight cellular concrete requirements.

Seismic performance criteria for the project adopted recommendations from AREMA (2014) for bridges. The three levels for design ground motion correspond to the following performance goals:

(1) During a Level 1 earthquake event the embankment should remain intact with no permanent deformation. This indicated that the seismic

loads at a Level 1 event must remain within the elastic range of the stress-strain curve of the embankment.

(2) During a Level 2 earthquake event the embankment structure can allow some minor permanent deformation but the structure should be repairable.

(3) During a Level 3 earthquake event the embankment structure must not collapse after experiencing permanent deformations.

For required service loads the AREMA recommended E-80 live loading was used during design to model rail loading. All train induced live loads are assumed to be distributed across 8.5-foot long ties with a critical wheel spacing of 5 feet, which equates to a design strip load of 1,882 psf for use in analyses. Live loads are assumed to act on the proposed embankment by two tracks.

Light weight cellular concrete criteria for the project adopted recommendation from manufacturer technical bulletins, AREMA (2014), and ACI (1999). Cellular concrete is an engineered, low density material having a homogeneous void or cell structure formed by the addition of a prepared foam or by the generation of gas within the fresh cementitious mixture. Cellular concrete is usually cast in densities ranging from about 20 to 120 pounds per cubic foot (pcf). Density control is achieved by adding a calculated amount of air as a prepared foam to a cementitious slurry with or without the addition of sand or other materials. The air cells created by the preformed foam may account for up to 80% of the total volume (Faoud, 2006). Maximum allowable shear and compression stresses for cellular concrete are functions of ultimate compressive strength of the material. The required compressive strengths for the cellular concrete used in the embankment structure were derived from estimated stresses from numerical modeling during the design phase of the project.

EMBANKMENT DESIGN

The Merchants Bridge west approach reconstruction embankment structure supports two railroad tracks. The typical embankment section consists of a ballasted track section supported by a stiffer upper 3-foot thick upper layer of Class IV cellular concrete overlying a variable thickness Class II cellular concrete section, which will make up the bulk of the embankment. The foundation of the embankment will consist of a 7-foot thick Class IV layer of cellular concrete underlain by a layer of crushed rock and geosynthetic fabric or geogrid embedded in the subgrade. The maximum embankment height is approximately 45 feet above existing grade at the east project limit and the minimum embankment height is approximately 25 feet above existing grade at the west project limit. Figure 7 details the typical cross section for the Merchants Bridge embankment structure.

During design, the evaluation of the foundation conditions for the lightweight cellular concrete embankment indicated that some form of ground improvement and/or deep foundations may be needed to minimize stresses and differential movement of the LCCF fill. A foundation system consisting of a combination of a geogrid reinforced rock matt used to transfer the embankment load to a series of

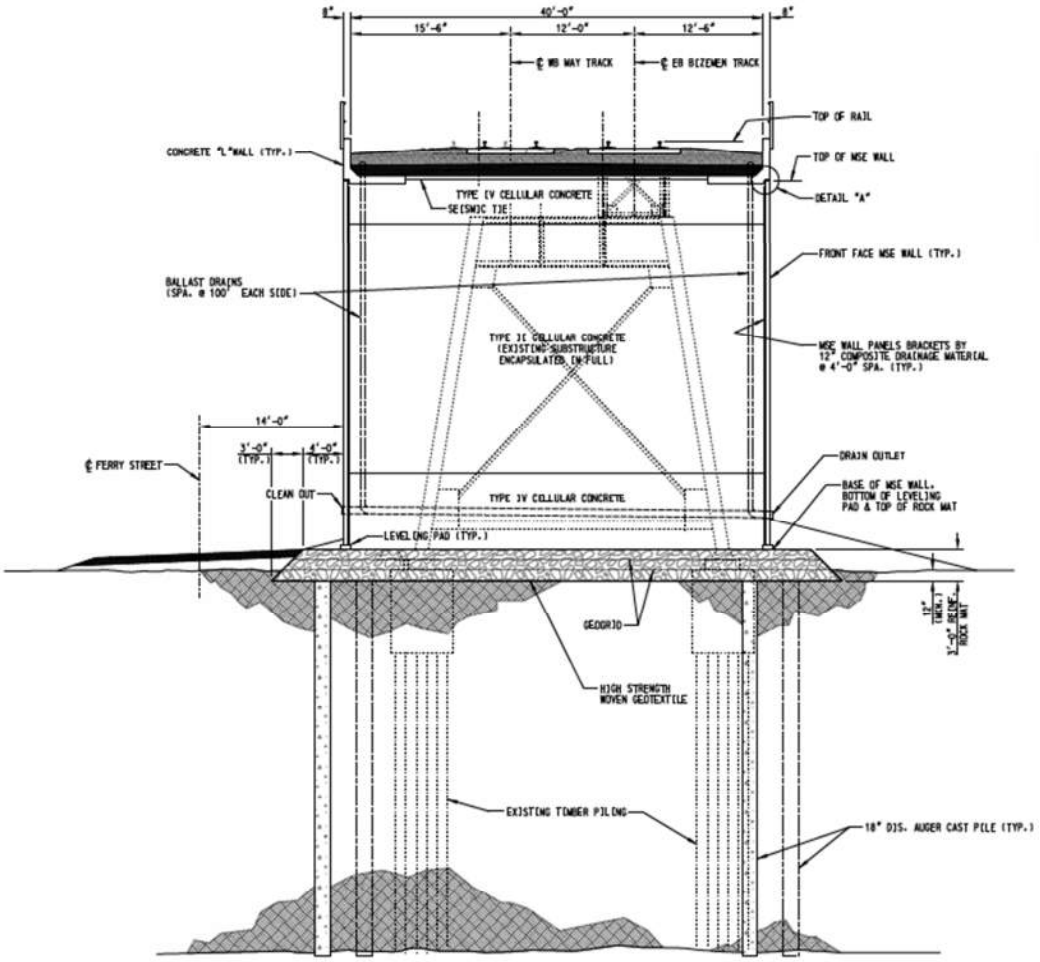

Figure 7. Typical Cross Section

auger-cast piles that would extend through the existing fill and soft fine alluvium and into the underlying medium dense coarse alluvium was selected for this project.

Auger-cast piles were primarily placed along the panel wall footings due to concentrated bearing requirements at these locations. The spacing of the auger-cast piles was determined as a function of the required bearing capacity along the project site. Auger-cast piles were also placed in the center of the embankment structure between existing bents when accessible by the construction equipment to help reduce shear and compressive stresses within the cellular concrete. It should be noted that to aid the design team in estimating foundation capacities, auger-cast pile load tests were performed prior to foundation design completion.

Since the embankment was designed to settle relatively uniformly, high stresses can build up at "hard points". Potential hard points were identified at the existing Bent W6 (at the east end of the project limits), the utility bridges, and the Ferry Street Bridge. The abutment at the west extent of the project was not expected to create a hard point due to the existing structure foundation consisting of timber piles believed to be founded in the same underlying medium-dense sand bearing layer

as the proposed LCCF embankment ACP. This abutment is expected to settle similarly to the rest of the timber pile/auger-cast pile supported embankment.

The existing W6 foundation consisted of 15 micropiles embedded into limestone bedrock. To reduce the stresses at this point and to transition into the typical embankment section, additional auger-cast piles were considered under the embankment between the two MSE wall panels. During analyses these auger-cast piles were deemed not feasible for construction (due to multiple existing utility conflicts) and alternative methods, such as installing geoinclusion to protect the existing W6 footing and abutment wall backface and a vertical control joint in the embankment structure, were used.

Ferry Street Bridge Abutments behave similarly to the BentW6, in that it creates a hard point within the embankment. The new Ferry Street Bridge is founded on six drilled shafts socketed into Limestone bedrock. Unlike the Bent W6, the Ferry Street Bridge does not have a footing as an additional pinch point to create higher stresses thus reducing the need for a geoinclusion. However, vertical control joints measured from both abutments of the bridge was still used to reduce the estimated shear stresses within the cellular concrete to below allowable levels.

Utility bridges presented a unique problem for the design team. The performance goal of the utility bridges was to limit and control the affects of settlement but not to eliminate it. In order to achieve this goal, the design team had to create multiple hard points in the embankment structure. The primary foundation element for the utility bridges was auger-cast piles tipped on bedrock. Placement of these elements is limited by overhead clearance due the equipment required for installation. Where auger-cast piles were not feasible micropiles were advanced to bedrock. The utility bridge foundations were topped by a reinforced concrete structural slab. The structural slab will be covered with a layer of low density compressible geofoam to allow settlement of the cellular concrete embankment above the underlying utility. By allowing for settlement to occur the design team eliminated the creation of a hard point below the embankment that could cause stress concentrating in the embankment under service or seismic loading, and also limit the transfer of loads to the utility below. The structural slab will act to protect the utility and distribute any loads that are transferred from the embankment to the foundation elements.

To better assess the utility company needs the utility lines crossing the embankment structure were categorized as shallow utilities (embedded between 0 to 10 feet below existing grade) and deep utilities (embedded greater than 10 feet below existing grade). The settlement contours created by the embankment structure further complicated the problem. Shallow utilities saw significant decrease in settlement due to the direct protection of the structural slab. The deep utilities did not see the same reduction due to the deep seated influence of the embankment structure. The treatments for each utility type differ in method. For shallow utilities a hanger cast into the structural slab was used to fix the utility to the rigid structural slab to minimize settlement due to the consolidation of the deeper soil layers. For deep utilities the spacing of the utility bridge foundation elements were adjusted to create a protective arching effect similar to a drilled shaft wall. These treatments reduced the expected settlements of the utilities on site to 1.0 inch or less.

Global stability, internal stability, external stability, and Load/Deformation analyses were conducted for the embankment design. Potential deep-seated failure surfaces were identified using the computer program SLOPE/W as part of the GeoStudios Program suite. Internal and external stability was checked using the computer program MSEW3.0 developed by ADAMA Engineering, Inc. (2009). Load/deformation analyses were performed using the finite element computer program SIGMA/W, which is also part of the GeoStudio 2012 software suite copyrighted by GEO-SLOPE International. The linear elastic material model is considered appropriate for small deformations of the system.

SEISMIC DESIGN

Seismic design methodologies generally followed those developed by HDR Engineering as part of the Union Pacific Railroad Colton Flyover Structure design in California. Seven design ground motions were selected and spectrally matched to the target bedrock acceleration response spectra. Spectral matching was generally performed within +/- 5% of the target spectrum.

In order to estimate the design seismic acceleration for the AREMA response spectra, it was necessary to estimate the fundamental period of the lightweight cellular concrete embankment. The fundamental period, which is based on the elastic properties of the cellular concrete and the geometry of the proposed embankment, is considered a more accurate estimate of the seismic acceleration within the embankment than simply using the peak ground acceleration (PGA) equally acting throughout the entire embankment. The fundamental period for the design analyses varied as a function of width and height of the cellular concrete embankment section along the project profile. The computational method used to estimate the fundamental period of the lightweight cellular concrete embankment is based on research performed by Dr. Steven Bartlett, John S. Horvath and others for seismic analyses of lightweight geofoam fill embankments (Bartlett, 2008; Horvath, 2004). This method is considered applicable to the elastic properties and response of lightweight cellular concrete fill.

Analyses were conducted using a one-dimensional, equivalent linear model using the computer software program SHAKE2000 and two finite-difference, two-dimensional models using the computer software program FLAC. The one FLAC models assumed the nonplastic silt below the design groundwater table will not liquefy, while the other assumed liquefaction did occur. If liquefaction does not occur, seismic settlement is expected to be less than an inch. However, if liquefaction does occur, settlement could be nearly 2 feet. Figure 8 shows the FLAC output resulting in large settlements, but overall remaining intact at an AREMA Level 3 earthquake event. Vectors are representative of the displacements that occur with liquefaction. The largest arrow corresponds to a displacement of approximately 22.5 inches.

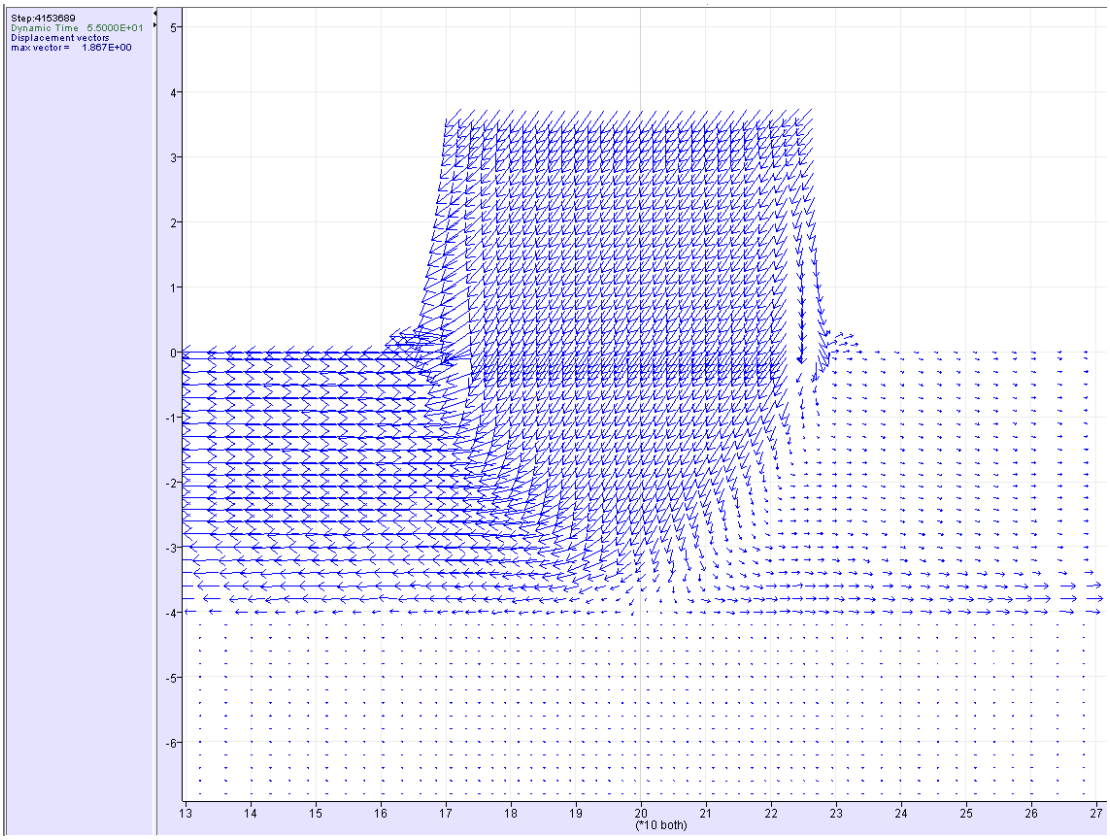

Figure 8. FLAC output for AREMA Level 3 earthquake event.

FINDINGS

The proposed cellular concrete embankment structure was found to be stable in both the global and internal stability analyses for all service load levels. The load/deformation analyses indicated that computed stresses and strains within the cellular concrete embankment were below the recommended limits for service loading. The elastic settlement calculations indicated small immediate differential and long-term settlement along the embankment alignment.

Seismic global and internal stability analyses indicate that the cellular concrete embankment will not yield under AREMA Level 1 and 2 seismic loading (F.S. ≥ 1.0), but will experience permanent deformations on the order of about 3 inches at the AREMA Level 3 earthquake (F.S. < 1.0).

CONCLUSIONS

This project presented challenges with operational and physical constraints which contributed to the innovative design of the Merchants Bridge west approach reconstruction. In addition to the numerous existing utilities and complex existing bridge structures, the subgrade soils were very soft and variable, requiring both a robust foundation system as well as lightweight fill to limit subgrade settlement and seismic inertial forces. Consequently, the complex nature of the proposed design

required the design team to develop an equally unique resolution. Using finite element modeling in addition to traditional analytical methods, the team was able to find matrix solutions to the challenges that arose throughout the design-build process.

REFERENCES

ACI (1999) ACI 213R-87 "Guide for Structural Lightweight-Aggregate Concrete" American Concrete Institute.

ADAMA (2009), MSEW (Version 3.0), by Adama Engineering, Inc.

AREMA (2014) "AREMA manual for Railway Engineering."

Bartlett (2008) "Evaluating the Seismic Stability and Performance of Freestanding Geofoam Embankment," 6th National Seismic Conference on Bridges and Highways, Charleston, S.C., July 27th -30th 2008. Invited Talk, prepared by Steven F. Bartlett and Evert C. Lawton, presented, 08/01/2008.

Denny (2003) "Bedrock Geology of Granite City Quadrangle Madison and St. Clair Counties, Illinois and St. Louis County, Missouri", compiled by F. Brett Denny of the Illinois State Geological Survey, 2003.

Fouad (2006) "Significance of Tests and Properties of Concrete and Concrete-Making Materials, STP 169D", ASTM International, 2006.

GEO-SLOPE (2012) Geostudio 2012 software by GEO-SLOPE International Ltd.

Horvath (2004) "Geomaterials Research Project - A Technical Note re Calculating the Fundamental Period of an EPS-Block- Geofoam Embankment". Manhattan College Center for Geotechnology Research Report No. CGT-2004-1 prepared by John S. Horvath, dated February 2004.

Pearce and Baldwin (2008) "Liquefaction susceptibility and probabilistic liquefaction potential hazard mapping, St. Louis Missouri and Illinois" National Earthquake Hazards Reduction Program, Final Technical Report, 2008, 51 p.

Sandia (2004) "Laboratory Constitutive Characterization of Cellular Concrete", Sand Report SAND2004-1030, Unlimited Release, March 2004, 76p.

Innovations in Rehabilitation of Aging Bridge Abutments

Justin Anderson, M.E., P.E.[1]

Abstract: Bridges throughout the United States are becoming unserviceable faster than they can be replaced. This paper presents a new concept in mitigating this mounting crisis. Current practice includes removal and replacement of the abutments and superstructures. There is now an innovative approach where the old abutment is left intact and used as a form during construction of a new abutment. This process can take as little as a few days and environmental concerns and permitting are avoided or minimized. The concept limits traffic disruption while minimizing costs; traffic flow can continue during non-construction hours. Costs are half or less, compared with the typical full removal and replacement.

This new concept combines several aspects of reinforced soil technologies into an integrated package that will allow designers and owners a new option when considering when and how to replace or reinforce an existing bridge or box structure. The technology is much faster and less expensive where it is compatible with local conditions and restraints.

[1] Senior Product Development Engineer, GeoStabilization International. Email: anderson@gsi.us

NOTES

NOTES

NOTES

NRC Research Press

ARTICLE

Three-dimensional levee and floodwall underseepage

Navid H. Jafari, Timothy D. Stark, Aaron L. Leopold, and Scott M. Merry

Abstract: Levee and floodwall seepage models based on two-dimensional (2D) conditions can underpredict landside vertical hydraulic gradients and uplift pressures due to excavations and convex bends. The Sherman Island levee system is used to calibrate a three-dimensional (3D) seepage model to evaluate the effect of finite landside excavations and convex levee bends on landside seepage. The model shows that a 3D analysis is required for a landside excavation with an aspect ratio (length to width) less than 1*L*:1.5*W*. For drainage canals and ditches that parallel a levee or floodwall and are wider than 15 m, gradients at the excavation center are essentially equal to 2D vertical gradients but greater than 2D gradients near the excavation sidewalls. The Sherman Island calibrated seepage model also confirms concave bends diverge seepage and yield lower vertical gradients than 2D models. Varying the degree of levee curvature (ω = 45°–100°) indicates that sharper convex bends (ω = 100°; axisymmetric radius, 150 m) cause vertical gradients that can be about 150% greater than 2D analyses.

Key words: two-dimensional (2D) seepage, three-dimensional (3D) seepage, levee, floodwall, concave, convex, excavation, axisymmetric, transient analysis, hydraulic gradient, uplift.

Résumé : Les modèles d'infiltration bidimensionnels (2D) appliqués aux digues et murs de protection contre les crues peuvent sous-estimer les gradients hydrauliques dans le sol et la sous-pression hydrostatique causés par des excavations et des courbures convexes. Le dispositif de digues de l'île Sherman sert à calibrer un modèle d'infiltration tridimensionnel (3D) qui permet d'évaluer les effets d'excavations creusées dans le sol et des courbures convexes de digues sur l'infiltration d'eau dans le sol. Le modèle montre qu'il est nécessaire de réaliser une analyse 3D dans le cas d'une excavation dont le rapport de forme (longueur sur largeur) est inférieur à (1.*L*)/(1,5.*l*). Dans le cas de canaux et de fossés de drainage qui sont parallèles à une digue ou à un mur de protection contre les crues et dont la largeur est supérieure à 15 m, les gradients au centre de l'excavation sont pratiquement égaux aux gradients verticaux 2D, mais supérieurs aux gradients 2D situés à proximité des parois de l'excavation. Le modèle d'infiltration calibré et utilisé à l'île Sherman confirme également que les courbures concaves font diverger les flux d'infiltration et produisent des gradients verticaux inférieurs à ceux obtenus dans les modèles 2D. En faisant varier le degré de courbure de la digue (ω = 45°–100°), on montre que les fortes courbures convexes (ω = 100°; rayon axisymétrique, 150 m) génèrent des gradients verticaux qui peuvent être supérieurs d'environ 150 % à ceux obtenus au moyen d'analyses 2D. [Traduit par la Rédaction]

Mots-clés : modèle d'infiltration bidimensionnel (2D), modèle d'infiltration tridimensionnel (3D), digue, mur de protection contre les crues, concave, convexe, excavation, axisymétrique, analyse transitoire, gradient hydraulique, sous-pression.

Introduction

Two-dimensional (2D) seepage models can underpredict landside hydraulic gradients under landside excavations and convex levee bend conditions (Money 2006; Cobos-Roa and Bea 2008; Ahmed and Bazaraa 2009; Benjasupattananan and Meehan 2012). For example, Money (2006) reports computed three-dimensional (3D) vertical hydraulic gradients that are ~45% and ~120% greater than 2D computed hydraulic gradients for infinite and finite landside excavations, respectively. Ahmed and Bazaraa (2009) show that neglecting seepage flow through excavation sidewalls can lead to errors in computing the landside uplift pressures and exit gradients. Benjasupattananan and Meehan (2012) and Merry and Du (2015) report higher 3D uplift pressures and hydraulic gradients at the landside toe for convex levee sections compared to 2D models. While 2D models underpredict hydraulic gradients for convex bends, concave bends diverge underseepage, resulting in 2D models that overpredict gradients. An industry guidance document (URS 2013) accounts for 3D effects by recommending an increase in average exit vertical gradient by 20%–30% for 60° levee angles.

The state of practice for examining levee and floodwall seepage is 2D finite element analyses (FEA) and (or) analytical solutions proposed in the U.S. Army Corps of Engineers (USACE) design manuals EM 1110-2-1901 and EM 1110-2-1913 (USACE 1993, 2000). The 2D FEA calculates uplift pressures and flow assuming levee geometry, soil stratigraphy, boundary conditions, and excavations are infinitely wide. However, urban levees and floodwalls are constructed to accommodate natural river meanders, and landside excavations are often present. Examples of limited extent landside excavations include borrow pits, building foundations, agricultural storage silos and tanks, residential swimming pools, burrowing animals, trees, utilities, conduits, pipelines, drainage canals, and culverts.

This study uses a segment of Sherman Island levees to field calibrate a seepage model and then perform a parametric analysis using the calibrated model to investigate the effects of 3D landside excavations and levee bends on landside hydraulic gradients. For 3D effects on landside excavations, the excavation width is varied to identify when a 3D analysis is warranted. Floodside excavations are not discussed herein because the maximum landside hydraulic gradients can be estimated using a 2D cross section

Received 17 August 2014. Accepted 18 June 2015.

N.H. Jafari and T.D. Stark. University of Illinois at Urbana-Champaign, 205 N. Mathews Ave., Urbana, IL 61801, USA.
A.L. Leopold. Shannon & Wilson Inc., 1321 Bannock St., Denver, CO 80204, USA.
S.M. Merry. University of the Pacific, 3601 Pacific Avenue, Stockton, CA 95211, USA.
Corresponding author: Navid H. Jafari (e-mail: njafari2@illinois.edu).

Can. Geotech. J. **52**: 1–13 (2015) dx.doi.org/10.1139/cgj-2014-0343

Published at www.nrcresearchpress.com/cgj on 19 June 2015.

that bisects the floodside excavation. Therefore, floodside excavations can be conservatively modeled using a 2D seepage analysis, whereas landside excavations require a 3D analysis (Stark and Jafari 2015). The levee bend analysis investigates the 3D vertical gradients along a curved segment of Sherman Island. A calibrated parametric analysis is performed to evaluate the effect of convex and concave meanders on 3D landside vertical gradients, and a methodology is proposed to simulate 3D bends with 2D axisymmetric models.

Sherman Island

The Sacramento – San Joaquin Delta (referred to herein as Delta) is located at the confluence of the Sacramento and San Joaquin Rivers in Northern California. The Delta is important to California's economy and infrastructure, including a source of water supply for about 25 million Californians, a source of irrigation for over 7 million acres (2.83 million hectares) of agricultural land, and an extensive infrastructure of state and local roads, railroads, pipelines, and shipping ports (CALFED 2000). A levee network protects the many islands in the Delta and directs water to San Francisco Bay. Combined with subsiding interiors and high flood levels, levees and their foundations are vulnerable to seepage and seepage-induced failures. In particular, subsidence is a major concern on Sherman Island because a lower landside elevation increases the hydraulic gradient from floodside to landside. From 1930 to the early 1980s, over 50 Delta islands or tracts flooded primarily due to levee foundation instability (Prokopovitch 1985). Significant consequences occur after a levee breach, such as in 2004 when the Lower and Upper Jones Tract flooded, resulting in economic impacts of greater than $100 million (California DWR 2005). Therefore, assessing seepage-induced levee performance on flood protection infrastructure is important to public health, commercial activities, and environmental safety of the Delta and Sherman Island.

Sherman Island lies at the western limit of the Delta where the Sacramento and San Joaquin rivers converge and is bordered to the northeast by Threemile Slough (see Fig. 1*a*; USDA (2014)). The island is located northeast of the city of Antioch, California, and is within the jurisdiction of Sacramento County. Sherman Island is currently protected by approximately 29 km of perimeter levees (Hanson 2009). The levees were originally constructed in the 1860s' over organic soils and have been enlarged periodically as the foundation soils subsided. Approximately 15 km of Sherman Island levees are constructed to federal standards and supervised by the USACE, while the remaining 14 km of levees are nonproject levees (maintained by the local levee district). Subsidence and substandard levee protection have resulted in major levee breaches that have inundated Sherman Island in 1904, 1906, 1909, and 1969.

In 1969, the levee segment on the San Joaquin River between levee Stations 520 and 525 (see Fig. 1*b*; USDA (2014)) failed, and the high-velocity flow from the levee breach eroded the island interior and created a scour hole about 6.5 m deep (see scour lake in Fig. 1*b*). Since 1969, seepage and stability problems have plagued the southern levees (south of Antioch Bridge to Station 545). Numerous piezometers, inclinometers, and settlement plates are being used to monitor levee performance between Stations 520 and 545 (see rectangle in Fig. 1*a*) to help prevent another breach (Hanson 2009). Borings from previous studies were utilized to develop a subsurface profile at cross section A–A′ in Fig. 1*b*, and a nearby piezometer was used to calibrate the 2D and 3D seepage models developed herein. These seepage models permitted an investigation of landside excavations and levee curvature on underseepage and landside vertical gradients and uplift pressures.

Levee profile and soil properties

The subsurface profile shown in Fig. 2 was developed using borings B-1, B-2, and B-3 from Hanson (2009). The boring locations shown in Fig. 1*b* were drilled as part of the levee improvements along landside of Sherman Island from approximately Stations 520 to 545. Borings B-1 and B-2 are located in the free field, i.e., beyond the landside levee toe, while B-3 is located at the landside toe. Borings B-1, B-2, and B-3 were drilled prior to the 2009 remedial measures. The aerial view in Fig. 1*b* was photographed in 2012 after construction of a landside stability berm began; therefore, borings B-1 and B-2 appear at the landside toe, and B-3 appears located at the levee crest after remediation.

The levee foundation is composed of a range of coarse-grained sediments, including gravels and loose clean sands, and silty sands. Thus, the profile in Fig. 2 starts at depth with a fine sand stratum below elevation (el.) –15 m NAVD88 (North American Vertical Datum of 1988). Above the sand is a layer of silty clay, locally known as Bay Mud, deposited as the sea level rose following the last ice age. The clay stratum is about 3.1 m thick and overlain by

Fig. 1. Aerial photographs: (*a*) Sherman Island (white box shows location of aerial photograph in *b*); (*b*) close-up showing location of cross section A–A′ and nearby instrumentation (USDA (2014), photos from 2012 [http://datagateway.nrcs.usda.gov/]).

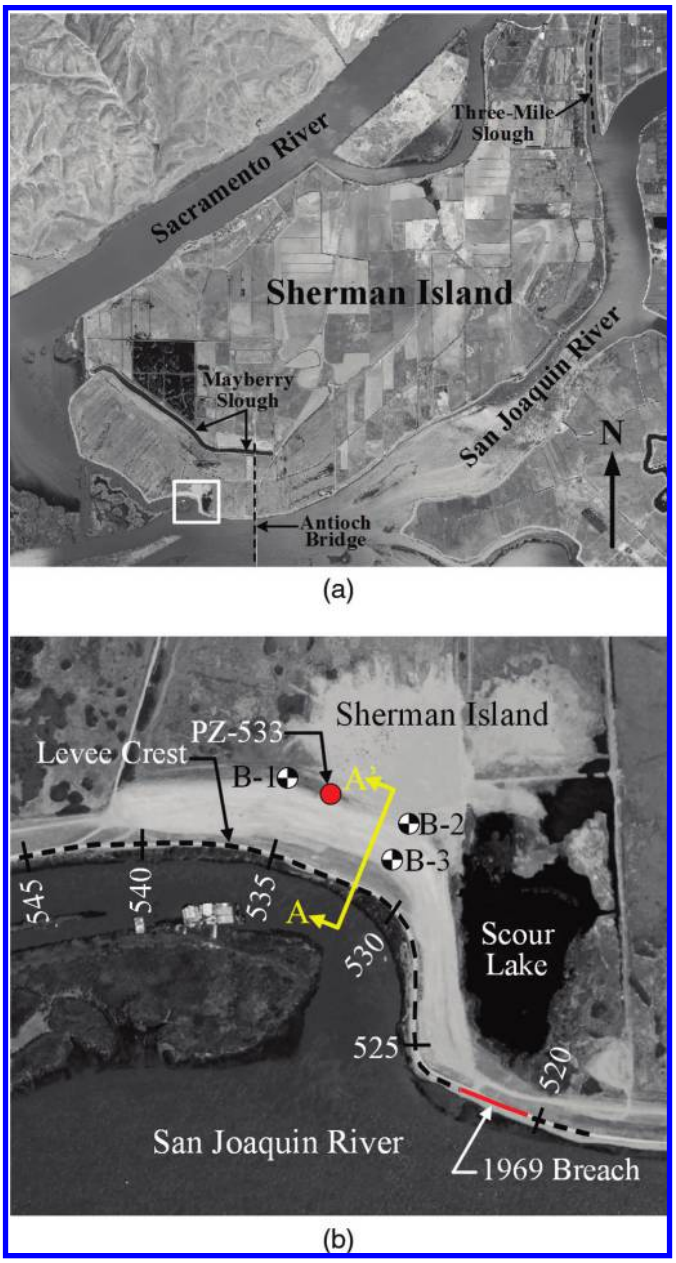

Fig. 2. Levee cross section A–A′ of Sherman Island at Station 532. h_t, total head; Q, flow rate.

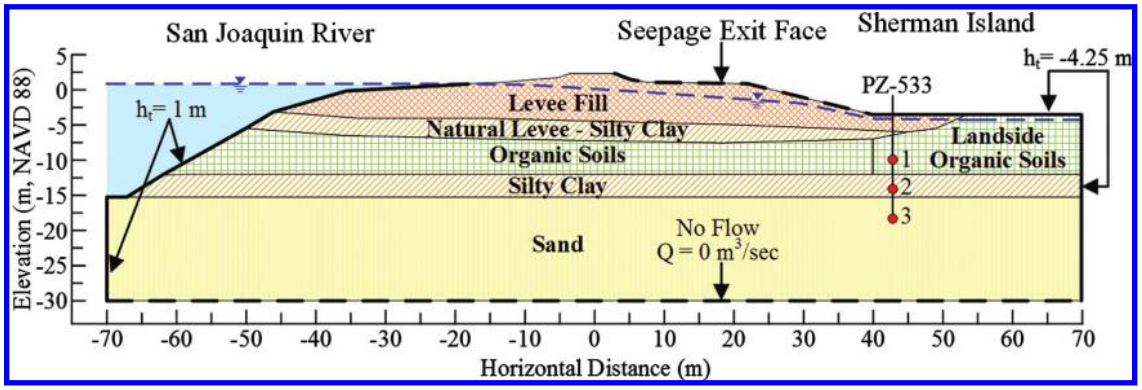

organic soils that extend to the ground surface. Shelmon and Begg (1975) report sea level rise in the past 7000 years created tule marshes that covered most of the Delta. The repeated burial of the tules and other vegetation growing in the marshes formed approximately 8 m of highly organic soils at cross section A–A′. The highly organic soils are not classified as peat because the organic content (ASTM D2974 (ASTM 2014)) and classification defined in ASTM D4427 (ASTM 2013) are not available to confirm sufficient organics for peat classification, i.e., greater than 75% organics.

The Sherman Island levee embankment is composed of dredged loose to medium sand and silt. Weight of the levee embankment has caused settlement of the organic soil layer and hence a decrease in horizontal hydraulic conductivity. In addition, the levee fill overlies natural levees of the San Joaquin River, which are represented by a layer of silty clay between the organic soil and levee fill. This natural levee material, known locally as overbank deposits, is found to be of limited lateral extent, grading into the thick organic soil stratum beneath the levee berms.

Water levels are maintained 0.6–1.5 m below land surface by an extensive network of drainage ditches. Foott et al. (1992) report an artesian condition in the sand substratum, causing upward seepage through the clays and organic soils. The foundation seepage is typically drained off, collected, and pumped out of the island via a series of levee toe drainage ditches flowing to a pumping station (see toe ditch in Fig. 2).

Table 1 summarizes index properties and engineering parameters used in the seepage analyses. Due to the weight of levee fill, the natural water content (w_o) of the organic soils under the levee ranges from 116% to 265%, while the landside organic soils have natural water contents from 224% to 408% (Weber 1969; Foott et al. 1992). The resulting organic soil saturated unit weight (11.6 kN/m^3) is greater than the landside organic soils (10.5 kN/m^3) and is in agreement with unit weights reported in Mesri and Ajlouni (2007). Available hydraulic conductivity tests are limited for the levee embankment, silty clay, and sand materials shown in Fig. 2. As a result, estimates of saturated horizontal hydraulic conductivity (k_h) for these soils in Table 1 were made using the Guidance Document for Geotechnical Analyses by URS (2013). The value of k_h for the organic soils is evaluated using Weber (1969), Mesri and Ajlouni (2007), and Mesri et al. (1997) and the appropriate average effective vertical stress (σ'_{va}). Weber (1969) utilized piezometer data to estimate k_h of the organic soils in the Delta using an inverse analysis and found k_h ranges from 1×10^{-7} to 1×10^{-4} cm/s for $\sigma'_{va} \leq 550$ kPa. The σ'_{va} of organic soils under the levee and landside toe is about 190 and 45 kPa, respectively, based on the cross section in Fig. 2. This σ'_{va} correlates to a k_h of about 3×10^{-5} and 3×10^{-4} cm/s for organic soils under the levee and landside, respectively. The anisotropy ratio, i.e., ratio of horizontal to vertical hydraulic conductivity (k_h/k_v), is 3–5 for surficial peats and about 10 for buried peat deposits (Mesri and Ajlouni 2007). Thus, the values of k_h/k_v chosen for Sherman Island organic soils are 10 and 3 for organic soils at the landside toe and under the levee, respectively. Based on URS (2013), the anisotropy ratio is assumed to be 4 for levee fill and 10 for the sand and natural silty clays. These values of saturated k_h and k_h/k_v ratios are consistent with those used for the certification of the nearby Natomas levees (Merry and Du 2015). Because this study is focused on underseepage during steady-state conditions, the unsaturated soil properties are not modeled for the levee embankment fill and landside organic clay.

Table 1. Soil index properties and hydraulic parameters for cross section A–A′ in Fig. 2.

Soil type	Soil classification (ASTM 2011)	γ_{sat} (kN/m^3)	w_o (%)	k_h (cm/s)	k_h/k_v
Levee fill	ML or SM	17.7	8–13	1×10^{-3}	4
Organic soil under levee	OL or OH	11.6	116–265	3×10^{-5}	10
Landside organic soil	OL or OH	10.5	224–408	3×10^{-4}	3
Silty clay	CL–ML	16.7	49–78	1×10^{-6}	10
Sand	SM or SP	19.5	25–35	1×10^{-2}	10

Note: CL, low-plasticity clay; ML, silt; OH, organic clay; OL, organic silt; SM, silty sand; SP, poorly graded sand; γ_{sat}, saturated unit weight.

Calibration of 2D seepage model

The 2D finite element program SEEP/W by Geo-Slope (2007) was used to estimate the phreatic surface through the levee fill and calibrate pore-water pressures in the substratum using available Sherman Island piezometer data. SEEP/W is a general seepage analysis program formulated to model saturated and unsaturated transient flow through soil and excess pore-water pressure dissipation estimated from a stress–deformation analysis within porous materials. Piezometer PZ-533 was installed in 2008 at Station 533 to monitor pore-water pressures during landside stability improvements (Hanson 2009). The initial pore-water pressures prior to construction of the stability berm were used to calibrate the 2D and 3D seepage models.

The initial floodside steady-state boundary condition is a total head (h_t) of el. +1 m NAVD88 and is consistent with canal water levels measured at the Antioch gage station. The "seepage exit face" option was selected from the levee crest to landside levee toe (40 m from levee centerline in Fig. 2) because the phreatic surface on the landside levee slope is unknown. The boundary condition from landside levee toe to the right-hand side (RHS) of the finite element mesh is assumed to be 0.75 m below the ground surface (el. –4.25 m NAVD88). The left-hand side (LHS) vertical boundary is specified as the steady-state river stage (el. +1 m NAVD88) because the sand stratum is hydraulically connected to the San Joaquin River (Foott et al. 1992). In addition, with the sand stratum hydraulically connected to the San Joaquin River, the results are insensitive to the vertical floodside boundary condition (Du and Merry 2014). The bottom boundary condition is defined as an impervious boundary to represent the low hydraulic conductivity clay under-

Table 2. Calibration of Sherman Island seepage model at steady-state conditions.

Piezometer	Depth (m)	Soil layer	Measured h_t (m)	SEEP/W h_t (m)
1	–9.6	Organic soil	–4.0	–4.2
2	–14.2	Silty clay	–3.0	–3.1
3	–18.8	Sand	–2.7	–2.8

lying the sand stratum. Figure 2 shows the soil profile and boundary conditions used in the calibration model.

The cross section in Fig. 2 is calibrated using data from PZ-533, which is located 43 m landside from the levee centerline and at ground surface el. –3.5 m NAVD88. Three piezometers shown in Fig. 2 were installed at el. –9.6 m (PZ-533-1), –14.2 m (PZ-533-2), and –18.8 m (PZ-533 = 3) in PZ-533 (Hanson 2009). The total heads in Table 2 were recorded prior to construction of the improvement activities. The total heads of –3 and –2.7 m measured by PZ-533-2 and PZ-533-3, respectively, indicate artesian conditions exist in the sand layer, which confirms the hydraulic connection between the San Joaquin River and sand stratum. A comparison of PZ-533 response and the SEEP/W results at steady state is shown in Table 2. The SEEP/W model slightly overestimates the pore-water pressures but is in close agreement with measured values. The phreatic surface computed in SEEP/W is shown in Fig. 2. Based on the initial pore-water conditions and phreatic surface, the 2D calibrated model was used to perform 3D simulations of landside excavations and levee bends.

Effect of landside excavations

The effect of floodside and landside excavations came to the forefront in litigation related to the floodwall breaches along the Inner Harbor Navigation Canal (IHNC) and was the impetus for this 3D study (Stark and Jafari 2015). Prior to Hurricane Katrina, the USACE contracted for the demolition and environmental cleanup of the East Bank Industrial Area (EBIA) in the IHNC to allow for widening of the shipping canal. The EBIA had a long history of industrial use and contamination (WGI 2005), as well as the presence of buried structures and foundations that could interfere with dredging of a bypass channel in the IHNC. Thus, the removal of contaminated soil and buried structures resulted in many floodside excavations along the IHNC floodwalls. If these excavations were backfilled with high hydraulic conductivity soils and penetrated to depths below the tip of the floodwall sheet pile, floodside underseepage could have been facilitated.

Stark and Jafari (2015) performed 3D seepage analyses to understand the IHNC floodwall breaches and found the maximum 3D landside vertical gradients correspond to a 2D cross section through the floodside excavation. In contrast, the 3D seepage analyses show that landside excavations cause 3D gradients to increase because of inward seepage from the excavation sidewalls. With landside drainage ditches, borrow pits, building foundations, residential swimming pools, and tree stumps located near levees, landside excavations were investigated to evaluate 3D flow on landside hydraulic gradients and provide recommendations on when a 3D seepage analysis is warranted.

Formation of 3D model

The 3D Sherman Island seepage model in Fig. 3 was developed using the software package RS^3 (Rocscience 2014) to compare the effect of finite landside excavations with the calibrated 2D SEEP/W model in Fig. 2. The soil profile, hydraulic properties, and levee geometry are identical between the two models (SEEP/W and RS^3). The 3D model geometry is constructed by extruding the 2D profile "into the page" in Fig. 2. The 3D model uses three extruded slices to model the excavation, with the center slice modified to include an open excavation. The outer two slices duplicate Fig. 2 and are 50 m wide to control end effects (see Fig. 3). The excavation width is varied by widening the center slice. The landside toe ditch is replaced with the landside excavation. The boundary conditions shown in Fig. 3 include a seepage exit face applied to the inside surfaces of the excavation because water can seep into the excavation during flood conditions. This boundary condition is applied in open excavations, e.g., during construction of building foundations, swimming pools, and underground utilities. The floodside and LHS vertical boundary conditions are assumed a maximum river stage of el. +1.8 m NAVD88. The boundary condition from the landside levee toe to the RHS of the finite element mesh is zero pressure head (h_p). The RHS vertical boundary is modeled as a total head boundary (h_t = el. –3.5 m or at the ground surface) to represent the landside groundwater conditions. The boundary condition along the bottom of the seepage model remains a no-flow boundary. Figure 4 shows the 2D flow field and total head contours at a river stage of el. +1.8 m. The total head contours decrease from +1.8 m at the floodside to –6 m at the bottom of the excavation. The contours in the sand stratum are horizontal, indicating head loss through the stratum is minimal. The total head contour of el. –6 m at the bottom of the excavation corresponds to hydraulic gradients close to 0.4.

Landside excavation parametric results

The multiple excavation widths used to compute the vertical hydraulic gradients at the center and edge of a landside excavation are shown in Fig. 5. Points 1 and 2 are positioned along the centerline of the landside excavation, and points 3 and 4 are located at the excavation edge (sidewall). At widths of 2 m, high gradients observed in the center of the excavation are attributed to inward seepage from the sidewalls. For excavations less than 3 m, the gradients measured at points 1 and 3 as well as points 2 and 4 are equal because of the short distance between the edge and center of the excavation. The lower gradients at points 2 and 4 as compared to points 1 and 3, respectively, are attributed to increased seepage length to the middle of the excavation. As the excavation width increases, gradients converge to 2D results (obtained from the cross section that bisects the excavation) and the effect of inward seepage is less at points 1 and 2.

For this analysis, points 1 and 2 approach 2D equivalent gradients when the excavation width is at least 15 m. This width corresponds to an excavation aspect ratio (length to width, *L*:*W*) of 1*L*:1.5*W* and is considered the threshold when vertical gradients in the excavation center are not influenced by 3D seepage. Vertical gradients are always higher at points 3 and 4 compared to the excavation center because of converging flow along the excavation sidewalls. For example, points 3 and 4 approach a constant hydraulic gradient of 0.66 and 0.44, respectively, at 10 m width. For widths >20 m, the vertical gradients at points 3 and 4 are about 150% and 190% greater than points 1 and 2, respectively. As a result, seepage-induced failures (heave or sands boils) can develop near the excavation sidewalls, as well as in the center for narrow excavations, having an aspect ratio of 1*L*:1.5*W* or less.

Figure 6 shows total head contours at steady-state flood condition with increasing excavation widths. The total head contours are el. –6.5 m at the excavation floor and el. –3.5 m on the landside surface. The concentrated total head contours for the 5 m excavation in Fig. 6*b* indicate greater change in total head and higher vertical exit gradients within the excavation. As the excavation width is increased in Figs. 6*b*–6*e*, the total head contours in front of the excavation straighten and the contours are spaced farther apart at the excavation sidewalls, thus arriving at 2D conditions. Total head contours in Fig. 6 corroborate the results in Fig. 5 by showing 3D seepage effects are limited for excavation widths greater than 15 m and the excavation sidewall is the critical zone to evaluate vertical hydraulic gradients and uplift pressures.

Fig. 3. 3D soil stratigraphy, boundary conditions, and landside excavation used in RS³.

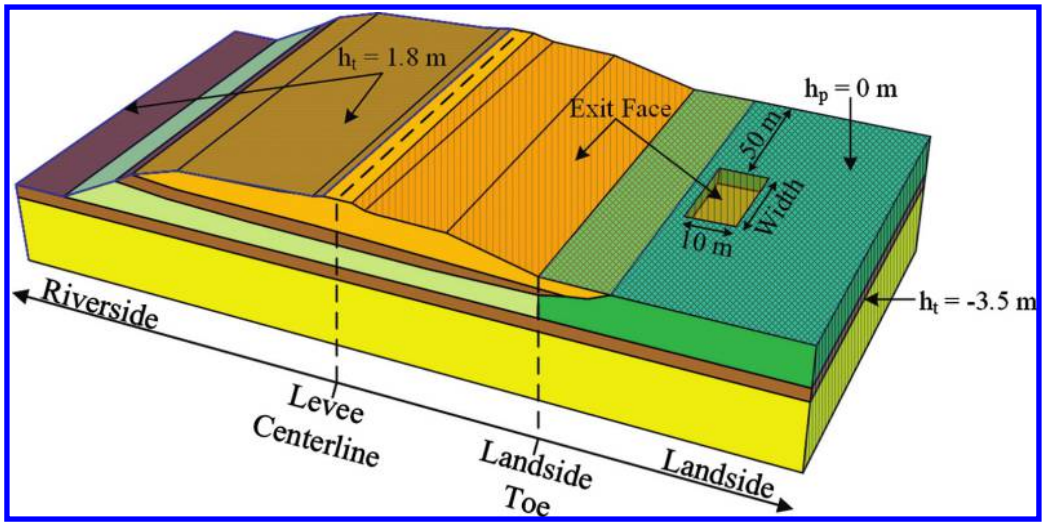

Fig. 4. 2D flow field and total head contours through excavation.

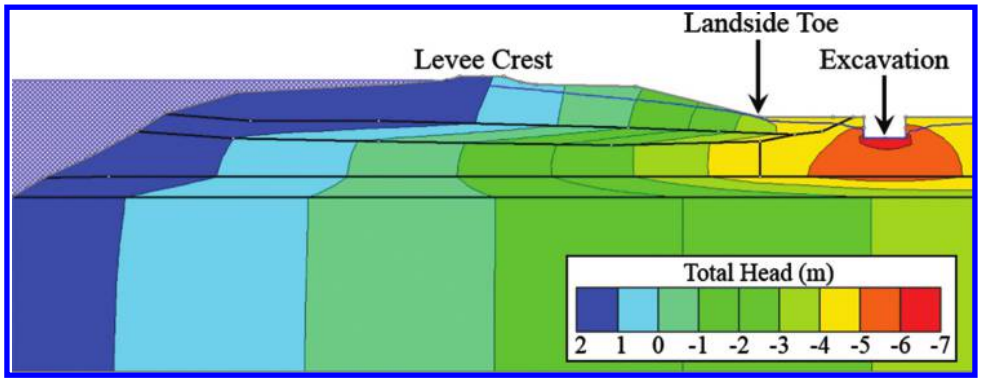

Fig. 5. Changes in vertical hydraulic gradient with increasing landside excavation width are compared with 2D seepage analyses through excavation.

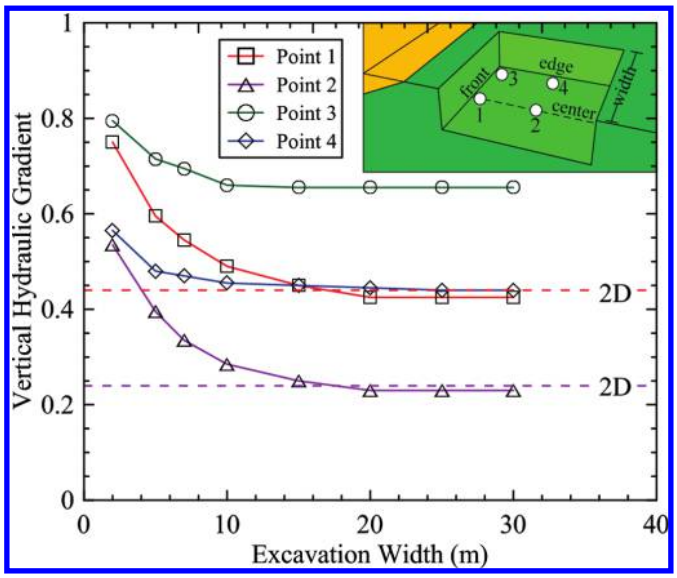

The analyses in Figs. 5 and 6 correspond to open excavations, which may be present for a temporary period. Closed excavations consist of an impermeable structure or lining, e.g., buried culverts, building foundations, and swimming pools, and can be prone to heave or sand boils around the excavation if excessive uplift pressures develop. Increases in uplift pressure can be facilitated by the structure not allowing migration of the hydraulic pressures and acting as a dam. Thus, it is necessary to compare the average uplift pressure in the excavation and the applied overburden stress. The uplift pressures were computed using RS³ by applying a no-flow boundary condition in the excavation bottom and sidewalls. This boundary condition yields an average 3D uplift pressure of 31 kPa. By estimating an overburden pressure due to the building or construction, the factor of safety against uplift for the building foundation can be computed.

The parametric analyses indicate that a 3D analysis should be used for a finite landside excavation with an aspect ratio less than 1*L*:1.5*W*. Because this aspect ratio is site specific and can depend on material hydraulic conductivity, soil profile, and excavation geometry and location from the landside toe, this example is used to simply illustrate the importance of 3D flow in landside excavations. Narrow excavations, e.g., trenches, pipelines, conduits, animal burrows, and tree stumps, are likely to impact floodwall or levee performance because vertical gradients rapidly increase below widths of 5 m. For cases such as drainage canals and toe ditches that run parallel to the levee and are greater than 15 m wide, the gradients at the center of the excavation are approximately equal to 2D vertical gradients, and therefore a 2D analysis can be performed.

Fig. 6. 3D total head contours for (*a*) model and landside excavation widths of (*b*) 5 m, (*c*) 10 m, (*d*) 20 m, and (*e*) 30 m.

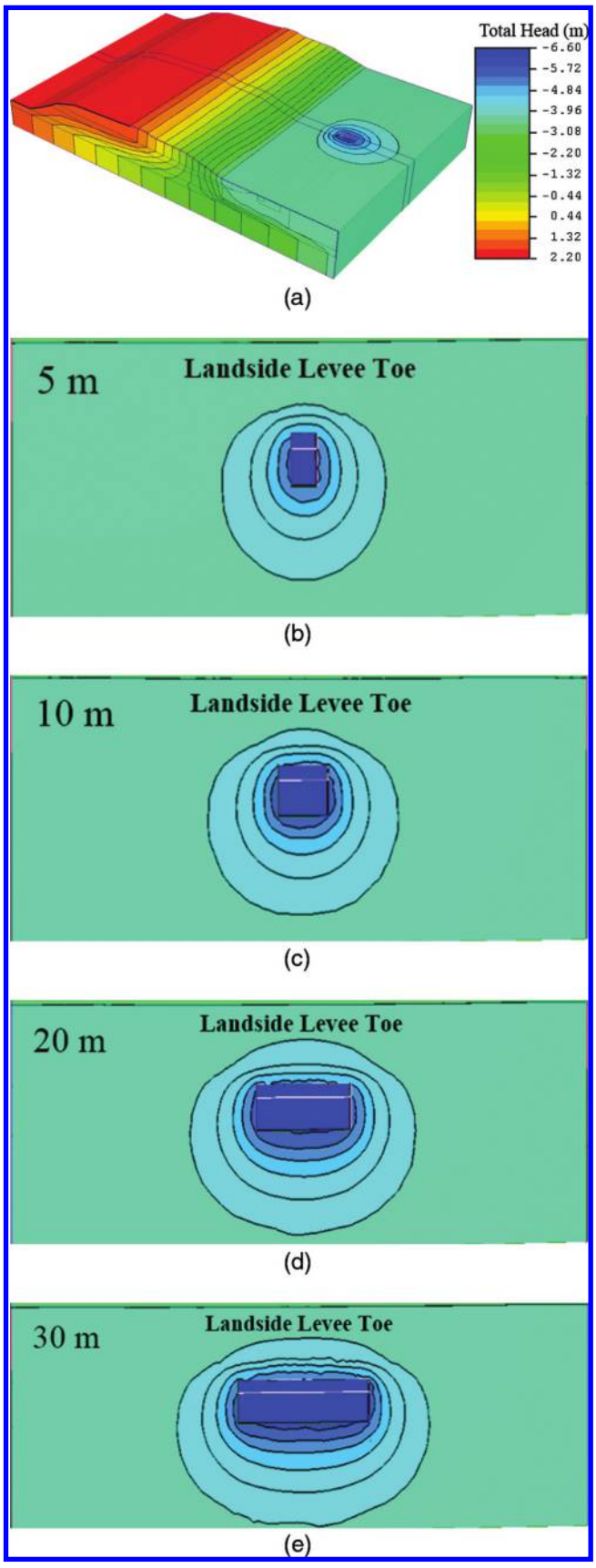

Unfortunately, Money (2006) reports that 3D vertical gradients can be 145% greater than 2D models for infinitely long landside excavations, e.g., toe drainage ditches. These results are in disagreement with Fig. 5, which illustrates long excavations, i.e., widths >15 m, approach 2D vertical gradients. The reason for this overprediction is not clear, but the authors recreated the Money (2006) 2D model and found that decreasing the mesh element size from 1.5 m (5 ft) to 0.15 m (0.5 ft) increased 2D hydraulic gradients closer to the 3D values. In other words, it appears the 2D values in Money (2006) are too low by about 145% possibly due to mesh size issues.

Effect of levee bends

The course of a river is classified as straight, meandering, or braided based on its sinuosity and other characteristics of the channel (Langbein and Leopold 1966; Morisawa 1985). Straight channels are slightly sinuous, and the occurrence of bends is random. Meandering channels can be highly convoluted or merely sinuous but maintain a single thread in curves having definite geometric shape. Braided channels are those with multiple streams separated by bars or islands, e.g., Sherman Island in Fig. 1*a*. Similar to the levees bordering Sherman Island in Fig. 1*b*, levee systems are constructed parallel to rivers and other water surfaces. As a result, levees consist of concave and convex bends, and these 3D effects can facilitate underseepage and instability.

Formation of 3D model

The 3D seepage model used to evaluate the effect of levee curvature was created in ModelMuse and input into MODFLOW 2005 (Harbaugh 2005). MODFLOW is a 3D groundwater model that can simulate steady and transient flow in an irregularly shaped flow system and with a combination of confined and unconfined aquifer layers. The surface and river topography for Sherman Island Stations 526–534 were developed from U.S. Geological Survey (USGS) geographic information system (GIS) data (Coons et al. 2008). The GIS data are imported into ModelMuse, and inverse distance square interpolation is used to create the 0.5 m surface contours in Fig. 7. MODLFOW uses the finite-difference solving method and discretizes the model into a grid. The grid spacing is defined in the *x*–*y* plane and then the model is constructed in the *z* direction by selecting a number of cells for each soil layer (see Fig. 7 for coordinate system). The grid consists of an equal spacing of 1 m by 1 m (each cell is 1 m^2) in the *x*–*y* plane, and 20 cells are specified in the *z* direction. The cells become denser in the *z* direction where changes in soil properties occur between layers.

Soil layers and material properties are defined by drawing polygons in the *x*–*z* plane and extruding these polygons in the *y* plane. Figure 8 shows the cross section that was used in MODFLOW. The subsurface profile in Fig. 8 is simplified compared to Fig. 2 because sufficient data are not present to accurately address spatial variations in soil stratigraphy and material properties. As a result, the soil layers in Fig. 8 are modeled as layers of constant thickness and elevation. For example, the organic soil layer is modeled with a thickness of 8.5 m and is located between el. –12 and –3.5 m NAVD88.

The boundary conditions used in MODFLOW are depicted in Figs. 7 and 8. To create the hydraulic connection (LHS h_t = 1.8 m), a line is specified along the center of the river and extruded in the *z* plane. A constant river stage of el. +1.8 m NAVD88 is applied to the cells that intersect this plane. For the floodside surface total head condition, a polygon is extended in the *x*–*y* plane at el. +1.8 m NAVD88 and is applied to only the surface cells. The landside surface boundary is assumed to be "free draining", which corresponds to the SEEP/W seepage exit face boundary. For the vertical landside boundary condition, a line parallel to the levee crest is drawn 70 m from the landside toe. The line is extruded in the vertical direction to create a plane. The vertical plane is set to a total head value of –3.5 m, i.e., the ground surface elevation. As a result, the LHS and RHS boundary conditions are applied so that

Fig. 7. ModelMuse surface geometry created from GIS topographical elevations and 3D boundary conditions.

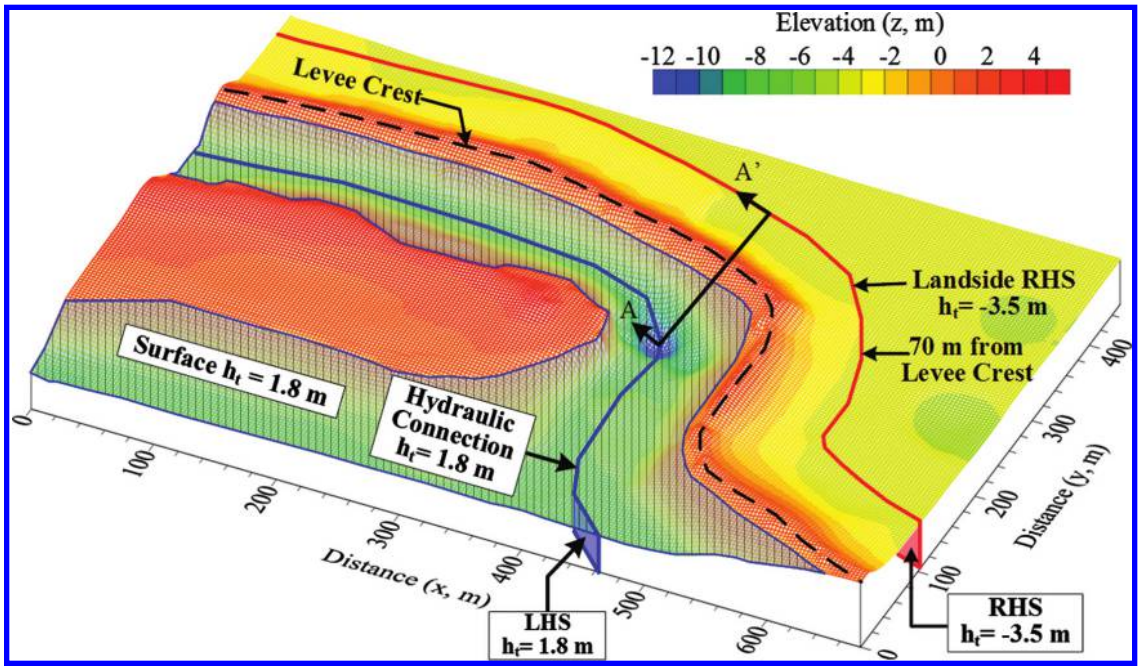

Fig. 8. Cross section A–A′ and boundary conditions of 3D model in MODFLOW at Station 532.

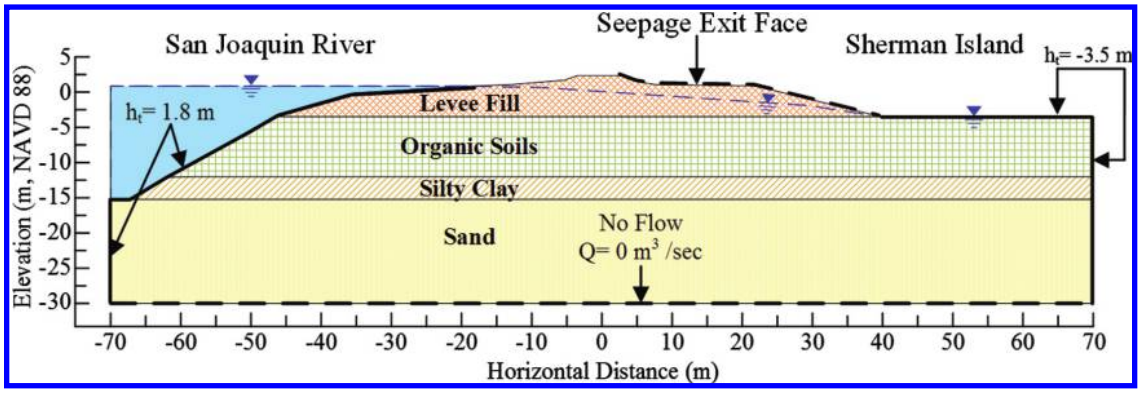

the model horizontal extents (–70–70 m) in Fig. 8 are the same as Fig. 2.

Sherman Island results

Figure 9 shows the MODFLOW hydraulic gradients at the landside toe from Stations 526 to 534. The aerial photograph in Fig. 1*b* shows the location of Stations 526–534 along the San Joaquin River. The vertical gradient is 0.36 at Station 526 and linearly decreases to a minimum of about 0.20 at Station 528. The vertical gradient remains in the range of 0.20–0.24 from Stations 528+00 to 532+50, and increases to 0.30 at Station 534. The low gradients between Stations 528 and 532 correspond to the concave curvature of the Sherman Island levee (see Fig. 1*b*). The corresponding 2D gradient at Station 532 in SEEP/W for the cross section in Fig. 8 is 0.32. This gradient comparison indicates that 2D results overpredict vertical gradients by about 160% (0.2–0.32) for concave bends. Hydraulic gradients approach the 2D model at Station 534 because the levee is transitioning to a straight segment. In addition, 3D vertical gradients are greater than 2D vertical gradients at Station 526+50 because of the convex curve at Station 525. Therefore, the 3D results in Fig. 9 highlight the important role of levee curvature and the necessity to evaluate 3D hydraulic gradients

Fig. 9. 3D vertical hydraulic gradients located between levee Stations 526 and 534.

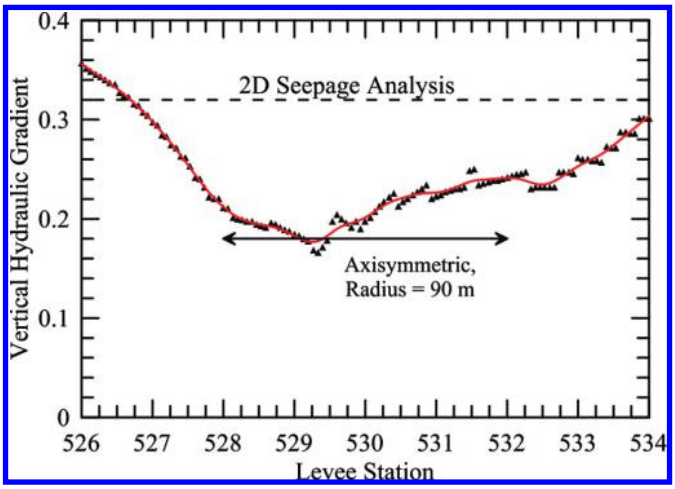

Fig. 10. Example of SGC for $\omega = 110°$: (*a*) channel direction; (*b*) levee meander.

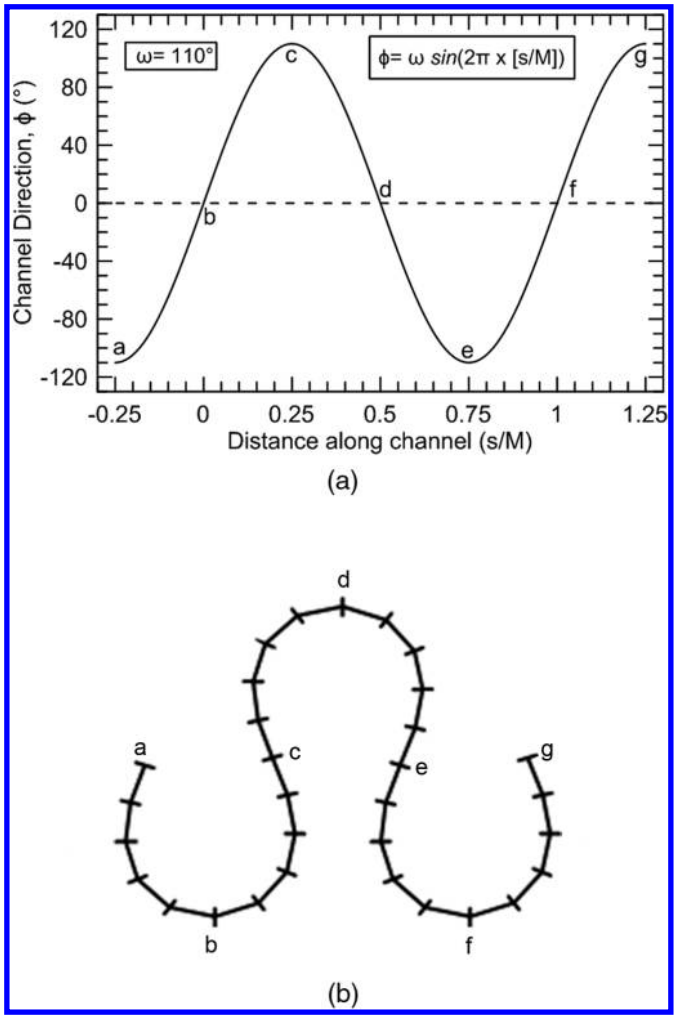

Fig. 11. Various SGC simulating levee bends used in 3D parametric analyses: (*a*) $\omega = 45°$; (*b*) $\omega = 60°$; (*c*) $\omega = 90°$; (*d*) $\omega = 100°$.

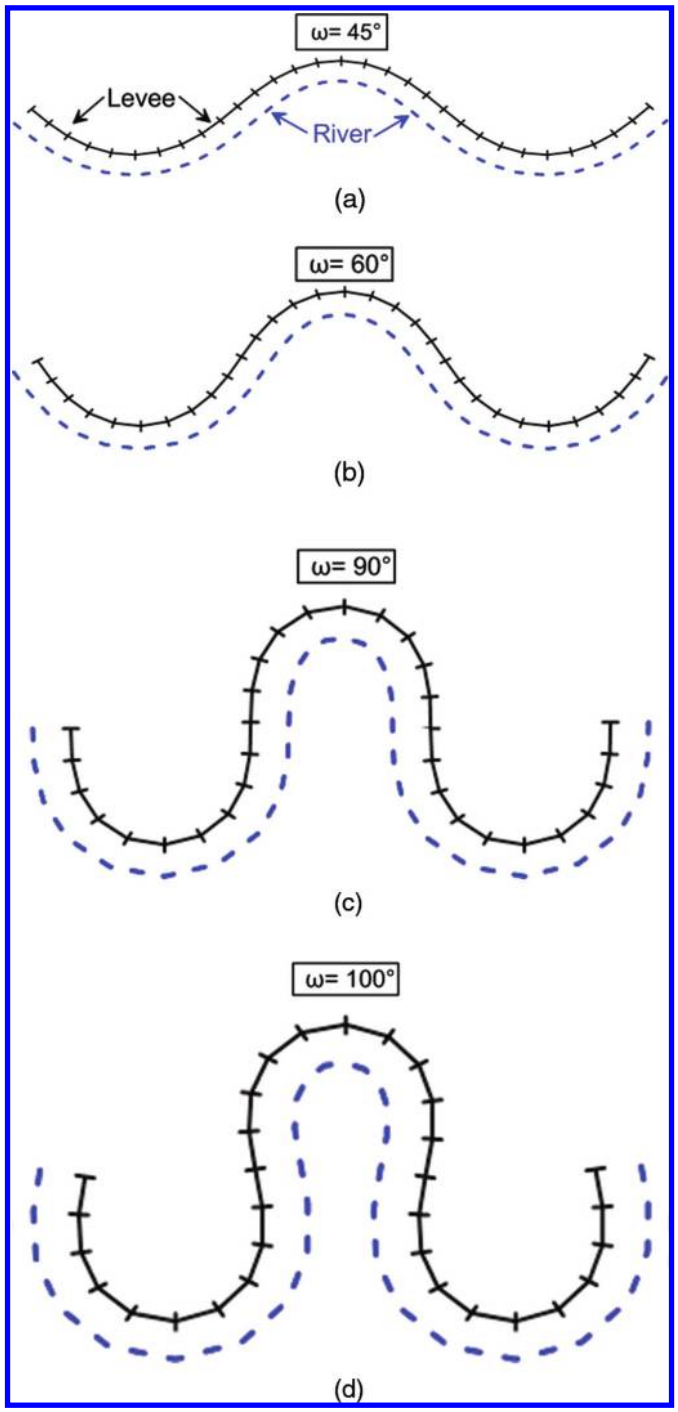

with methods that go beyond 2D plane strain analyses, especially where convex bends are present.

Levee bend parametric analyses

Typical river meanders do not follow common geometric curves, therefore Langbein and Leopold (1966) describe meander loops as sine-generated curves (SGC). They reason the SGC curve is statistically probable because it requires the smallest variation in change of direction and hence represents the least amount of work by the river. The SGC is recognized as descriptive of a self-forming river planform geometry (Yalin 1992; Soar and Thorne 2001). The planimetric geometry described in Langbein and Leopold (1966) of river meanders is defined as

$$\phi = \omega \sin\left(\frac{s}{M} 2\pi\right) \quad (1)$$

where ϕ equals the meander direction (angle) at location s, ω is the maximum angle the meander takes to the general direction of levee, and M is the levee length of a meander. Equation (1) defines the angular direction of the curve at various meander distances. Figure 10 shows an example of the SGC using $\omega = 110°$ in eq. (1) to calculate the channel direction (ϕ). The value of ϕ is zero at the curve apex (see points b, d, and f in Figs. 10*a* and 10*b*). The value of ϕ is equal to ω at points of inflection, which are illustrated in Fig. 10*b* at points c and e. Therefore, the angle ω is the critical parameter for specifying the amount of sinuosity or horseshoe looping and ranges from zero for a straight levee to a maximum of 125°.

The SGC is adopted herein for characterizing levee bends because levees are constructed parallel to rivers. Figure 11 shows four SGC examples of levee meanders used in the parametric analyses. As the value of ω increases, the meander changes from a sinuous curve to a horseshoe shape. The river in Fig. 11 is depicted at a constant distance perpendicular to the levee. In this parametric analysis, the various levee meander profiles in Fig. 11 are modeled in MODFLOW (see Fig. 12 for $\omega = 60°$) and are used to evaluate the effect of levee curvature on 3D vertical gradients. The soil

Fig. 12. MODLFOW topography and boundary conditions used in levee curvature parametric analyses (Fig. 9 shows 2D cross section of soil profile).

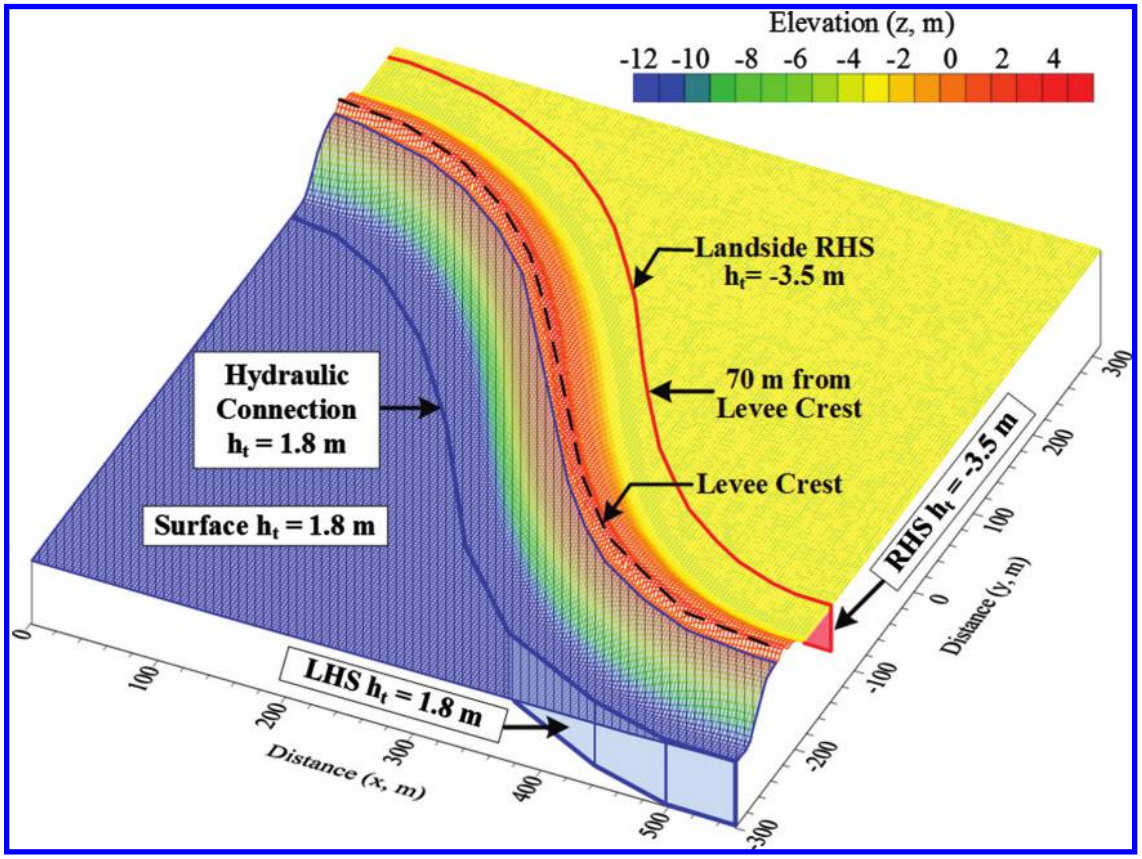

profile and boundary conditions are illustrated in Figs. 8 and 12, and are applied in the same procedure as the MODFLOW Sherman Island 3D analysis. Because the levee meanders in Fig. 11 are symmetric, the segment between points b and d in Fig. 10*b* is modeled and shown in Fig. 12.

Parametric results

Figure 13 shows the landside levee toe hydraulic gradients for ω values of 45°, 60°, 90°, and 100°. The gradients for all ω values are equal to the 2D gradient of 0.32 at the inflection point, where the levee segment is straight between convex and concave bends. From distance 0 m (the inflection point) to 200 m (maximum convex curvature), the vertical gradients increase to a maximum value at the convex bend apex. For ω of 90° and 100°, the maximum gradients approach 0.5 while gradients of about 0.4 correspond to ω of 45° and 60°. Thus, increasing convex curvature results in vertical gradients that are about 150% greater than the 2D model. Concave bends yield hydraulic gradients in the range of 0.22–0.28 for all ω values, which are slightly less than 2D values. Figure 13 shows that the concave gradients at maximum curvature are within a narrower range (~0.06) than convex bends (~0.12). Because the levee changes to a horseshoe shape at ω of 100° (see Fig. 11*d*), this causes the floodside boundary to enclose the landside area. As a result, the 3D underseepage concentrates flow into the landside and gradients increase more rapidly. In contrast, concave bends divert seepage away from the landside so 3D effects between ω values are less pronounced. As the levee curvature transitions from ω of 60° to 90°, the convex gradients in Fig. 13 increase from ~0.39 to ~0.48. The increase in gradient of ~25% indicates a critical ω value and levee curvature between 60° and 90° where 3D effects can contribute more to landside vertical hydraulic gradients.

Figure 14 presents the landside toe vertical gradients along the levee meander (distance from 0 to ±200 m) as a function of radius. The meander distance from 0 to ±200 m is divided into 200 nodes. A radius is determined for each node (n) by inscribing a circle that is tangent to the node n and neighboring nodes ($n+1$ and $n-1$). In Fig. 15, the radii for ω of 45°, 60°, 90°, and 100° corresponding to the levee bend apex (see Fig. 10 point b) are 305, 220, 155, and 150 m, respectively. These radii represent the maximum curvature of meanders in Fig. 11 and hence signify the critical section for evaluating vertical hydraulic gradients. Figure 14 shows the vertical gradients converge to the 2D value of 0.32 when radii are above ~1000 m, or close to the inflection point. The vertical gradients in Fig. 14 are also independent of ω because the 3D flow has been transformed from Cartesian to radial coordinates, i.e., equivalent radii correspond to equal gradients.

Axisymmetric model and results

The steady-state equation for radial flow is

$$\frac{k_r}{r}\frac{\partial h_t}{\partial r} + k_r\frac{\partial^2 h_t}{\partial r^2} + k_z\frac{\partial^2 h_t}{\partial z^2} = 0 \quad (2)$$

where k_r and k_z are the hydraulic conductivities in the radial and vertical directions, respectively; r is the radius; and h_t is the total head (Connor and Brebbia 1976; Bennett et al. 1990; Reddy 1993; Rao 1999). Because steady-state flow is present in eq. (2) and the hydraulic conductivity values remain constant, the rate of change

Fig. 13. Results of 3D levee curvature analyses and comparison with values from 2D seepage analyses.

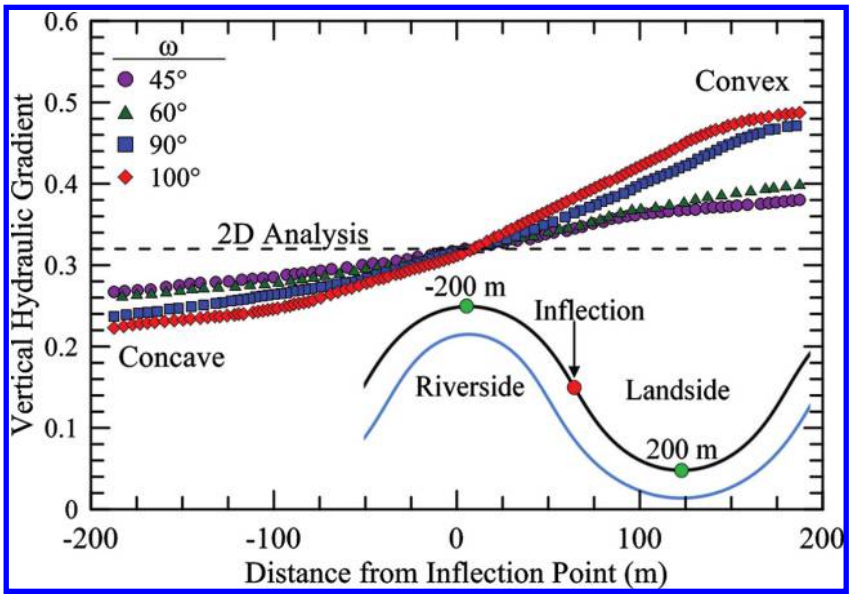

Fig. 14. Comparison of 3D MODFLOW parametric analysis and axisymmetric model.

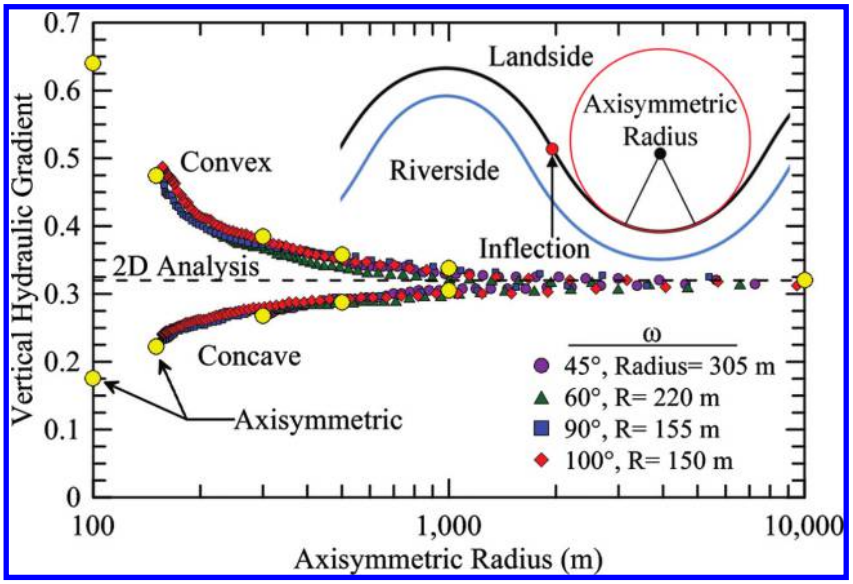

in total head in the radial direction ($\partial h_t/\partial r$) must increase as radius decreases. To compensate for the progressive decrease in flow area (radius is decreasing), $\partial h_t/\partial r$ must increase towards the axis of symmetry, which is similar to a drawdown curve. In a concave bend where the axis of symmetry is located in the floodside, decreasing the radius causes more head loss to occur before reaching the landside toe. In contrast, decreasing the radius of a convex bend generates higher total heads and vertical gradients near the landside toe before the sharp drawdown curve at the axis of symmetry.

Merry and Du (2015) use an axisymmetric model to compare hydraulic gradients of plane strain and curved levees, but do not investigate whether or not an axisymmetric analysis can accurately model 3D levee meanders. The Sherman Island cross section in Fig. 8 and levee meander parametric analysis in Fig. 11 provide an opportunity to use 3D MODLFOW results to evaluate the accuracy of axisymmetric models in curved levee seepage analyses. An axisymmetric formulation involves a 2D cross section where the origin of the horizontal axis is taken as the axis of symmetry. In an axisymmetric analysis, a concave levee bend rotates with respect to the floodside while a convex bend rotates with respect to the landside. An assumption in axisymmetric modeling is the LHS, RHS, levee centerline, and levee landside toe should all lie within concentric circles. For example, if a levee radius of 300 m describes a concave bend and the levee toe is located 20 m from the levee centerline, the radius at the levee toe is assumed to be 320 m. SEEP/W also rotates the model about the origin, so the model cannot transverse into the negative x axis.

When developing a plane strain 2D analysis, the LHS of the model is extended to the river or hydraulic boundary centerline. The RHS boundary is recommended to be extended sufficiently such that the boundary condition does not affect pore-water pressures near the levee. Several trial analyses are required to locate the RHS boundary. An axisymmetric model can be developed once the limits (RHS and LHS) of the plane strain model are selected. The axisymmetric radius describing the levee meander must be outside of the horizontal extent of the plane strain model. For example, Fig. 15 shows the calibrated Sherman Island cross section in

Fig. 15. Axisymmetric model of Sherman Island.

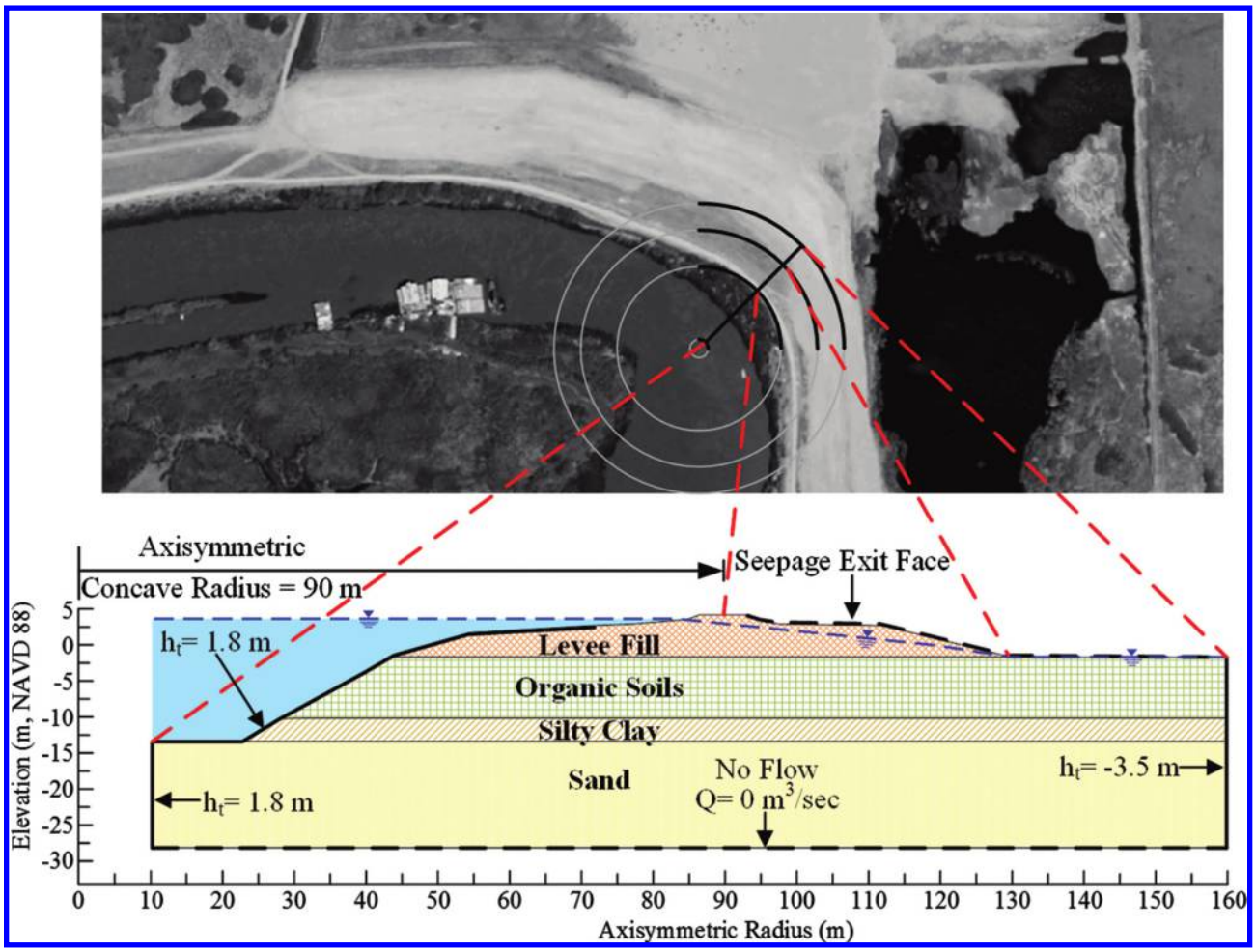

Fig. 2 in terms of an axisymmetric formulation. The axis of rotation in Fig. 15 is located at the origin or r = 0 m, and the 2D model starts at r = 10 m. The axis of rotation is located on the floodside because of the concave bend. The axisymmetric radius, defined from levee centerline to model origin, is determined by specifying three points along the levee crest and the following graphical procedure:

1. Draw two chords through points 1 and 2 and points 2 and 3.
2. Draw a perpendicular line from the midpoint of each chord so they intersect. The point of intersection is the center and origin of the axisymmetric analysis, and the distance between the center and any of the points is the radius of the circle.

An axisymmetric radius of 90 m is computed between Stations 528 and 532 in Fig. 15. The concave curve at Station 528 is modeled in SEEP/W with the boundary conditions depicted in Fig. 15. The axisymmetric vertical gradient of 0.18 between Stations 528 and 532 is displayed in Fig. 9 and shows that the 3D model and axisymmetric analysis in SEEP/W are in close agreement at the point of maximum curvature. The axisymmetric model and MODFLOW gradients separate after Station 530 because the axisymmetric model assumes the levee section is a circle, but the levee section (see Fig. 15) is straightening and therefore gradients begin to increase to 2D plane strain condition.

An axisymmetric model is also developed for the levee meander parametric analysis because convex (converging) and concave (diverging) flow conditions are present. The axisymmetric boundary conditions and soil profile are applied in a similar manner as in Fig. 15. Various radii ranging from 100 to 10 000 m are conducted to compare axisymmetric results with the levee meander vertical gradients in Fig. 14. The circular dots in Fig. 14 represent the axisymmetric vertical gradients and are found to match the MODLFLOW parametric analysis. Because the meanders in Fig. 11 are reduced to a series of radii (using the node procedure), equivalent radii develop the same vertical gradients independent of ω. Therefore, the radius of curvature can be used in an axisymmetric analysis to evaluate vertical gradients at a levee bend.

Table 3 summarizes the 3D and 2D vertical gradients for the levee meander parametric analysis. The MODFLOW and axisymmetric vertical gradients are 0.64 at r = 100 m, and thus a factor of 2 greater than the 2D gradient of 0.32. As the radius approaches 1000 m, the normalized values approach 1.05. The concave 3D results show 2D gradients overpredict gradients by about 1.8 and similarly approach 2D gradients at r = 1000 m. Based on the specific soil properties and cross section modeled, Table 3 shows that 3D analyses via MODFLOW and (or) axisymmetric are necessary to capture 3D effects of levee underseepage that are missed with a 2D analysis.

Axisymmetric analyses can be used to develop a design chart similar to Fig. 14 and Table 3 for levee segments with consistent subsurface profiles, boundary conditions, and material properties. The design chart can provide an approximation of 3D gradients for a range of radii. The radius of the levee bend is determined by the graphical procedure using three points along the levee centerline. If 3D uplift pressures that may cause sand boils or heaving are predicted, the uplift pressures or vertical

Table 3. Comparison of 3D and 2D vertical gradients for convex and concave levee bends.

	Convex vertical gradient		Concave vertical gradient	
Radius (m)	Axisymmetric and MODFLOW	Normalized[a] (3D/2D)	Axisymmetric and MODFLOW	Normalized[a] (3D/2D)
100	0.64	2	0.18	0.55
150	0.48	1.5	0.22	0.7
300	0.39	1.2	0.27	0.85
500	0.36	1.1	0.29	0.9
1000	0.34	1.05	0.31	0.95

[a]2D vertical gradient, 0.32.

gradients also can be used as input for design of remedial measures, such as relief wells, seepage berms, and cutoff walls.

Summary and conclusions

The state of practice to examine levee and floodwall seepage performance includes 2D plane strain FEA and analytical equations proposed in the USACE design manuals EM 1110-2-1901 and EM 1110-2-1913 (USACE 1993, 2000). The Sherman Island levee system is used to develop a calibrated seepage model and evaluate the effect of finite landside excavations and levee curvature on landside seepage results. This study shows that 2D analyses underpredict hydraulic gradients for convex levee bends and landside excavations with aspect ratios less than 1*L*:1.5*W*. The following observations and recommendations were derived from the 3D seepage analyses.

1. For the specific case of Sherman Island, a 3D analysis is required for a landside excavation with aspect ratios less than or equal to 1*L*:1.5*W*. The parametric analysis shows that narrow landside excavations, e.g., trenches, pipelines, conduits, animal burrows, and tree stumps–trunks, are important because vertical gradients rapidly increase below widths of 5 m. For cases such as drainage canals and ditches that parallel the levee toe and are greater than 20 m wide, the gradients at the center of the excavation are essentially equal to 2D vertical gradients. The critical location at a finite width excavation occurs near the edge of the excavation because of seepage inflow from the sidewalls.
2. The 3D MODFLOW model of Sherman Island levee shows concave levee bends diverge seepage, leading to lower vertical hydraulic gradients compared to 2D plane strain seepage models. The analyses also show convex bends, e.g., near Station 525, yield gradients greater than 2D values while the vertical gradients approach the 2D value when the levee is straight (close proximity to Station 535).
3. The pattern of levee curvature is defined herein using the SGC developed by Langbein and Leopold (1966), which can be used to describe river channels. Sine-generated curves are defined by a circular arc in the bend portion and transition from a circle at the apex to a straight segment at the point of inflection. By varying ω from 45° to 100°, the field-calibrated parametric analyses indicate sharper convex bends ($\omega = 100°$) cause vertical gradients that are about 150% greater than a 2D seepage model. Concave bends yield similar gradients for all values of ω because seepage is diverging in many directions away from the landside toe. When a segment of a levee bend is defined in terms of a radius, the vertical gradients compared to a 3D seepage model are approximately equal. Radial flow depends on the radius; hence, equivalent radii produce equivalent gradients.
4. Axisymmetric seepage models can be used to evaluate 3D vertical hydraulic gradients for convex levee bends. Although levee geometry can be irregular, a circular arc can approximate the maximum curvature by defining a three-point circle for a levee bend. The three-point circle graphical procedure can be used to identify the center and radius of a circle. The axisymmetric radius along with a 2D plane strain subsurface profile, material properties, and boundary conditions can be used in an axisymmetric seepage model to estimate 3D vertical gradients.

Acknowledgements

The authors thank Emily MacDonald of Wagner & Bonsignore for sharing Sherman Island piezometer data. This material is based upon work supported by the National Science Foundation through a Graduate Research Fellowship to Navid H. Jafari. Any opinions, findings, and conclusions or recommendations expressed in this material are those of the authors and do not necessarily reflect the views of the NSF, USACE, USDOJ, or any other agency or individual.

References

Ahmed, A., and Bazaraa, A. 2009. Three-dimensional analysis of seepage below and around hydraulic structures. Journal of Hydrology Engineering, ASCE, **14**(3): 243–247. doi:10.1061/(ASCE)1084-0699(2009)14:3(243).

American Standards and Test Methods (ASTM). 2011. Standard practice for classification of soils for engineering purposes (Unified Soil Classification System). ASTM standard D2487. American Society for Testing and Materials, West Conshohocken, Pa.

American Standards and Test Methods (ASTM). 2013. Standard Classification of Peat Samples by Laboratory Testing (D4427). *In* 2013 Annual Book of ASTM Standards, Volume 04.08. American Society for Testing and Materials, Philadelphia. doi:10.1520/D4427.

American Standards and Test Methods (ASTM). 2014. Standard Test Methods for Moisture, Ash, and Organic Matter of Peat and Other Organic Soils (D2974). *In* 2014 Annual Book of ASTM Standards, Volume 04.08. American Society for Testing and Materials, Philadelphia. doi:10.1520/D2974-14.

Benjasupattananan, S., and Meehan, C.L. 2012. Deterministic and probabilistic approaches for two- and three-dimensional levee underseepage analyses. *In* Proceedings Dam Safety 2012, ASDSO, Denver, CO, pp. 1–21.

Bennett, G.D., Reilly, T.E., and Hill, M.C. 1990. Technical training notes in ground-water hydrology: Radial flow to a well. U.S. Geological Survey, Water Resources Investigations Report 89-4134.

CALFED (CALFED) Bay Delta Program. 2000. Levee system integrity program plan, Final Programmatic EIS/EIR Technical Appendix.

California Department of Water Resources (DWR). 2005. Flood warnings: Responding to California's flood crisis, Resources Agency of California.

Cobos-Roa, D., and Bea, R. 2008. Three-dimensional seepage effects at three New Orleans levee breaches during Hurricane Katrina. Electronic Journal of Geotechnical Engineering, **13**(Bund. K): 1–26.

Connor, J.J., and Brebbia, C.A. 1976. Finite element techniques for fluid flow, Newnes-Butterworths, Boston, MA.

Coons, T., Soulard, C., and Knowles, N. 2008. High-resolution digital terrain models of the Sacramento/San Joaquin Delta region, California. USGS Data Series, **359**: 1–12. Available from http://pubs.usgs.gov/ds/359/.

Du, R. and Merry, S.M. 2014. The effect of the waterside boundary condition on the seepage and slope stability analyses of the Natomas Levees – A case study. *In* Proceedings of the GeoCongress 2014, Atlanta, GA, February 23–36, ASCE Geotechnical Special Publication 234, pp. 1511–1524.

Foott, R., Sisson, R., and Bell, R. 1992. Threatened Levees on Sherman Island. *In* Proceedings Stability and Performance of Slopes and Embankments II, ASCE, Berkeley, California, pp. 756–774.

Geo-Slope. 2007. Slope/W software Users Guide. Geo-Slope International Ltd., Calgary, Canada.

Hanson, J.C. (Hanson) Consulting Civil Engineer. 2009. Reclamation District 341 Sherman Island five-year plan, SH 08-3.0. California DWR, Sacramento, CA.

Harbaugh, A.W. 2005. MODFLOW-2005, The U.S. Geological Survey modular ground-water model—the ground-water flow process, USGS Techniques and Methods 6-A16.

Langbein, W.B., and Leopold, L.B. 1966. River meanders – Theory of minimum variance, physiographic and hydraulic studies of rivers, U.S. Geological Survey Professional Paper 422- H, H1-H15.

Merry, S.M., and Du, R. 2015. Plane strain versus axisymmetric modeling of convex levees. accepted for publication. Journal of Geotechnical and Geoenvironmental Engineering, ASCE, **141**(4): 04014121. doi:10.1061/(ASCE)GT.1943-5606.0001255.

Mesri, G., and Ajlouni, M. 2007. Engineering properties of fibrous peats. Journal of Geotechnical and Geoenvironmental Engineering, ASCE, **133**(7): 850–866. doi:10.1061/(ASCE)1090-0241(2007)133:7(850).

Mesri, G., Stark, T.D., Chen, C.S., and Ajlouni, M. 1997. Secondary compression of peats with and without surcharging. Journal of Geotechnical and Geoenvironmental Engineering, ASCE, **123**(5): 411–421. doi:10.1061/(ASCE)1090-0241(1997)123:5(411).

Money, R. 2006. Comparison of 2D and 3D seepage model results for excavation near levee toe. *In* Proceedings Geo-Congress 2006: Geotechnical Engineering

in the Information Technology Age, Atlanta, GA, 26–28 February 2006, American Society of Civil Engineers, 1–4.

Morisawa, M. 1985. Rivers: Form and process, Geomorphology Texts, Longman, New York.

Prokopovitch, N.P. 1985. Subsidence of peat in California and Florida. Environmental & Engineering Geoscience, **22**(4): 395–420. doi:10.2113/gseegeosci.xxii.4.395.

Rao, S.S. 1999. The finite element method in engineering, 3rd ed. Butterworths-Heinemann, Boston, MA.

Reddy, J.N. 1993. An introduction to the finite element method, 2nd Ed., McGraw-Hill, Hightstown, NJ.

Rocscience. 2014. RS^3 User's Guide. Rocscience Inc. Toronto, Canada.

Shelmon, R.J., and Begg, E. 1975. Late quaternary evolution of the Sacramento-San Joaquin Delta, California. *In* Quaternary Studies Bulletin, **13**. *Edited by* R.P. Suggate and M.M. Creswell. Wellington, NZ, pp. 259–266.

Soar, P.J., and Thorne, C.R. 2001. Channel restoration design for meandering rivers, ERDC/CHL Report CR-01-1, USACE Engineer Research and Development Center, Vicksburg, Mississippi.

Stark, T.D., and Jafari, N.H. 2015. Ruling on IHNC floodwall failures during Hurricane Katrina. Journal of Legal Affairs and Dispute Resolution, ASCE, **7**(3): 06715001. doi:10.1061/(ASCE)LA.1943-4170.0000167.

URS. 2013. Guidance document for geotechnical analyses, DWR Urban levees evaluations project, Version 13, Sacramento, CA.

U.S. Army Corps of Engineers. (USACE). 1993. Seepage analysis and control for dams. EM 1110-2-1901, Department of the Army, Washington, D.C.

USACE. 2000. Engineering and design—design and construction of levees. EM 1110-2-1913, Department of the Army, Washington, D.C.

USDA. 2014. Geospatial Data Gateway. Available from http://datagateway.nrcs.usda.gov/GDGHome.aspx [accessed 18 October 2013].

Washington Group International (WGI). 2005. Post-NFAATT groundwater characterization report, Inner Harbor Navigation Canal, East Bank Industrial Area. Washington Group International, Inc.

Weber, W.G. 1969. Performance of embankments constructed over peat. Journal of the Soil Mechanics and Foundations Division, ASCE, **95**(SM1): 53–76.

Yalin, M.S. 1992. River mechanics, Pergamon Press, Oxford.

NOTES

Asphalt Resurfacing after a Geohazard Repair

Paul Travis, E.I., P.L.S.[1]

Abstract: Landslides are a common occurrence on many roads in the United States and beyond. This class of geohazard usually begins as cracks in the asphalt pavement and then a "drop" in the pavement elevation; usually occurring on the roadway's outboard side away from any slope. A common remedy is to pave over the "dropped" portion of the roadway to "even up" the surface. This works for a short time; however, the additional weight of asphalt actually makes the slip accelerate and the road to fail at a faster pace. Permanent repair for these geohazard involves an engineered solution that provides additional resistive forces to retain the failing slope section. Reducing driving or causative forces is usually not an option.

After a repair system has been installed, roadway managers typically apply an asphalt pavement patch over the existing repair area to restore the cracked or dropped pavement. If this re-surfacing operation is performed too soon or improperly, reflective cracking most assuredly will reappear in the repaired surface pavement.

This paper will provide recommendations for re-surfacing roadways following geohazard repairs based on assessments of project instrumentation, other observations, and our general experience.

[1] Senior Project Development Engineer, Geostabilization International, Richmond, Kentucky.
Email: paul@gsi.us

NOTES

NOTES

NOTES

Earthquake Hazard Mitigation in Memphis

Ashraf S. Elsayed, Ph.D., P.E., D.GE[1]

Abstract: Earthquakes have resulted in significant damages to buildings, transportation and infrastructure facilities over the years. The Memphis area is prone to damage from earthquakes from the New Madrid seismic zone (NMSZ). Memphis is located within the Upper Mississippi embayment. The embayment is a trough like depression that plunges southward along an axis that approximates the course of the Mississippi River. The deep soil deposits of the Mississippi embayment have a pronounced yet not fully understood influence on the amplification and attenuation of ground motions associated with NMSZ. Young river deposits are susceptible to liquefaction, which can result in significant damage to foundations, slopes and buried structures. Geotechnical engineers are striving to better understand the liquefaction phenomenon, the likelihood of its occurrence and how to mitigate its impact by utilizing various ground improvement techniques. Advanced site-specific hazard and ground response analyses performed on medium to large projects have resulted in code-allowed reductions in design seismic accelerations and consequently significant cost savings in the design and construction of foundations and superstructures. Geotechnical Seismic retrofit/mitigation was recently performed on two projects in the Memphis area. These are the Bass Pro Shop at the Pyramid and the I-40/I-240 Interchange Phase II. Geotechnical seismic mitigation will also be performed at the site of the new TVA Combined Cycle power plant. This presentation includes a brief overview of the seismic hazard in the Memphis area, a typical approach to its assessment from geotechnical standpoint and details about the case histories mentioned above.

[1] Chief Engineer, Geotechnology, Inc., Memphis, Tennessee. Email: aelsayed@geotechnology.com

GEOTECHNOLOGY INC
FROM THE GROUND UP

EARTHQUAKE HAZARD MITIGATION IN MEMPHIS

Presented by:
Ashraf S. Elsayed, Ph.D., P.E., D.GE

Ohio River Valley Soil Seminar XLVIII
November 17, 2017

QUALITY · INTEGRITY · RESPONSIVENESS · PARTNERSHIP · OPPORTUNITY · SAFETY

Outline

- Why do earthquakes happen
- Earthquake hazards in Memphis
- What we typically do to investigate
- Mitigation case studies
  - The Pyramid (Bass Pro Shops)
  - The I-40 / I-240 East Interchange (Phase II)
  - TVA Allen
- Q's

The Earth's Crust

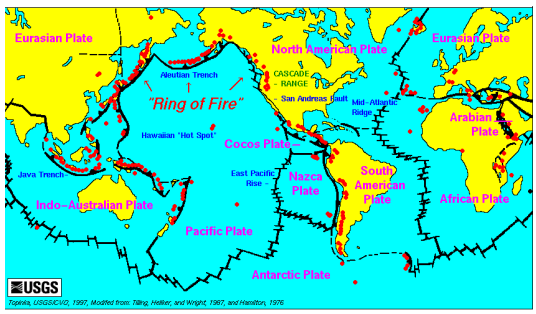

Why Do Earthquakes Happen?

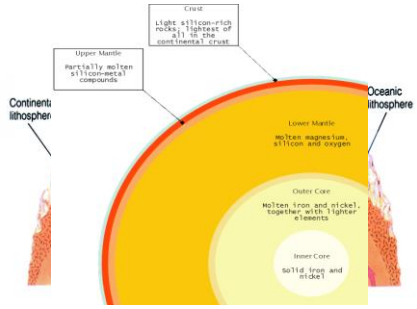

1964 Niigata, Japan (M_W 7.5)

Seismic Activities in Central U.S.

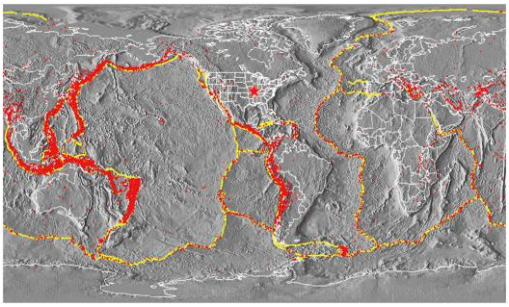

New Madrid Seismic Zone

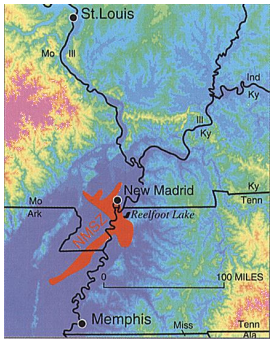

Geologic-Tectonic Setting

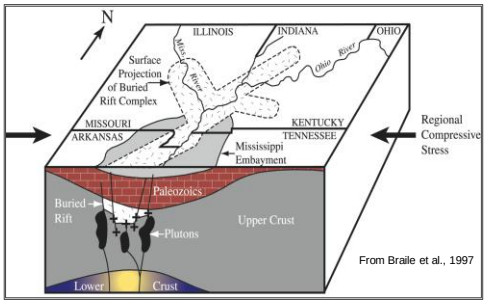

From Braile et al., 1997

New Madrid Seismic Zone

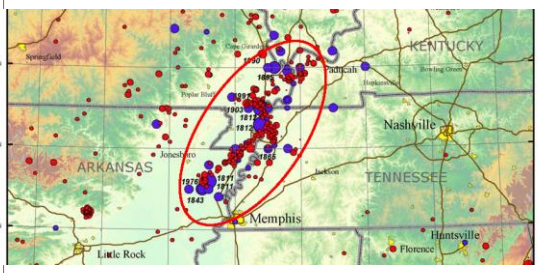

- Most seismically active area east of Rocky Mountains
- Produces 200 earthquakes annually in M 1.5-4 range
- Largest recorded event M 5 near Marked Tree in 1976

Provided By M. Tuttle

Why is the NMSZ different?

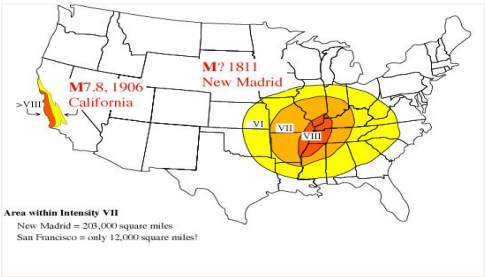

Earthquake Hazards

- Mainly liquefaction-related
  - Bearing capacity loss
  - Lateral soil reaction and downdrag of deep foundations
  - Floating of buried structures
- Dynamic settlement
- Flow slide & lateral spreading
- Retaining wall failures
- Slope instability

Seismic Hazard Evaluation

- Applicable building code(s)
- Subsurface exploration
- Geotechnical evaluation
  - Preliminary site assessment
  - Liquefaction analysis
  - Site-specific seismic study

Evaluation of Liquefaction Potential

- Simplified Procedure
  - Seed & Idriss, 1982
  - Boulanger & Idriss, 2014
    - Calculate CSR (demand)
    - Calculate CRR (resistance)
  - FOS = (CRR/CSR) * *MSF*

How Do We Evaluate

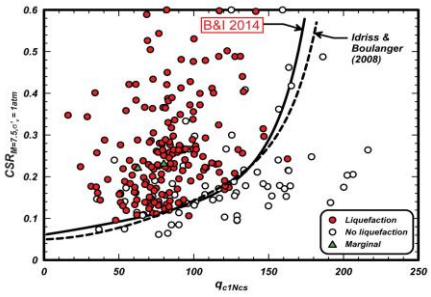

Probabilistic Approach to Liquefaction

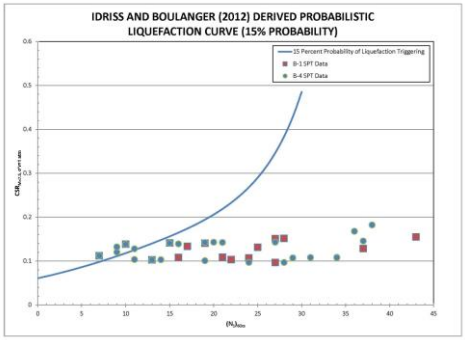

Standard Penetration Testing (SPT)

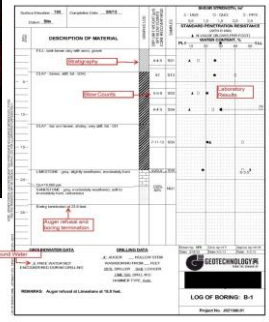

CPT

CPT

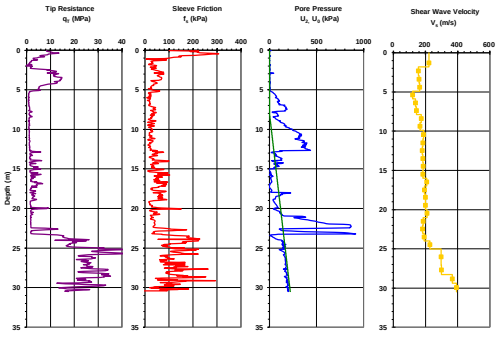

Site-Specific Seismic Study

- Two sub-studies:
  - Site-specific hazard analysis
  - Site-specific ground response analysis
- Results can allow for reduction in design seismic accelerations:
  - Up to 20% (IBC)
  - Up to 33% (AASHTO)

What do we do to mitigate the hazard

- Typically: nothing below ground surface
  - We make the design team & Owner aware
  - Superstructure is designed by the applicable code, with no ground improvement or modifications
- Three Exceptions:
  - Bass Pro Shops (The Pyramid)
  - I-40/I-240 East Interchange Phase II
  - TVA Allen Power Plant

Outline

- Background
- Due Diligence & Subsurface Exploration
- Seismic Concerns
- Retrofit & Construction details

Background

- Former Basketball arena opened in 1991
- Designed per the 1982 Standard Building Code
- In 2004 the Grizzlies moved to the FedEx Forum

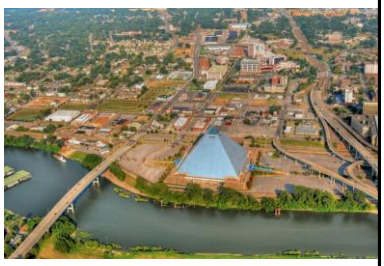

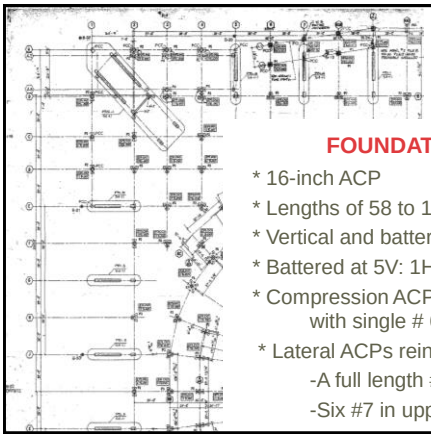

FOUNDATIONS

* 16-inch ACP
* Lengths of 58 to 113 ft
* Vertical and battered ACP
* Battered at 5V: 1H
* Compression ACPs reinforced with single # 6 full length
* Lateral ACPs reinforced
  - -A full length #7 bar
  - -Six #7 in upper 20 feet

Corner Buttress Detail

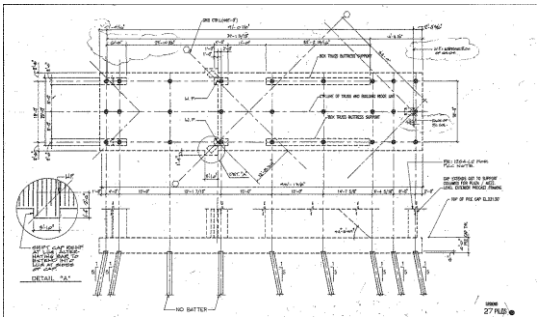

New Development

- After years of negotiation, the City of Memphis entered into an agreement with Bass Pro Shops:
  - A 55-year lease; $1M per year
  - The City: $78M investment, including ~$30M for seismic upgrade
  - Bass Pro: $191M of total investment

Due Diligence

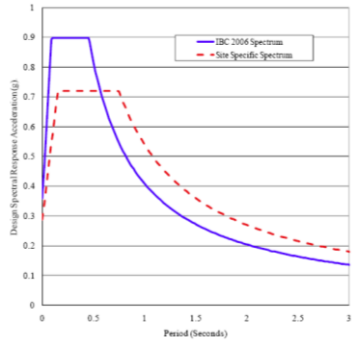

Figure 5. Design Response Spectra.

Subsurface Exploration

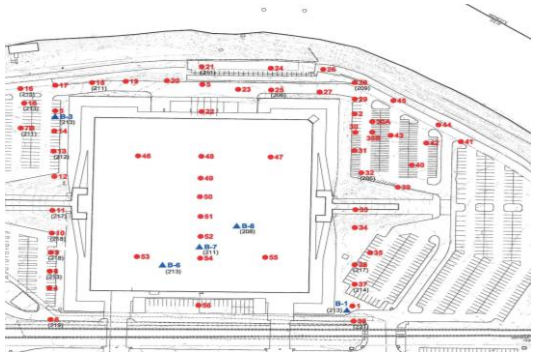

Site Exploration

SPT

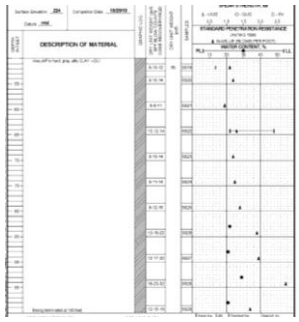

CPT

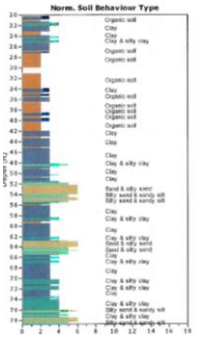

Typical Section

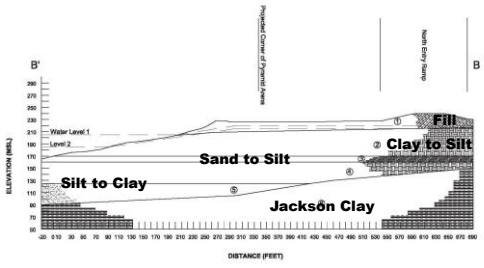

Liquefaction Potential

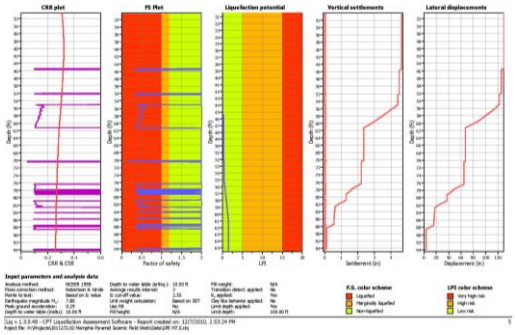

Potential Slope Instability

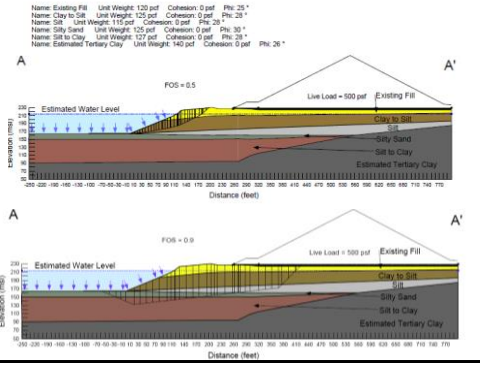

Pyramid Seismic Upgrade

- Upgrades included three Approaches
- Mitigating risk of seismically induced slope instability and lateral spread.
- Underpinning existing Pyramid foundations
- Additional strengthening of Pyramid structure

Below Ground Seismic Upgrade

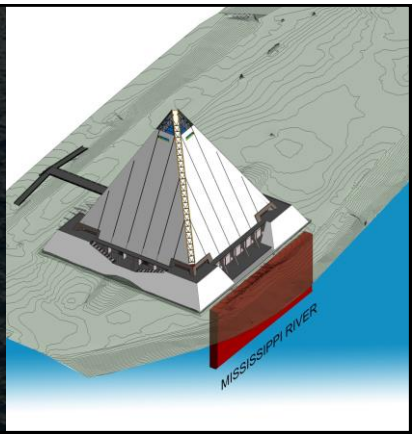

Above Ground Seismic Upgrade

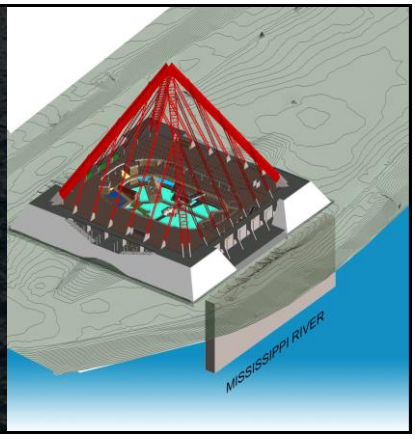

Reducing Effects of Lateral Spread

- Proposed Barrier Wall / Buttresses

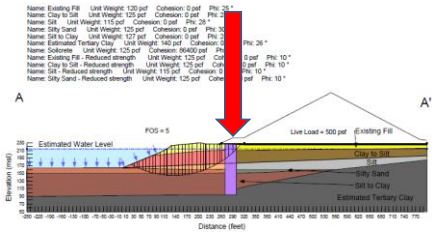

Performance Specification

Structural Engineer provided criteria for pile cap lateral displacement using ASCE SEI 41-06 Seismic Rehabilitation of Existing Buildings

- Case 1, 10% PE in 50 years (Life Safety Performance)
  PGA = 0.20g
- Case 2, 2% PE in 50 years (Collapse Prevention)
  PGA = 0.37g

Criteria for Analysis

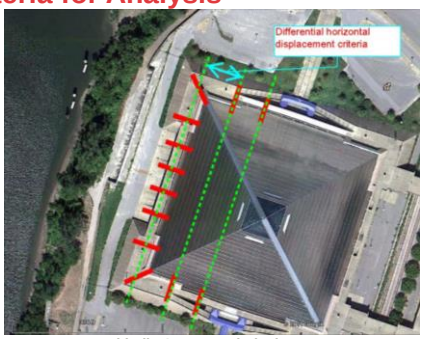

Pyramid Pile Cap Lateral Displacement
1 inch in 100 feet

Chris-Hill Construction Co. "Shear Fins"

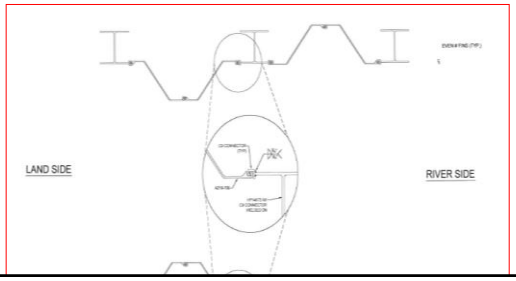

Shear Fin Layout

Shear Fin Installation

Existing Foundation Strengthening

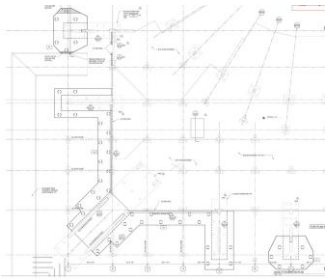

Combination of :

- Dual drilled displacement piles, 24-inch
- Driven Pipe Piles, 24-inch

FAMBO Hydraulic Hammer

I-40/I-240 East Interchange

Outline

- Need for better design information
  - Site-Specific Seismic Study
  - CPT Soundings
- Seismic concerns
  - Seismic Stability of slopes and Retaining walls
  - Driven pile embedment

Site Specific Study

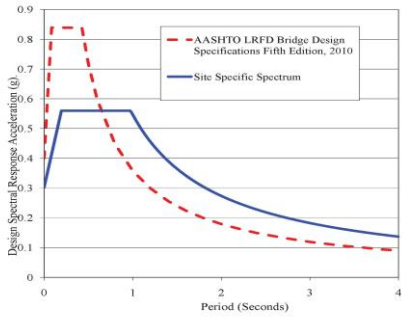

Benefit of Site-Specific Study

I-40/I-240 Interchange Bridge1, Memphis, TN

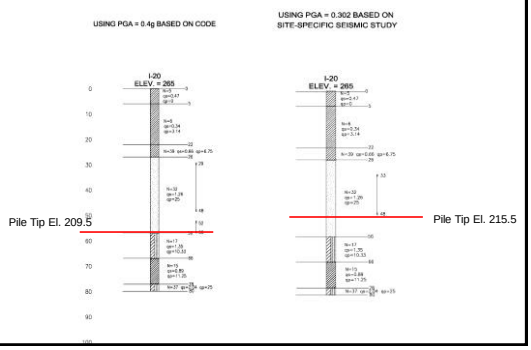

Supplemental Liquefaction Study

Impact of Pile Driving

CPT Areas of Study

Supplemental Liquefaction Study

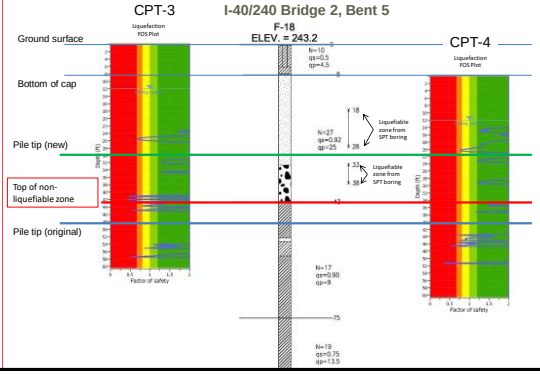

Walls 17 and 19

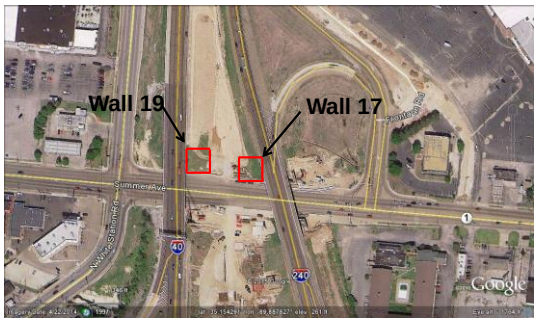

Wall No. 19

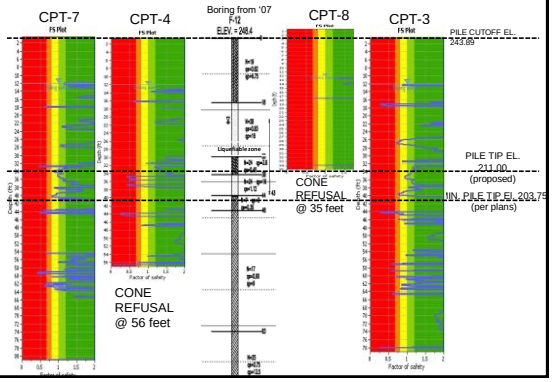

Walls 15 and 16

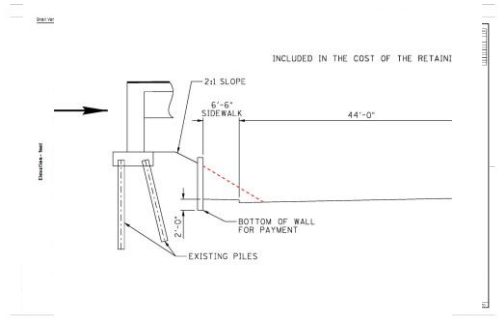

Wall 10

- Two approved wall types
  - Soldier Pile (embedded in drilled shafts) & Lagging Wall
  - Pile-supported Cantilever Wall
- TDOT set maximum deflection (6 inches)
- Procedure:
  - Determine the required force per shaft (based on wall configuration and pile spacing) to achieve a FoS of 1.10
  - Perform LPILE analysis (Chapter 10 Duncan & Wright) to determine min. shaft embedment below failure surface, bending moment and lateral deflection

Wall 10

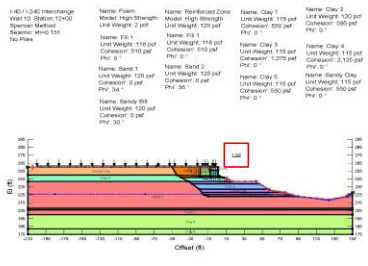

Wall 10

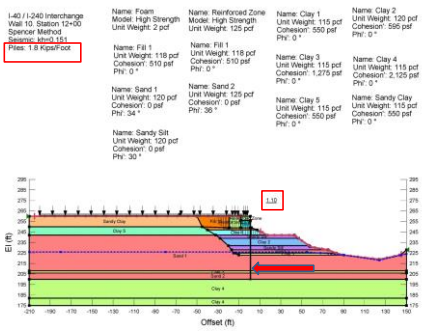

Wall 10: Design Concept

- Pile-Supported, CIP wall with geofoam backfill

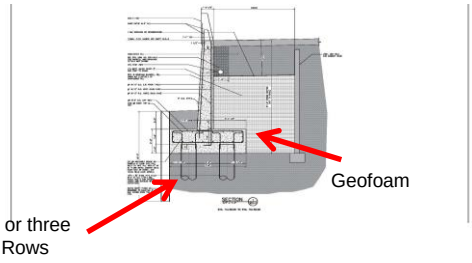

LPILE Analysis

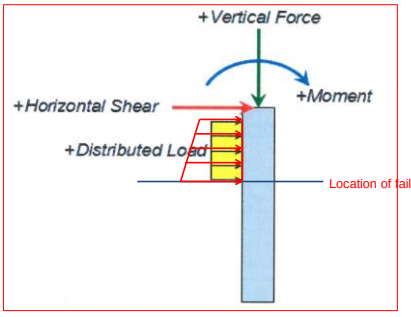

Wall 10 Construction

TVA Allen Combined Cycle Plant

Project Information

- $160M Design / Build Project
- Primary structures:
  - Two combustion turbine-generators (CTGs)
  - A turbine hall building
  - Two heat recovery steam generators (HRSGs)
  - One steam turbine generator (STG)
- Seismicity is a major concern

Subsurface Exploration

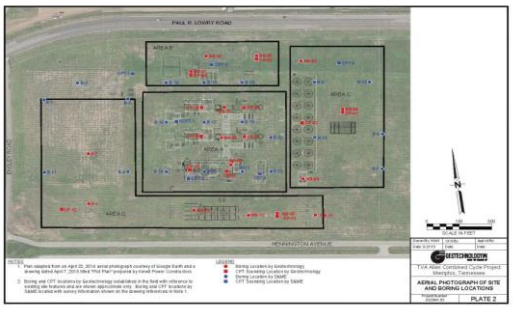

Geotechnical Evaluation

- Site-Specific seismic study
- Two events: 2% and 10% PE in 50 years
- SPT- & CPT-based liquefaction hazard evaluation
- Analysis indicated significant potential for liquefaction and post-earthquake dynamic settlement

Site-Specific Seismic Study

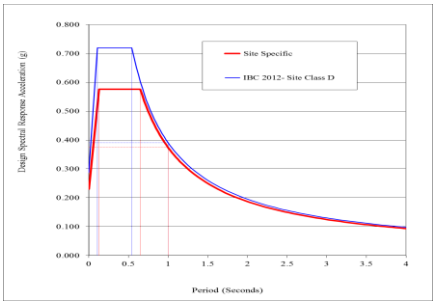

Geotechnical Evaluation cont.

- Kiewit to utilize Cast-in-Place Ground Improvement Elements (CGEs) for ground improvement, settlement control and liquefaction mitigation
- CFA Deep foundation (Augercast & drilled-displacement piles)
- Static and post-liquefaction capacity recommendations

Main Geotechnical Challenge: Lateral Displacement (LD)

- Initial study concluded LD of 60 inches to be used in the structural design
- Impact:
  - Tighter CGE and pile installation
  - Addition cost: $30M
- Geotechnology was asked to perform additional LD evaluation

Lateral Spreading

Lateral Displacement (LD) Evaluation

- Geotechnology collected additional information and performed LD analyses using 2 different methods
  - Zhang et al. (2004)
  - Youd et al. (2002)

Analysis Results

Youd et al. | Based on 10 SPT Borings				
Estimated Lateral Displacement, inch Distance to the nearest Seismic Energy Source = 63 km				
Method	Sloping Ground Without Free Face			Level Ground With Free Face
	Slope = 0.33%	Slope = 0.50%	Slope = 0.67%	
Range	0-9	0-10	0-11	Negligible
Average	4	5	6	
Standard Deviation	3	3	4	

- Conclusion: estimated LD =3-6 inches
- Cost saving: ~$30M

Project Status

Geotechnical Challenges – The I-40/I-240 Interchange Phase II

Ashraf S. Elsayed, Ph.D., P.E., D.GE[1]

Abstract: The I-40/I-240 interchange is formed by I-40 to the north and east, I-240 to the south, and Sam Cooper Boulevard (SCB) to the west. The current average daily traffic (ADT) on I 40 is approximately 200,000 vehicles and is expected to be over 350,000 vehicles by 2035. The project includes modifying four existing bridges, constructing two new bridges and 23 retaining walls. The existing low-speed ramps will be replaced by two-lanes, high-speed fly-over structures. The final interchange configuration will include four levels, the first of its kind in west Tennessee. The estimated construction period is 39 months and started in October 2013. Two types of driven piles are used to support the bridges. These are 14-inch-square, pre-stressed concrete piles and open-ended steel pipe piles. The pile embedments vary from 15 to 85 feet. Approximately 97,500 feet of concrete and steel pipe piles will be driven to support the bridges. Additional concrete piles were also required to support ten, wrap-around retaining walls. The design team concluded that utilizing dynamic testing of at least two production piles per site condition, but no less than 2% of the production piles would yield a more economical approach because of reduced testing cost and expedited pile installation time. The project created several geotechnical challenges and the geotechnical team needed to answer the following questions

1. Can pile setup in western Tennessee be estimated with an acceptable accuracy?
2. Can one or more of the available pile driving formulae (i.e., dynamic formulae), be used to predict the long-term nominal axial resistance indicated by the dynamic testing results?
3. How should the pile terminal driving resistance be used for quality control?
4. How can the impact of driving displacement piles be into liquefiable soils, in terms of increasing the soil driving and liquefaction resistance be assessed and utilized?
5. How can the global stability of existing bridge approaches that will be widened be improved to meet the minimum required factors of safety in both static and seismic conditions without flattening side slopes due to right-of-way restrictions?
6. How can the abutment slopes of existing bridges be upgraded to current AASHTO seismic requirements without closing the bridges?
7. How can the bearing resistance of existing soil be significantly improved to support retaining walls up to 35 feet in height?

These challenges created opportunities for innovation. The geotechnical team developed a formula for predicting long-term pile resistance using early-stage test results. Recommendation for specific pile driving formulae and the terminal blow counts were

[1] Chief Engineer, Geotechnology, Inc., Memphis, Tennessee. Email: aelsayed@geotechnology.com

made based on statistical analyses of the available data. The team also utilized soil reinforcement techniques to improve soil bearing resistance. A combination of soil nails and anchors was utilized to stabilize existing abutment slopes. Light-weight backfill was utilized for constructing specific retaining walls. The impact of pile driving on liquefaction mitigation was assessed using Cone Penetration Testing (CPT) and consequently utilized to reduce pile embedments. The team also utilized deep foundation to improve the factor of safety against global stability failure for the first time in West Tennessee.

GEOTECHNICAL CHALLENGES: I-40/I-240 INTERCHANGE PHASE II

Presented by
Ashraf S. Elsayed, Ph.D., P.E., D.GE

Ohio River Valley Soil Seminar XLVII
Cincinnati, OH
November 17, 2017

OUTLINE

- Project Overview
- Pile dynamics
- Seismic issues
- Retaining walls
- Q's

I-40/I-240 EAST INTERCHANGE

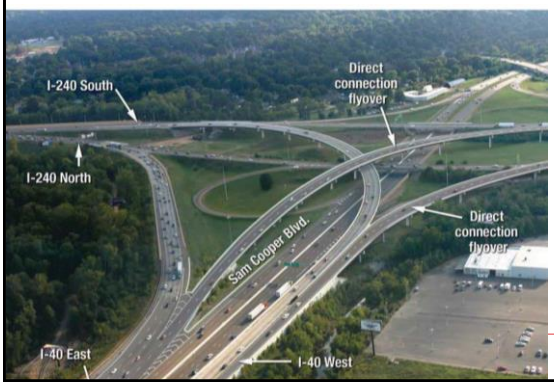

PROJECT SUMMARY

- Busiest intersection in TN (more than 200,000 vehicles currently, over 350,000 vehicles by 2035)
- Largest project contract awarded by TDOT (~$110M) at the time
- Design is accordance with 2012 AASHTO LRFD
- Six bridges: 2 new direct flyovers, Improvement of 4 existing bridges
- 23 retaining walls
- Noise walls
- More than 100,000 feet of piles
- Construction period: 42 months

GEOTECHNICAL SUBSURFACE EXPLORATION

- Started in 1999
- Completed in 2013
  - 340 SPT borings
  - Conventional sampling & testing
  - Supplemental Cone Penetration Testing (CPT)
- Two site-specific seismic studies

GENERAL SUBSURFACE CONDITIONS

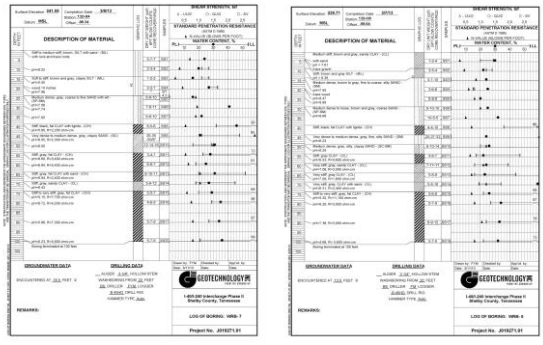

SITE-SPECIFIC SEISMIC STUDY

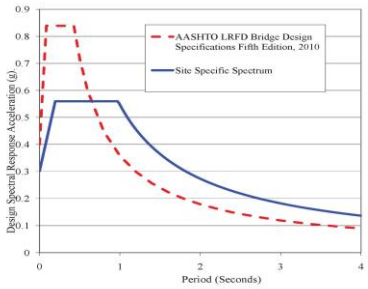

BENEFIT OF SITE-SPECIFIC STUDY

I-40/I-240 Interchange Bridge1, Memphis, TN

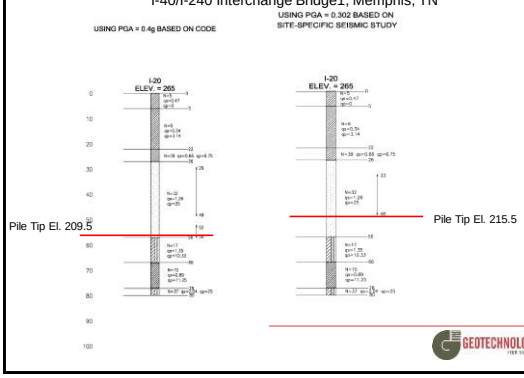

PILE DYNAMICS

- Pile resistance has been typically evaluated by performing static load tests
- Installation blow counts of driven piles have been used as a QC tool
- The Engineering News (EN) formula has been used to assess the capacity (FoS = 6.0)
- TDOT decided to allow high-strain dynamic testing of piles as the sole method of resistance evaluation

PILE DYNAMICS cont.

- A resistance factor of 0.65 in the design (dynamic testing of at least two production piles per site condition, but no less than 2% of the production piles)
- Testing was performed on production piles during initial driving and 7-day restrike
- The nominal axial resistances were then estimated using the CAse Pile Wave Analysis Program (CAPWAP)

TEST PILE INSTALLATION SUMMARY

Test No.	Bridge No.	Bent No.	Pile No.	Embed. (ft.)	Average of Bottom 5 feet		Average of Bottom One foot	
					Stroke (ft.)	Blow Count (blows/ft.)	Stroke (ft.)	Blow Count (blows/ft.)
1	1	3	71	29.0	7.60	60	8.50	64
2		5		37.0	7.80	112	7.80	117
3		7	64	28.0	7.70	69	7.60	75
4		RW17	8	45.0	7.90	83	8.00	70
5	2	RW19	23	49.0	7.70	74	7.70	79
6		2	1	34.0	7.80	87	8.00	98
7		4	1	19.0	7.50	116	7.80	118
8		5	64	23.0	8.70	53	9.00	52
9		7	64	37.0	9.00	59	9.00	62
10		9	1	30.0	7.90	141	8.30	117
11		11	72	30.0	5.90	67	6.60	150
12		12	8	14.5	6.60	33	7.10	41
13		Abut. 2	1	31.0	5.60	155	5.70	201
14	4	RW12	1	18.0	7.50	50	7.70	60

SUMMARY OF TEST RESULTS

Test No.	Static Resistance (kip)	End-of-Drive CAPWAP Resistance (kip)	Restrike Age (Days)	Restrike CAPWAP Resistance (kip)		
				Total	Side	Tip
1	371	290	7	337	303	34
2	612	409	8	545	521	24
3	420	393	7	399	297	102
4	826	335	7	788	742	46
5	660	306	7	630	574	56
6	410	330	8	345	219	126
7	400	379	7	393	100	293
8	425	397	7	415	226	189
9	328	258	7	274	196	78
10	450	397	7	439	93	346
11	400	327	7	344	277	67
12	238	222	5	227	78	149
13	304	253	7	272	64	208
14	403	305	7	356	117	239

OBJECTIVES

- Can pile setup in western Tennessee be estimated with an acceptable accuracy?
- Can one or more of the available pile driving formulae (i.e., dynamic formulae) be used to predict the long-term nominal axial resistance indicated by the dynamic testing results?
- How should the terminal driving resistance be used for quality control?
- Can we detect pile damage due to overstressing during driving?

ESTIMATING SETUP

Modified Bogard & Matlock (B-M) equation:

$$Q(t) = Q_u\left\{\alpha + (1-\alpha)\left[\frac{\frac{t}{T50}}{1+\frac{t}{T50}}\right]\right\}$$

Q(t): the resistance at time t,

Q_u: the nominal resistance with 100% of setup realized

T_{50}: the time required to realize 50% of pile setup

α: empirical coefficient in the range of 0.2 to 0.5

SITE CORRELATION

- T_{50} was estimated to be 0.5 to 2 days, based on site conditions (low-plasticity clays, silts and sands)
- An α value of 0.2 appears to be suitable when tip resistance is less than 40 percent of the total resistance
- When tip resistance is more than 40 percent of the total resistance, an α value of 0.5 appears to be suitable

RESULTS

Bridge 1 Bent 3 (Test 1) α = 0.2 & 0.5

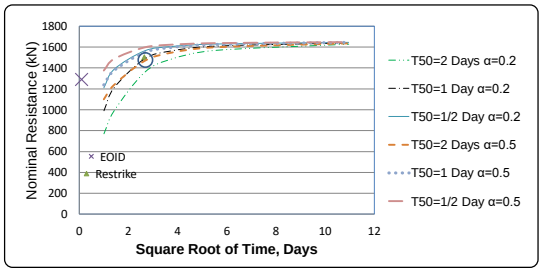

RESULTS cont.

Bridge 2 Abutment 2 (Test 13) α = 0.2 & 0.5

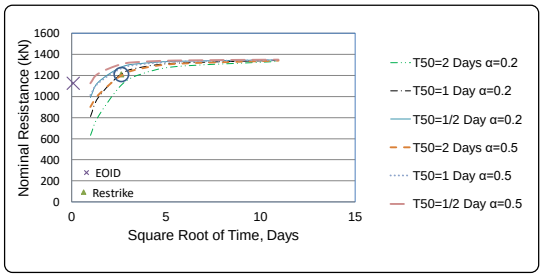

PILE DRIVING FORMULA

Three formula:

- Engineering News (EN)
- Modified Gates (MG)
- Washington DOT (WSDOT)

FORMULA COMPARISON

Test No.	Eng. News (EN) kips		Modified Gates (MG) kips		WSDOT kips	
	5 feet	1 foot	5 feet	1 foot	5 feet	1 foot
1	1221	1424	420	460	286	326
2	1814	1855	511	517	341	344
3	1354	1408	443	450	301	303
4	1556	1420	475	455	322	313
5	1415	1473	452	461	306	311
6	1579	1733	477	501	322	339
7	1776	1863	504	518	330	345
8	1284	1311	439	446	317	327
9	1429	1477	464	471	338	342
10	2056	1974	547	537	363	366
11	1018	1767	371	499	229	307
12	686	871	311	354	211	242
13	1521	1720	455	490	262	281
14	1063	1237	393	424	270	290

GEOTECHNOLOGY

FORMULA EVALUATION

Test No.	EN		MG		WSDOT	
	Diff. kips	DR_{u1}/R_{u5}	Diff. kips	R_{u1}/R_{u5}	Diff. kips	R_{u1}/R_{u5}
1	-204	1.17	-39	1.09	-39	1.14
2	-41	1.02	-6	1.01	-3	1.01
3	-54	1.04	-8	1.02	-2	1.01
4	136	0.91	20	0.96	9	0.97
5	-58	1.04	-9	1.02	-5	1.02
6	-153	1.1	-24	1.05	-18	1.05
7	-87	1.05	-14	1.03	-14	1.04
8	-27	1.02	-7	1.01	-9	1.03
9	-48	1.03	-7	1.02	-4	1.01
10	82	0.96	10	0.98	-3	1.01
11	-748	1.73	-127	1.34	-78	1.34
12	-185	1.27	-43	1.14	-31	1.15
13	-199	1.13	-35	1.08	-19	1.07
14	-174	1.16	-31	1.08	-21	1.08
Mean	-125.7	1.1	-22.8	1.1	-17.0	1.1
STDEV	206.0	0.2	35.0	0.1	21.7	0.1
COV,%	-163.9	17.8	-153.2	8.8	-127.4	8.8

GEOTECHNOLOGY

FORMULA COMPARISON cont.

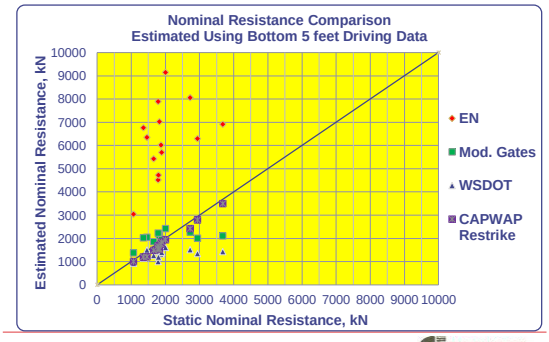

GEOTECHNOLOGY

CONCLUSIONS

•The MG and WSDOT driving formulae are more accurate than the EN formula in estimating nominal static resistance in west Tennessee. The use of the EN formula should be discontinued.

•The average driving data (blow count and hammer drop height) over the bottom 5 feet of driving is appropriate for friction piles in west Tennessee.

•The average should be taken over the bottom one foot if a layer of very dense material is present at or above the pile tip elevations.

•The Modified Bogard & Matlock equation can be used to provide a fairly accurate estimate of the CAPWAP restrike resistance in west Tennessee using the nominal long-term static resistance, α values of 0.2 to 0.5 and T_{50} values of ½ to 2 days.

PILE INTEGRITY

F = Zv Z = Impedance = EA/c

PILE INTEGRITY-cont.

- F = Zv Z = Impedance = EA/c
- When Impedance changes, part of the downward traveling stress wave is reflected up and part continues to travel down
- When the cross section of the pile is reduced, the up reflected stress wave is tensile, its magnitude indicates the extent of the cross section change

PILE INTEGRITY-cont.

- PDA calculates a relative integrity factor (β)
- When Impedance does not change, $\beta = 1$
- GRL recommendations (2007):
  - $\beta > 0.8$ → slight damage
  - $\beta < 0.6$ → serious damage

DETECTING DAMAGED PILES HAMMER MALFUNCTION


DETECTING DAMAGED PILES POOR SPLICING

PILE EMBEDMENT

- Piles are to penetrate through liquefiable soils into non-liquefying stratum
- There were difficulties achieving the design tip elevations at some locations
- Need to assess:
  - Pile resistance
  - Liquefiable zones
  - Change in subsurface conditions due to pile driving
- Need for reliable, quick subsurface information

CPT

CPT

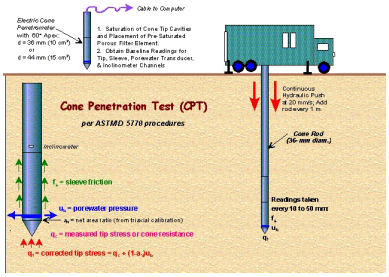

CPT

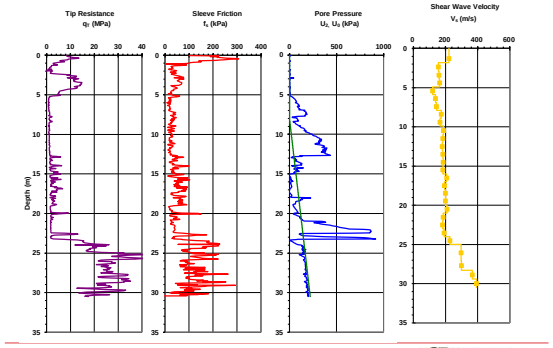

GEOTECHNOLOGY

CPT AREAS OF STUDY

GEOTECHNOLOGY

SUPPLEMENTAL LIQUEFACTION STUDY

GEOTECHNOLOGY

IMPACT OF PILE DRIVING

SUPPLEMENTAL LIQUEFACTION STUDY

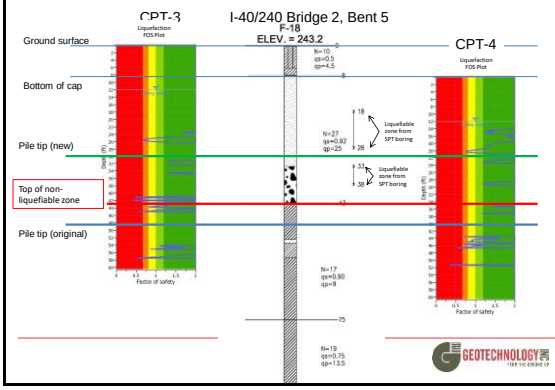

WALLS 17 AND 19

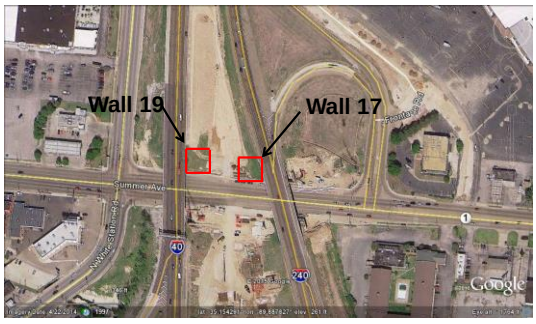

WALL NO. 19

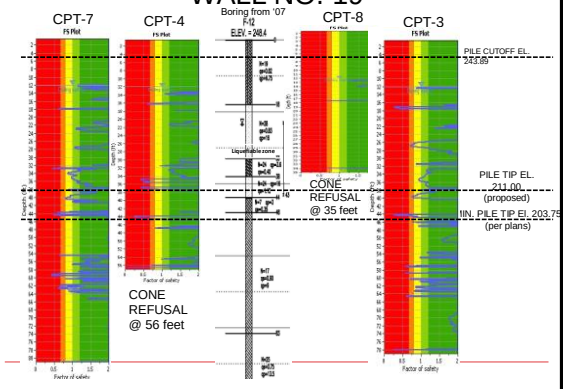

WALLS 15 &16

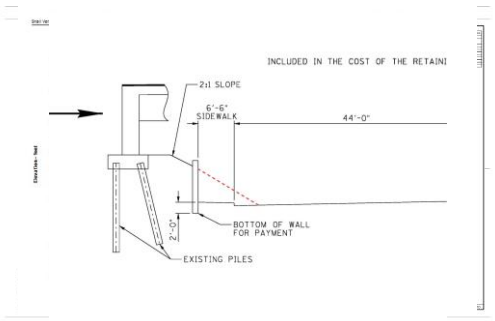

WALL 21

- Problem: Insufficient factors of safety against global instability in seismic conditions
- Solution: Ground improvement using rammed aggregate piers

WALL 21

WALL 10

- Needed to widen I-40 WB ramp
- Two approved wall types
  - Soldier Pile (embedded in drilled shafts) & Lagging Wall
  - Pile-supported Cantilever Wall
- TDOT set maximum deflection (6 inches for soldier pile wall and 2 inches for CIP wall)
- To reduce lateral pressure, EPS foam blocks & light-weight flowable fill are to be used for backfill

GEOTECHNOLOGY

WALL 10

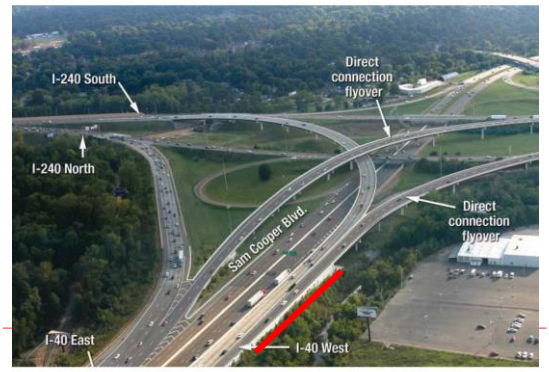

WALL 10 CHALLENGE

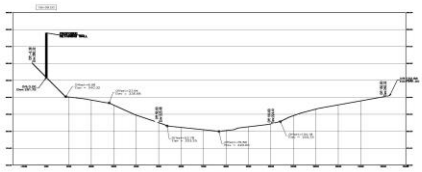

WALL 10 CHALLENGE cont.

- Global stability minimum factors of safety have to be satisfied:
  - 1.30 static
  - 1.1 seismic
- Initial design utilized soldier pile wall
- Procedure:
  - Determine the required force per pile (based on wall configuration and pile spacing) to achieve a FoS of 1.10
  - Perform LPILE analysis (Chapter 10 Duncan & Wright) to determine min. shaft embedment below failure surface, bending moment and lateral deflection

WALL 10

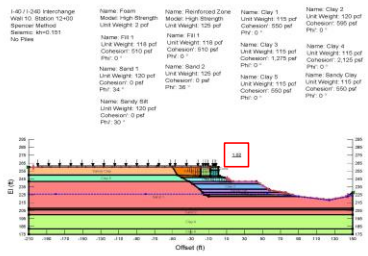

WALL 10

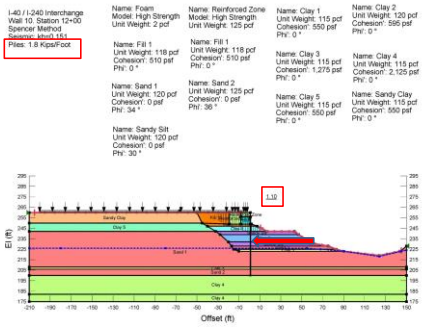

GEOTECHNOLOGY

LPILE ANALYSIS

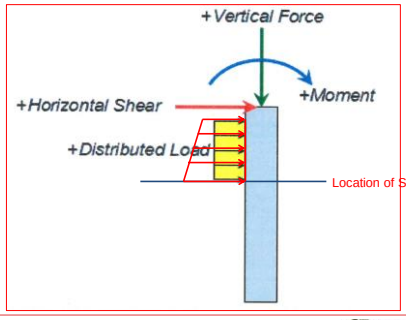

GEOTECHNOLOGY

WALL 10

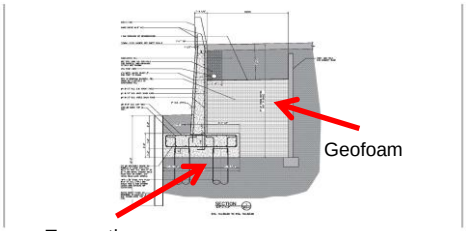

GEOTECHNOLOGY

WALL 10 – GROUP ANALYSIS

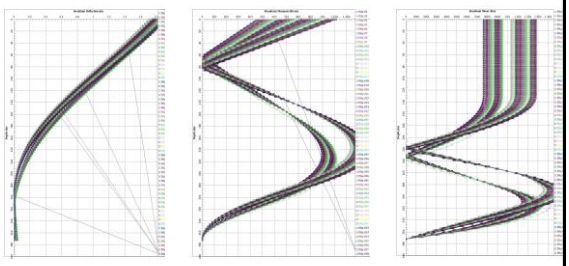

WALL 10 CONSTRUCTION

WALL 10 CONSTRUCTION

PROJECT PROGRESS (JUNE 2015)

GEOTECHNOLOGY

GEOTECHNOLOGY

BRIDGE 2

GEOTECHNOLOGY

BRIDGE 1

PROJECT PROGRESS (August, 2016)


aerial

Presentation Topics

1. Project Description
2. Site Introduction / Characteristics
3. Seepage Challenges
4. Dam-Related Improvements Overview
5. Spillway Improvements
6. Road Widening / Dam Armoring
7. Constructed Views

Project Location

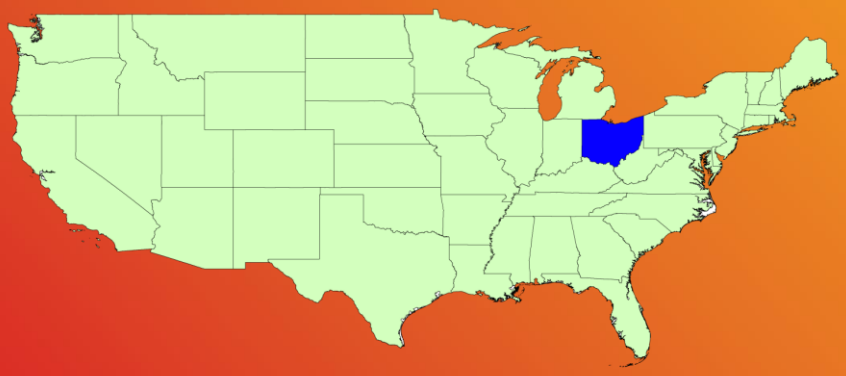

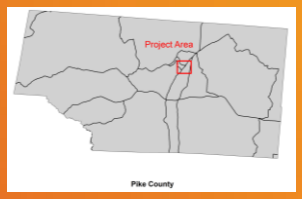

Location: Pike County, Ohio (near Waverly)
Lake Usage: Recreational

Stantec

Project Description

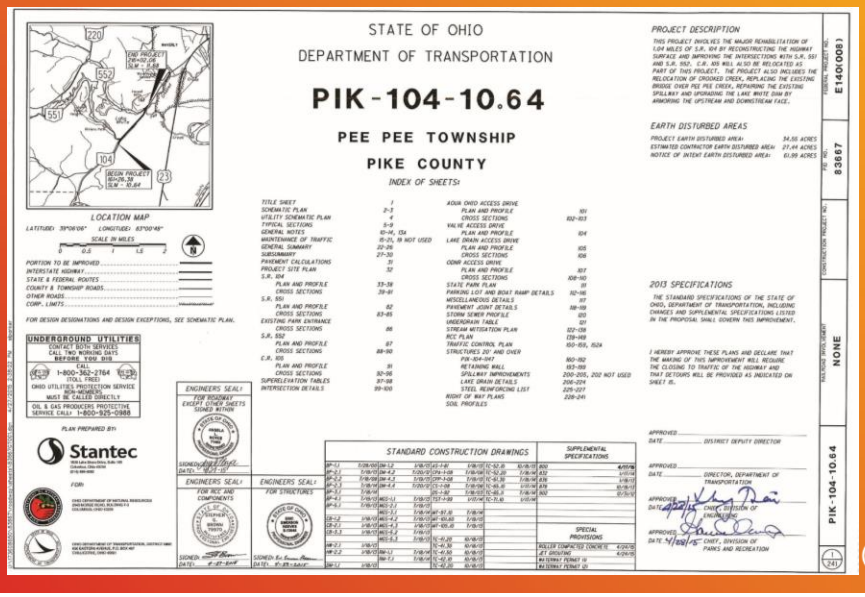

STATE OF OHIO
DEPARTMENT OF TRANSPORTATION

PIK-104-10.64

PEE PEE TOWNSHIP
PIKE COUNTY

INDEX OF SHEETS:

PROJECT DESCRIPTION

EARTH DISTURBED AREAS

2013 SPECIFICATIONS

LOCATION MAP

UNDERGROUND UTILITIES

STANDARD CONSTRUCTION DRAWINGS

SUPPLEMENTAL SPECIFICATIONS

SPECIAL PROVISIONS

PIK-104-10.64

Stantec

Project Description

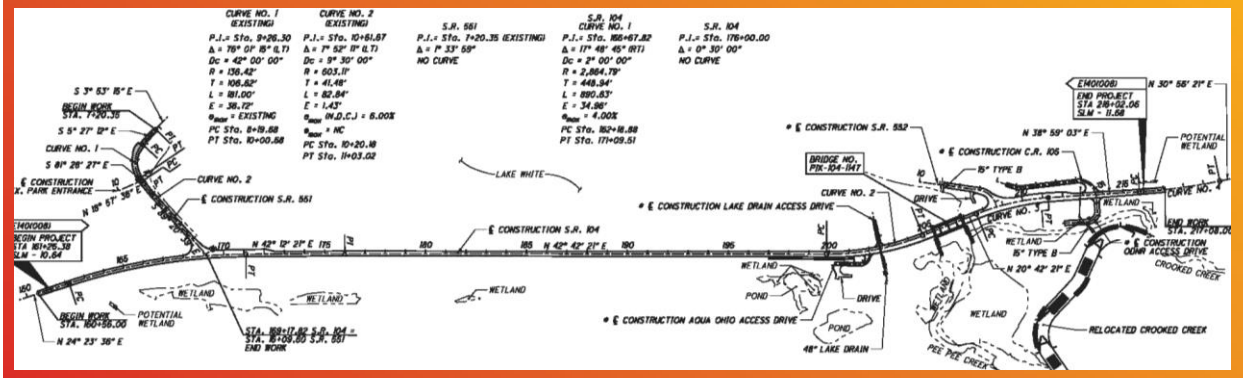

Stantec

Site Characteristics

Dam Classification: Class I (High-Hazard)
Crest: Roadway (State Route 104)
Dam Length: 5,100 feet
Maximum Dam Height: 39 feet
Downstream Slope: 2.5 (H) to 1.0 (V)

Total Drainage Area: 35 square miles
Lake Surface Area: 400 acres
Storage Capacity: 1.9 billion gallons
Waterway: Crooked Creek / Pee Pee Creek
Adjacent River: Scioto River (south)

Stantec

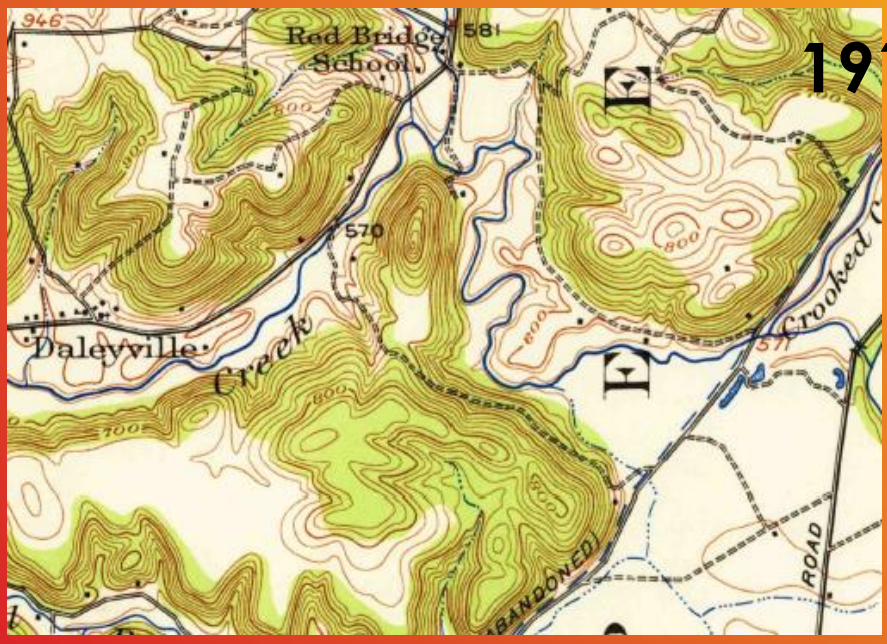

1915 USGS

Stantec

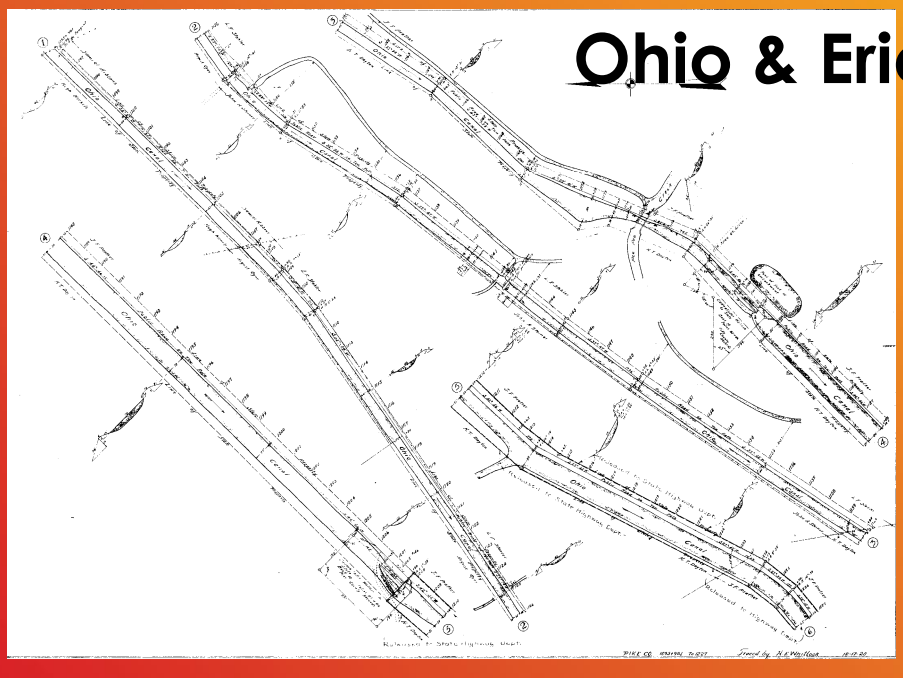

Ohio & Erie Canal

Stantec

Prior to Construction

Stantec

Site Characteristics

Spillway Info
Width: 140 feet
Height: 16 feet
Type: Stair-stepped concrete structure
Control: Remote operated hydraulic gates

Stantec

2006 Overtopping Event

Site Characteristics

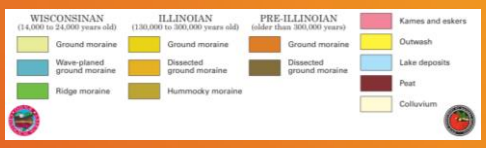

Geologic Conditions

Unglaciated

Steep terrain with varying bedrock depths

Within the glacial outwash

Silty clay, coarse sand and gravel

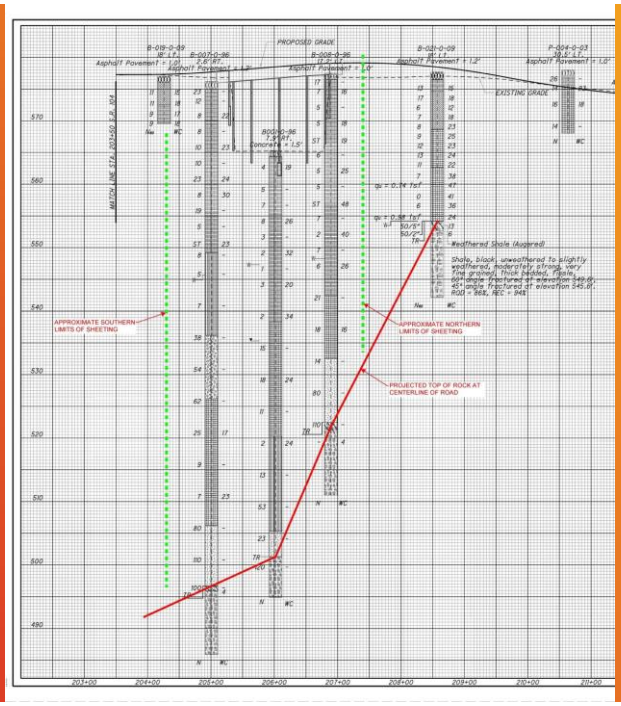

Stantec

Seepage Challenges

July 22, 2014

Stantec

Seepage Challenges

August 29, 2014

Stantec

Seepage Challenges

August 29, 2014

Stantec

Seepage Challenges

August 31, 2014

Stantec

Seepage Challenges

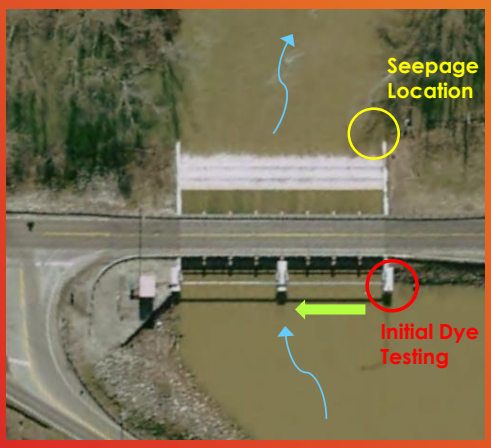

September 4, 2014

Stantec

Seepage Challenges

September 4, 2014

Stantec

Seepage Challenges

- Round the clock observations and monitoring complete.
- Roadway reopened to traffic.
- Seepage area protected.
- Pool level lowered.
- Siphons installed and ready for operation.
- Design of long-term repairs in the works.

September 17, 2014

Stantec

Lake White Dam
Emergency Response

Figure E.1

Stantec

Station 206+00
South of Spillway

Loading Condition: Summer HW

Soil Layers & Loading Conditions

Headwater = Summer Pool = El. 560.3 ft

Tailwater = El. 542.0 ft

Material Name	Kh-Sat (ft/sec)	Kratio Kv/Kh
Silty Clay (Fill) and Sandy Silt	4.41e-008	0.25
Sand and Gravel and Silty Sand	3.28e-005	1
Clay (Residual)	1.1e-008	0.1
Shale	3.28e-009	1
Concrete	3.3e-012	1

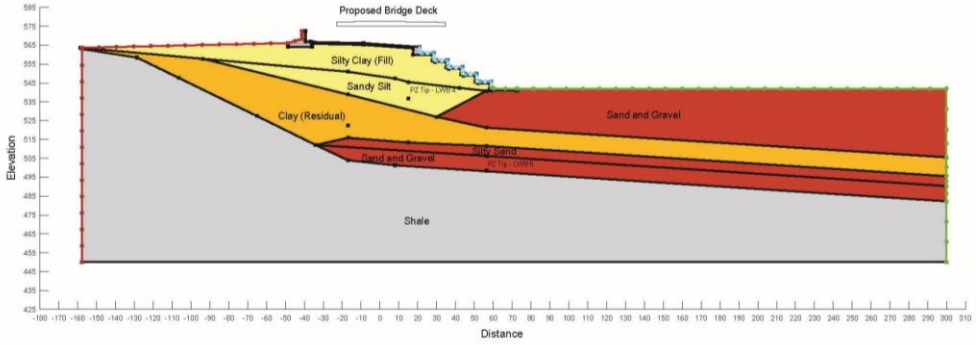

Stantec

Lake White Dam
Emergency Response

Figure E.3

Stantec

Station 206+00
South of Spillway

Loading Condition: Summer HW

Pressure Head (ft)

Headwater = Summer Pool = El. 560.3 ft

Tailwater = El. 542.0 ft

Material Name	Kh-Sat (ft/sec)	Kratio Kv/Kh
Silty Clay (Fill) and Sandy Silt	4.41e-008	0.25
Sand and Gravel and Silty Sand	3.28e-005	1
Clay (Residual)	1.1e-008	0.1
Shale	3.28e-009	1
Concrete	3.3e-012	1

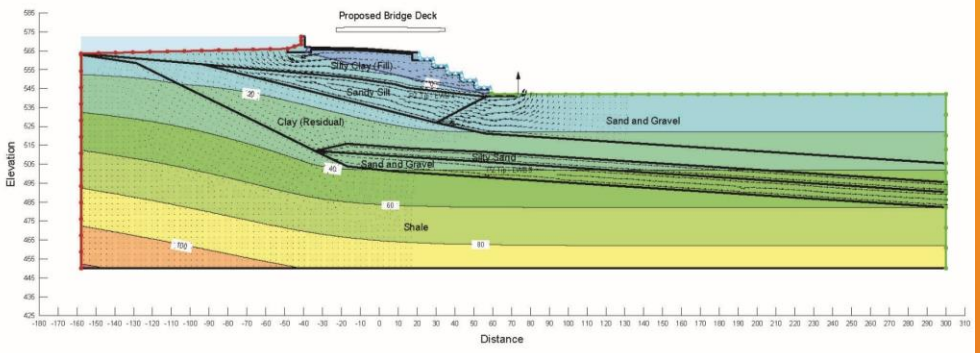

Stantec

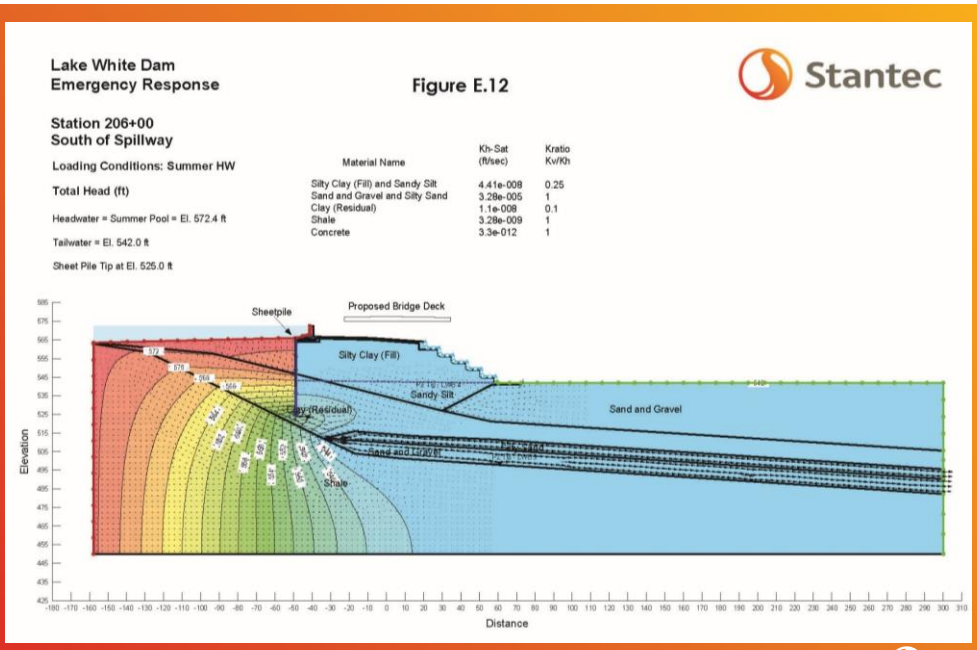

Stantec

Dam-Related Improvements Overview

- Spillway Remediation/Improvements
  - Upstream Cutoff Wall System – sheeting & jet grouting
  - Flowable Fill Enhanced With Bentonite
  - Spillway Toe Relief Wells
- Dam Widening / Armoring
- Install Lake Drain

Stantec

Spillway Remediation/Improvements

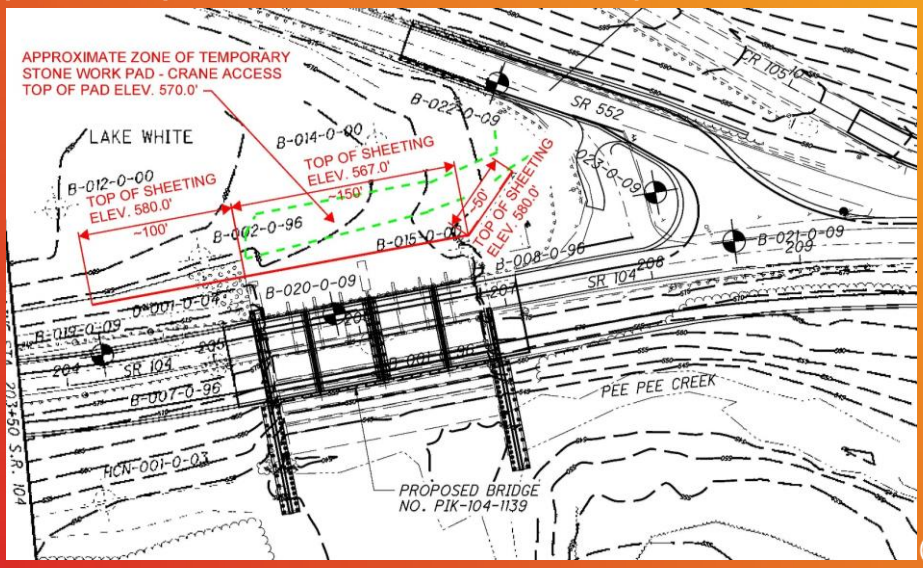

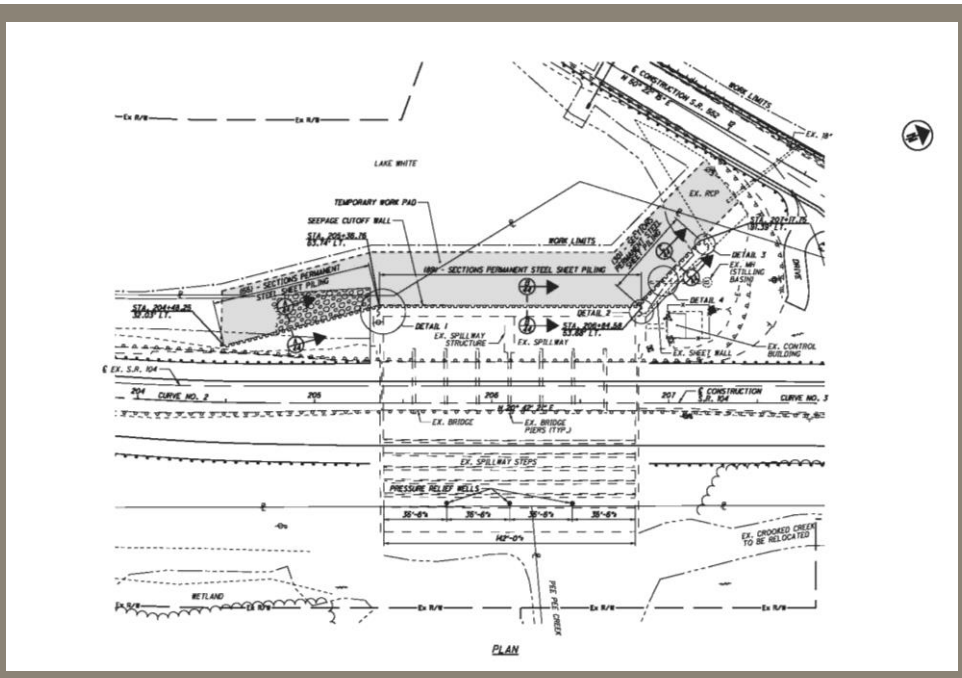

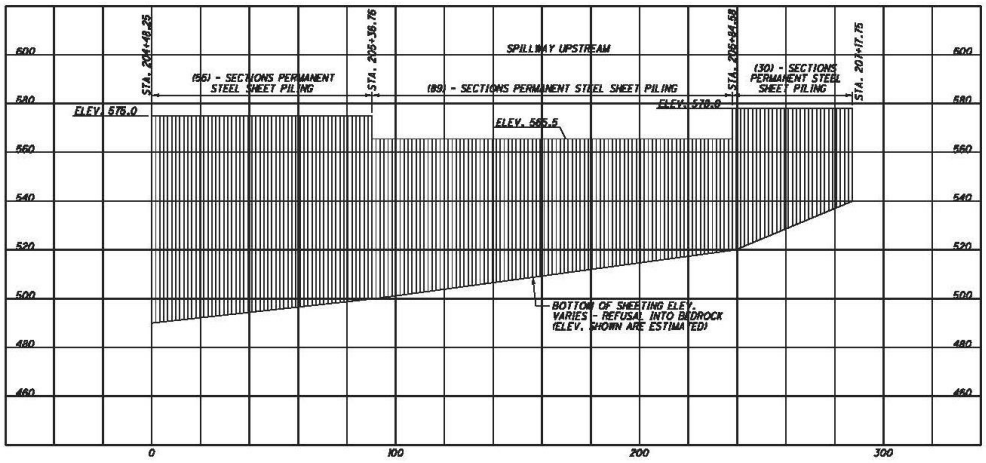

SEEPAGE CUTOFF WALL DEVELOPED ELEVATION

(FOR SEEPAGE CUTOFF WALL PLAN SEE SHEET 41/68)

Stantec

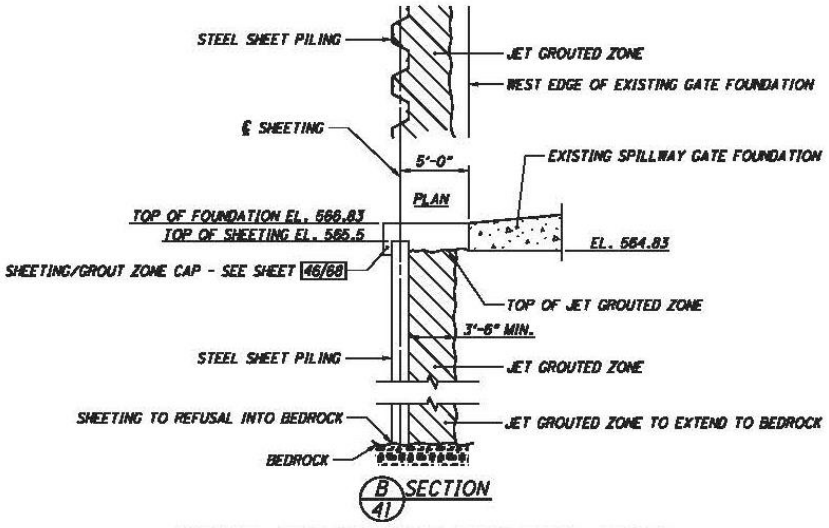

B/41 SECTION

(LAKE WHITE - SPILLWAY CUTOFF WALL TYPICAL SECTION @ SPILLWAY)

Stantec

Sheeting

Stantec

Jet Grouting

Stantec

Jet Grouting

Stantec

Jet Grouting

Stantec


11:53 OCT/24/2016
Stantec


11/18/2016 11:59
Stantec

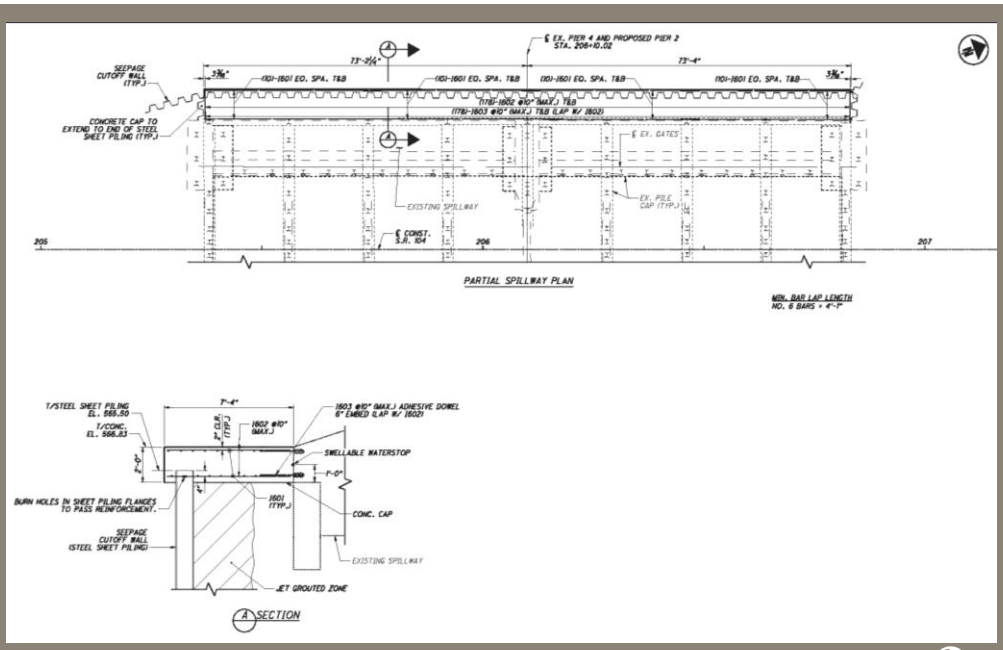

Stantec

Cutoff Wall Cap

Stantec

Cutoff Wall Cap

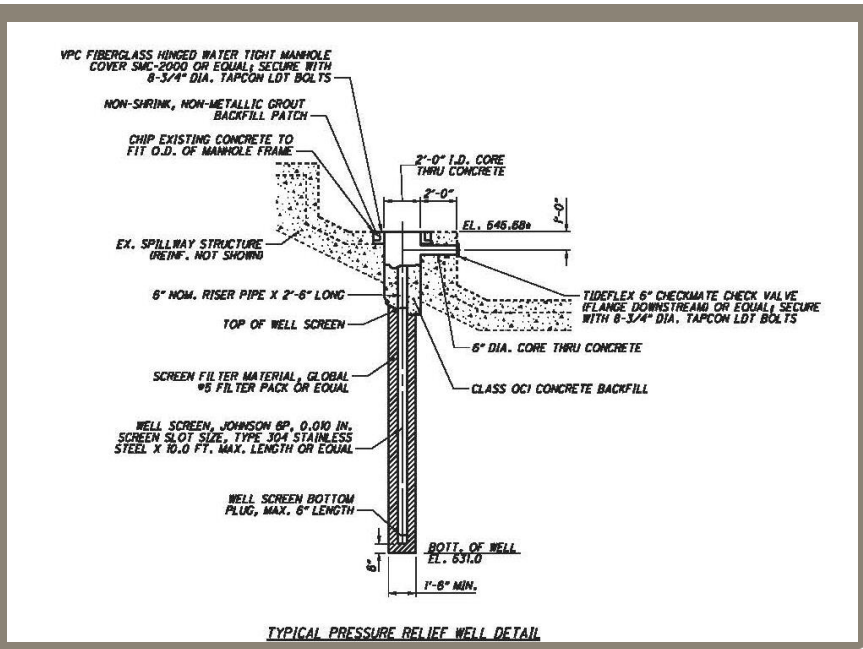

Relief Wells

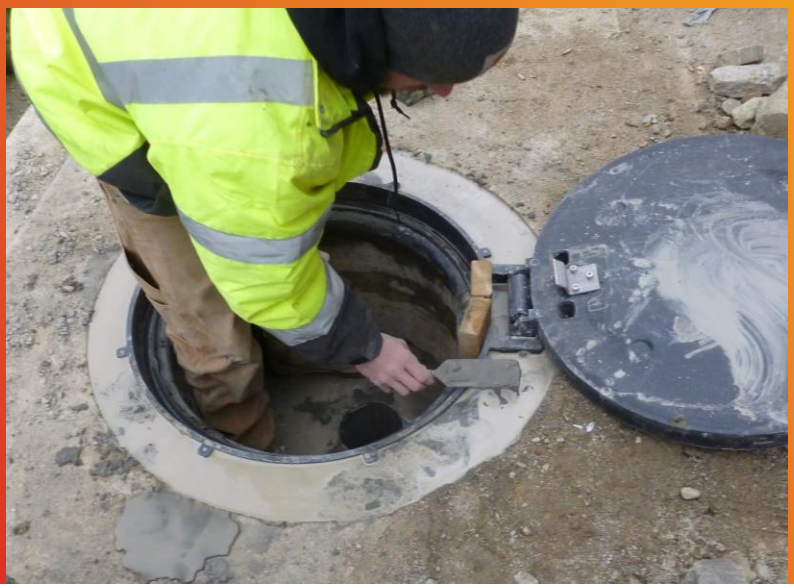

Stantec

Relief Wells - Tideflex

Stantec

Relief Wells

Stantec

Flowable Fill

Stantec

Dam Widening /Armoring

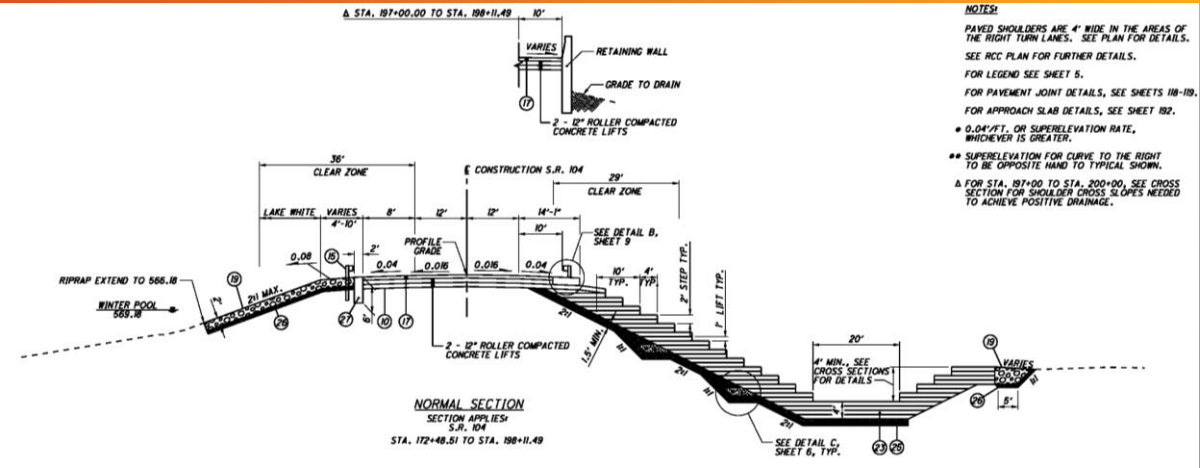

Stantec

Dam Widening / Armoring

Stantec

Dam Widening / Armoring

Stantec

Dam Widening / Armoring

Stantec

Dam Widening / Armoring

Stantec

Dam Widening / Armoring

Stantec

Dam Widening / Armoring

Stantec

Dam Widening / Armoring

Stantec

Dam Widening / Armoring

Dam Widening / Armoring

Dam Widening / Armoring

Stantec

Lake Drain

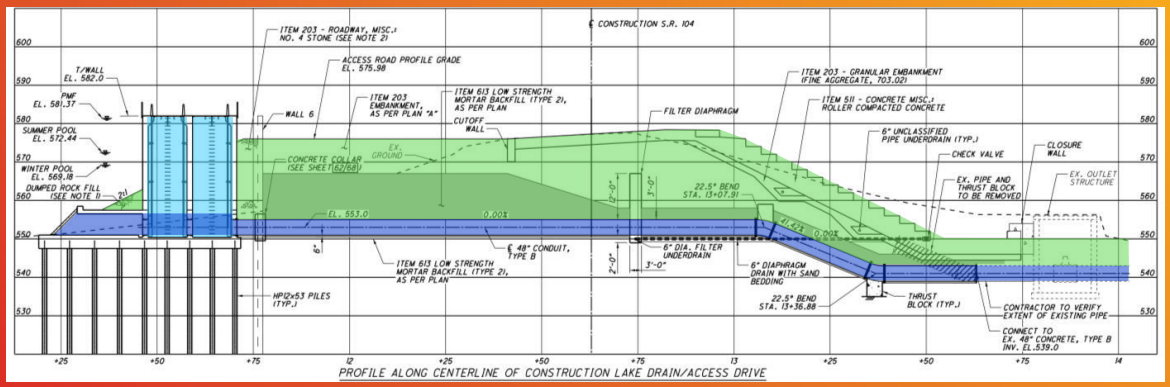

PROFILE ALONG CENTERLINE OF CONSTRUCTION LAKE DRAIN/ACCESS DRIVE

- New concrete structure.
- Dual-chamber, multiple gates, influent tower
- Outlet Pipe Size: 48-inch diameter

Stantec

Lake Drain

Stantec

Elevated Water

Stantec


Constructed
Stantec

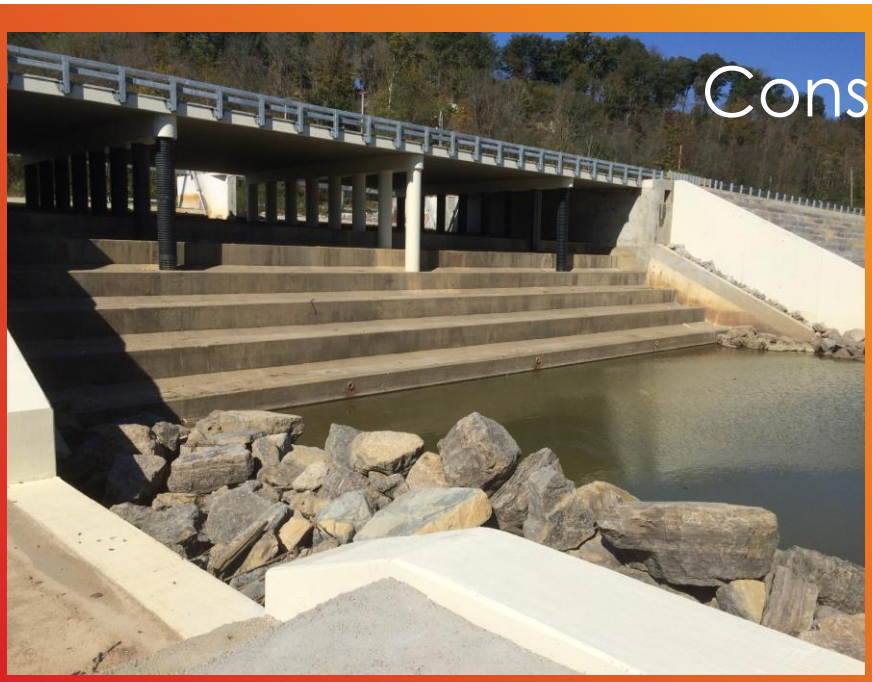
Constructed
Stantec

Stantec

THANKS TO THE DREAM TEAM

- Ohio Department of Natural Resources – Div. of Engineering
- Ohio Department of Transportation District 9 Construction
- Ohio Department of Natural Resources – Div. of Water Resources, Ohio Dam Safety
- Ohio Department of Transportation District 9 Planning & Design

Stantec


Thank You!
QUESTIONS?
Stantec

NOTES

NOTES

NOTES

CHRONOLOGY OF OHIO RIVER VALLEY SOIL SEMINARS

ORVSS I	BUILDING FOUNDATION DESIGN AND CONSTRUCTION, October 16, 1970, Lexington, KY
ORVSS II	EARTHWORK ENGINEERING, START TO FINISH, October 15, 1971, Louisville, KY
ORVSS III	LATERAL EARTH PRESSURES, October 27, 1972, Fort Mitchell, KY
ORVSS IV	GEOTECHNICS IN TRANSPORTATION ENGINEERING, October 5, 1973, Lexington, KY
ORVSS V	ROCK ENGINEERING, October 18, 1974, Clarksville, IN
ORVSS VI	SLOPE STABILITY AND LANDSLIDES, October 17, 1975, Fort Mitchell, KY
ORVSS VII	SHALE AND MINE WASTES: GEOTECHNICAL PROPERTIES, DESIGN, AND CONSTRUCTION, October 8, 1976, Lexington, KY
ORVSS VIII	EARTH DAMS AND EMBANKMENTS: DESIGN, CONSTRUCTION AND PERFORMANCE, October 14, 1977, Louisville, KY
ORVSS IX	DEEP FOUNDATIONS, October 27, 1978, Fort Mitchell, KY
ORVSS X	GEOTECHNICS OF MINING, October 5, 1979, Lexington, KY
ORVSS XI	EARTH PRESSURE AND RETAINING STRUCTURES, October 10, 1980, Clarksville, IN
ORVSS XII	GROUNDWATER: MONITORING, EVALUATION AND CONTROL, October 9, 1981, Fort Mitchell, KY
ORVSS XIII	RECENT ADVANCES IN GEOTECHNICAL ENGINEERING PRACTICE, October 8, 1982, Lexington, KY
ORVSS XIV	FOUNDATION INSTRUMENTATION AND GEOPHYSICAL EXPLORATION, October 14, 1983, Clarksville, IN
ORVSS XV	PRACTICAL APPLICATION OF DRAINAGE IN GEOTECHNICAL ENGINEERING, November 2, 1984, Fort Mitchell, KY
ORVSS XVI	APPLIED SOIL DYNAMICS, October 11, 1985, Lexington, KY
ORVSS XVII	NATURAL SLOPE STABILITY AND INTRUMENTATION, October 17, 1986, Clarksville, IN
ORVSS XVIII	LIABILITY ISSUES IN GEOTECHNICAL ENGINEERING AND CONSTRUCTION, November 6, 1987, Fort Mitchell, KY
ORVSS XIX	CHEMICAL AND MECHANICAL STABILIZATION OF SOIL SUBGRADES, October 21, 1988, Lexington, KY
ORVSS XX	CONSTRUCTION IN AND ON ROCK, October 27, 1989, Louisville, KY
ORVSS XXI	ENVIRONMENTAL ASPECTS OF GEOTECHNICAL ENGINEERING, October 26, 1990, Fort Mitchell, KY
ORVSS XXII	DESIGN AND CONSTRUCTION WITH SYNTHETICS, October 18, 1991, Lexington, KY
ORVSS XXIII	IN-SITU SOIL MODIFICATION, October 16, 1992, Louisville, KY
ORVSS XXIV	GEOTECHNICAL ASPECTS OF INFRASTUCTURE RECONSTRUCTION, October 15, 1993, Fort Mitchell, KY
ORVSS XXV	RECENT ADVANCES IN DEEP FOUNDATIONS, October 21, 1994, Lexington, KY
ORVSS XXVI	SITE INVESTIGATIONS: GEOTECHNICAL AND ENVIRONMENTAL, October 20, 1995, Clarksville, IN
ORVSS XXVII	FORENSIC STUDIES IN GEOTECHNICAL ENGINEERING, October 11, 1996, Cincinnati, OH

CHRONOLOGY OF OHIO RIVER VALLEY SOIL SEMINARS (CONTINUED)

ORVSS XXVIII	UNCONVENTIONAL FILLS: DESIGN, CONSTRUCTION AND PERFORMANCE, October 10, 1997, Lexington, KY
ORVSS XXIX	PROBLEMATIC GEOTECHNCIAL MATERIALS, October 16, 1998, Louisville, KY
ORVSS XXX	VALUE ENGINEERING IN GEOTECHNICAL CONSULTING AND CONSTRUCTION, October 1, 1999, Cincinnati, OH
ORVSS XXXI	INSTRUMENTATION, September 15, 2000, Lexington, KY
ORVSS XXXII	REGIONAL SEISMICITY AND GROUND VIBRATIONS, October 24, 2001, Louisville, KY
ORVSS XXXIII	GROUND STABILIZATION AND MODIFICATION, October 18, 2002, Covington, KY
ORVSS XXXIV	APPLICATIONS OF EARTH RETAINING SYSTEMS AND GEOSYNTHETIC MATERIALS, September 19, 2003, Lexington, KY
ORVSS XXXV	ROCK ENGINEERING AND TUNNELING, October 20, 2004, Louisville, KY
ORVSS XXXVI	GEOTECHNICAL INNOVATIONS IN TRANSPORTATION ENGINEERING, October 14, 2005, Covington, KY
ORVSS XXXVII	INNOVATIONS IN EXPLORATION OF SUBSURFACE VOIDS, October 27, 2006, Lexington, KY
ORVSS XXXVIII	CIVIL INFRASTRUCTUREAND THE ROLE OF GEOTECHNICAL ENGINEERING, November 14, 2007, Louisville, KY
ORVSS XXXIX	URBAN CONSTRUCTION, October 17, 2008, Covington, KY
ORVSS XL	GEOTECHNICAL ENGINEERING AND ENERGY INFRASTRUCTURE, November 13, 2009, Lexington, KY
ORVSS XLI	NATIONAL INFRASTRUCTURE: DAM AND LEVEE SAFETY, October 20, 2011, Louisville, KY
ORVSS XLII	LESSONS LEARNED: FAILURES AND FORENSICS, October 21, 2011, Cincinnati, OH
ORVSS XLIII	WALLS: ABOVE AND BELOW GRADE, November 19, 2012, Lexington, KY
ORVSS XLIV	THE APPLICATION OF GEOLOGY TO GEOTECHNICAL ENGINEERING PRACTICE, November 15, 2013, Louisville, KY
ORVSS XLV	GEOTECHNICAL ASPECTS OF WATERFRONT DEVELOPMENT, October 17, 2014, Cincinnati, OH
ORVSS XLVI	GROUTING SOLUTIONS TO GEOTECHNICAL PROBLEMS, December 16, 2016, Lexington, KY
ORVSS XLVII	GEOTECHNICAL ASPECTS OF THE LOUISVILLE-SOUTHERN INDIANA OHIO RIVER BRIDGES PROJECT, November 16, 2016, Louisville, KY
ORVSS XLVIII	INFRASTRUCTURE INNOVATION IN GEOTECHNICAL DESIGN, November 17, 2017, Cincinnati, OH